

Exploring Statistical Index Criteria for Transformer Frequency Response Interpretation

Adilet Sultanbek, BSc in Electrical and Electronic Engineering

**Submitted in fulfilment of the requirements
for the degree of Masters of Science
in Electrical and Electronic Engineering**



**School of Engineering
Department of Electrical and Computer Engineering
Nazarbayev University**

53 Kabanbay Batyr Avenue,
Astana, Kazakhstan, 010000

Supervisors: Mehdi Bagheri
Co-Supervisor: Amin Zollanvari

December 2018

DECLARATION

I hereby, declare that this manuscript, entitled “Exploring Statistical Index Criteria for Transformer Frequency Response Interpretation”, is the result of my own work except for quotations and citations, which have been duly acknowledged. I also declare that, to the best of my knowledge and belief, it has not been previously or concurrently submitted, in whole or in part, for any other degree or diploma at Nazarbayev University or any other national or international institution.

Name: Adilet Sultanbek

Date: December 14, 2018

ABSTRACT

Large power transformers are considered as the most expensive assets in power system network after hydro generators. Therefore, monitoring of such equipment needs to take special attention. Frequency Response Analysis (FRA) is one of the efficient methods to examine the mechanical condition of the transformer without opening the transformer tank. FRA is a comparative method, where the measured response is compared to the reference fingerprints. Therefore, interpretation of the FRA results needs to be done by an expert in the field. To overcome this problem, so that untrained personnel would be able to use FRA for transformer condition monitoring the interpretation of the frequency response should be based on standard or on some criteria. In this study, various statistical indices for frequency response results interpretation will be introduced and evaluated. Frequency responses of single-phase 0.4-1kVA transformers and three-phase transformers up to 40kVA are interpreted by statistical indices. Outcome of each indicator is discussed and the most reliable ones for FR interpretation are suggested. The simulation of inter-disk short circuit was performed by the rheostat connected in parallel with the winding of transformer. The voltage taps of the transformers were used in order to have the access to different percentage of the transformer winding. With the help of different voltage taps and different resistances in parallel, the two levels of critical values were found and advised to use.

ACKNOWLEDGEMENT

I would first like to thank my thesis advisor Dr. Mehdi Bagheri of the School of Engineering at Nazarbayev University. The Prof. Bagheri always provided me with valuable advises and was available for me 24/7. He allowed to this paper to be my own work, but guided me whenever I had trouble with it.

I would also like to acknowledge Dr. Amin Zollanvari of the School of Engineering at Nazarbayev University as the co-supervisor of this thesis, and I am gratefully indebted to him for his very valuable comments on this thesis.

Finally, I must express my very profound gratitude to my parents and to my partner for providing me with unfailing support and continuous encouragement throughout my years of study and through the process of researching and writing this thesis. This accomplishment would not have been possible without them.

PUBLICATION LIST

The Conference paper for this topic was submitted.

A. Sultanbek, A. Khassenov, Y. Kanapyanov, M. Kenzhegaliyeva, and M. Bagheri, "Intelligent wireless charging station for electric vehicles." In *Control and Communications (SIBCON), International Siberian Conference on IEEE*, pp. 1-6, 2017

M. Bagheri, A.Sultanbek, O. Abedinia, M. S. Naderi and N. Ghadimi, "Multi-objective Shark Smell Optimization for Solving the Reactive Power Dispatch Problem." *IEEE International Conference on Environment and Electrical Engineering and IEEE Industrial and Commercial Power Systems Europe (EEEIC/I&CPS Europe)*. pp. 1-6, 2018

V. Nurmanova, M. Bagheri, A. Sultanbek, A. Hekmati, H. Bevrani, "Feasibility Study on Wind Energy Harvesting System Implementation in Moving Trains." *Control and Communications (SIBCON), International Siberian Conference on. IEEE*, 2017.

Table of Contents

ABSTRACT	2
Acknowledgement	3
Publication list	4
List of Tables	6
List of Figures	7
Chapter 1 – Introduction	8
1.1 Motivation and Objectives.....	8
1.2 Literature review.....	11
Chapter 2 – Methodology and experimental setup.....	20
2.1 Methodology.....	20
2.1.1 Euclidean Distance(ED).....	21
2.1.2 Standard Deviation (SD).....	21
2.1.3 Absolute Sum of Logarithmic Error (ASLE).....	22
2.1.4 Absolute Difference (DABS).....	22
2.1.5 Root Mean Square Error (RMSE).....	23
2.1.6 Correlation Coefficient (CC)	23
2.1.7 Sum Squared Error (SSE)	23
2.1.8 Complex Distance (CD).....	24
2.1.9 Comparative Standard Deviation (CSD)	24
2.1.10 Cross-correlation coefficient (CCF)	25
2.1.11 Maximum of Difference (MAX)	25
2.1.12 Minimum-Maximum Ratio (MM)	25
2.1.13 Normalized Correlation Coefficient (ρ).....	26
2.1.14 Sum squared ratio error (SSRE)	26
2.1.15 Sum squared max-min ratio error (SSMMRE)	27
2.2 Experimental Setup.....	27
2.3 The effect of the rheostat connected in parallel to the transformer winding	29
Chapter 3 – Results and Discussion	32
3.1 Results of FR with calculated SIs	32
3.2 Criteria for each SIs	55
Chapter 4 – Conclusion	64
References	66

LIST OF TABLES

Table 3.1. The CC results for all transformers	37
Table 3.2. The SD results for all transformers	38
Table 3.3. The SSE results for all transformers	39
Table 3.4. The ASLE results for all transformers	41
Table 3.5. The DABS results for all transformers.....	42
Table 3.6. The RMSE results for all transformers	43
Table 3.7. The ED results for all transformers	45
Table 3.8. The CD results for all transformers.....	46
Table 3.9. The CSD results for all transformers	47
Table 3.10. The CCF results for all transformers.....	49
Table 11. The MAX results for all transformers	50
Table 3.12. The MM results for all transformers	51
Table 3.13. The SSRE results for all transformers.....	53
Table 3.14. The SSMMRE results for all transformers.....	54
Table 3.15. The ρ results for all transformers	56
Table 3.16. The results of current flowing through the rheostat	57
Table 3.17. The critical values of SIs for fault detection	58
Table 3.18. The results of CC during 0.005% of nominal current flow through the rheostat..	61
Table 3.19. The SIs values for yellow border.	61

LIST OF FIGURES

Figure 2.1. Experimental setup	28
Figure 2.2. End-to-end open circuit FRA measurement. A) Open circuit. B) Partial short circuit via rheostat. C) Short circuit.	29
Figure 2.3. The total impedance at different voltage taps of 1kVA transformer	31
Figure 3.1. Frequency response of 5 V tap with different resistances.	33
Figure 3.2. Frequency response of 12 V tap with different resistances	33
Figure 3.3. Frequency response of 24 V tap with different resistances	34
Figure 3.4. Frequency response of 36 V tap with different resistances	34
Figure 3.5. Frequency response of 110 V tap with different resistances	35
Figure 3.6 Frequency response of 220 V tap with different resistances	35
Figure 3.7. The criteria zone separation for 1kVA transformer	62

CHAPTER 1 – INTRODUCTION

The maintenance of transformer in healthy condition is the motivation of this research. The modern technique to evaluate the transformer condition is FRA. Thus, to overcome the necessity in trained expert in order to interpret the frequency response some evaluation criteria should be proposed. Based on the literature review provided in this chapter it could be concluded that numerical indices could be used for frequency response interpretation. The objective of this work is to analyze the FRA results of several transformers under predefined fault, and based on the results create the criteria for numerical indices, that could be used during transformer maintenance.

1.1 Motivation and Objectives

One of the most important pieces of equipment in power systems, especially in the field of transmission, distribution and generation, is the power transformer. Power transformers operate under various environmental, electrical and mechanical conditions, which expose them to different hazards during their operation. Any kind of unexpected transformer failure may lead to electricity shortages and significant economic losses. For this reason, proper transformer operation and maintenance are required [1].

One of the main causes of transformer failure is mechanical defects. Mechanical defects can occur due to short circuit currents, overvoltage, inappropriate transportation, explosion of combustible gases generated in the

transformer oil or natural hazards such as an earthquake [2]. Mechanical defects include axial and radial winding deformation, hoop buckling, overall bulk movement, tilting, intermittent internal connections, broken clamping structures, etc. Approximately 70-80% of all transformer failures are initiated by internal winding defects [1]-[5]. Transformer aging is the main cause of these types of failures. Hence, early detection of winding defects helps prevent continuous degradation of transformers and unexpected failure [3]. Transformers can operate with slight winding damage, but this damage may eventually worsen, leading to the total breakdown of the equipment.

A short circuit current, which travels through the transformer winding, can initiate a winding defect [4]. These large currents can be generated due to a single line to ground fault, fault of the equipment at the station, turn-to-turn insulation degradation, etc. and create a large electromagnetic force, consequently damaging the structure of a winding [6]-[9].

Frequency response analysis (FRA) is a widely used method to evaluate the mechanical condition of transformer active parts: the winding, core and leads [10], [11]. The transform frequency response is usually evaluated in the range of 20 Hz to 2 MHz. To determine the transformer condition, input reference and output response signals are required. Any variation between the two responses means that mechanical damage may exist in the equipment. The main challenge of using the FRA test is to correctly interpret the results and determine the reason for the

deviation in the FRA spectra [12]. In many cases, the interpretation of the FRA results is performed visually. Visual interpretation requires that a trained expert review the FRA spectra to identify the faults and their tendencies and to carry out a proper diagnosis [13]. Thus, the FRA interpretation depends on the experience of the personnel interpreting the FRA data. CIGRE reported that some of the reports based on FRA interpretation were not clear and that uncertainties existed in the fault criteria [14]. Another interpretation method includes the calculation of the transfer function (TF) of the transformer. A TF was obtained with the help of frequency-partitioned mathematical models, and another TF was calculated from measured data. Then, the two TFs were compared to predict the fault based on the differences in the TFs. However, this method has high computational complexity and uncertainties arising from the use of mathematical models for the TF calculation, thus, can only identify severe faults [15].

Another method to interpret the FRA spectra is to use numerical or statistical indicators (SIs). SIs allow the interpretation of the results even by inexperienced personnel. However, to use SIs for the interpretation of FRA results, some criteria for fault detection should be obtained. For different fault types and their severity levels, the SIs have different values. This difference arises because different faults distinctively affect the frequency response by increasing the amplitudes of resonances or shifting them horizontally. These changes

differentially affect each SI. Therefore, to use SIs, the effect of faults on SI values should be analyzed and some criteria proposed.

The first standard regarding FRA was issued in China in 2005, DL 911/2004; other international standards were later established by IET and IEEE [16]-[18]. Statistical indices are used to analyze recorded signals; however, the criteria for statistical indices are still a research topic [19]-[21].

In this research work, FRA measurements of various distribution transformers with predetermined transformer faults are conducted, various types of statistical indices are calculated and analyzed, and two levels of criteria are suggested for each index. The first level is the critical value, which describes the healthy condition of the transformer without any fault. The second level is the boundary value, which indicates that the transformer can still operate but that some faults are present.

1.2 Literature review

The idea that generated FRA arose from the concept that the transformer is a gray box [22] and energized by high frequency electromagnetic waves. As FRA should detect the faults, to observe the fault response, creating predefined faults is important. For this reason, the modeling of the transformer is important; however, modeling and simulating the transformer are very challenging tasks. To address the frequency-dependent elements of the transformer and not increase the complexity of the model calculation, the complex permeability approximation

should be used. Due to the macroscopic observation of the conductors, a sparse mesh is obtained. Moreover, for the frequency-dependent elements for program calculation, the rational approximation, passivity enforcement and state space equations are used. The comparison of the proposed model and real transformer results showed adequate similarity.

After modeling of the transformer, the next important step is to analyze the performance of the system. The technique that can confirm the transformer validity over the frequency range is FRA [23]. The FRA response is usually presented in a Bode plot and can be analyzed in three different frequency ranges [24], where the low band corresponds to the core, the midrange to the windings and the high range to the connections of the equipment. For windings observation, focusing on the midrange is necessary, where, with the help of traveling wave theory and multiconductor line theory, the response of the windings can be analyzed. Mathematical calculations can be used to clarify the resonance points of the FRA trace; moreover, the trend of the dependency between the inductance and shunt capacitance has been explored. Real transformers were used to practically prove the calculations, as well as to practically derive the dependence of the FRA response on parameters such as the initial voltage distribution coefficient for windings [25], [26]. The theoretical and practical values agreed with each other in the analysis.

FRA is not the only technique used for transformer maintenance; however, it is the most recently developed. Different techniques that can be used for transformer diagnosis were analyzed in [27]. The techniques used to analyze the mechanical integrity of the transformer were no-load loss and no-load current, insulation resistance, dielectric dissipation factor, short circuit and vibration analysis [28], [29]. These techniques were all performed for a real 400 MVA transformer and practically tested. For the mechanical defects considered, such as buckling and tilting of windings, the conventional tests could not produce accurate results when data for only a few parameters were available. If the transformer is a black box with available output terminals, then the best possible analysis that can produce accurate results is FRA.

FRA is an off-line technique; however, the ability to move to an on-line mode is now a topic of research. The benefit that can be obtained from real-time data analysis of a transformer and accurate and real-time fault diagnosis cannot be ignored. Therefore, [30] conducted a study to move to an on-line FRA. The paper discusses different on-line and off-line winding deformation analyses and proposes a setup for on-line FRA. The main point of the FRA setup was to take into account the bushing effects [31] of a terminal, as they have a capacitance that affects the FRA response. Moreover, the power frequency penetration should be filtered [32]. A practical test of the setup showed adequate results; however, these results were not identical to those of off-line FRA.

FRA can be effectively used to identify a problem with the mechanical integrity of a transformer. However, as the FRA equipment needs to be connected to the transformer, the connection is also important. Samimi et al. [33] applied six different connections for FRA and tried to determine the best terminating resistor (TR) and measurement impedance (MI) in order to obtain the best sensitivity. All connections were applied for three different types of deformation, such as radial and axial, and for disk space variation of the transformer. To compare the obtained results, SIs such as the correlation coefficient (CC) and Euclidean distance were used. Moreover, to use them simultaneously, the change ratio was used, which includes both the CC and ED. The results showed that the capacitive interwinding connection had the best sensitivity to mechanical defects and that higher TR and MI values provide better noise reduction but lead to larger amplitudes. A 1 M Ω resistance provides more sensitivity, but at least a 50 Ω resistor should be used to eliminate reflections.

FRA is a comparative method and requires a trained expert to interpret the results. To make FRA more convenient for untrained personnel, scientists have tried to set some standards that people can rely on, but this research is still in progress. To help interpret the results, Nirgude et al. [34] tried to set a criteria with which FRA users could identify faulty transformers. In their studies, they used three reliable SIs, the CC, standard deviation (SD) and absolute sum of logarithmic error (ASLE). Numerical methods were applied to the results obtained

from a transformer with a predefined axial displacement and to a transformer with a known radial displacement. Additionally, the transformer of an operating substation was tested. As the axial displacement of 1% is not in the tolerable range according to Nirgude, it was used as a reference point, based on which a critical point was found for the three SIs. People can thus use these critical points, which are a CC greater than 0.9998, an SD less than 1 and an ASLE less than 0.4, to identify whether a transformer is healthy. In addition, this approach does not require special knowledge of FRA interpretation.

A transformer consists of many parts, several of which are active. Each of them affect the FRA results. Murthy et al. [35] analyzed the effect of the winding clamping structure on the frequency response. FRA was performed on transformers with and without a clamping structure, and several numerical methods were used to identify the difference. The results showed that the clamping structure affects the response under 2 kHz and that Pearson's, Kendall's and Spearman's CCs and the cross-correlation coefficient are not sensitive to small changes in the frequency response of the transformer under 2 kHz caused by the clamping structure. However, the root mean square error (RMSE) is sensitive to small changes, as is the hypothesis test (F-test).

Senobari et al. [36] applied FRA to a transformer and showed that FRA is an effective tool for fault detection. However, they also showed that many variables could affect the FRA. The connection type and the transformer structure

and type affect the FRA trace. A recommended frequency range for FRA was proposed [37]. Moreover, the FRA interpretation was also problem, so they proposed numerical methods as a solution. They claimed that different SIs could be used but that the absolute average difference (DABS) provides more precise results. The SD turned out to be more robust to different uncertainties. External factors, such as humidity and temperature, also affect the frequency response. The problem regarding the CC is that for data with the same shape but different magnitudes, incorrect results are obtained, and for the SD, a horizontal shift of a peak has a significant effect, while a large horizontal shift in a valley does not have a proper effect. Thus, the sum squared max-min ratio error (SSMMRE) should be used to overcome this problem.

The FRA technique has been used for the past fifteen years [38], and during this time, several connection methods have been used almost as a standard. Picher et al. [39] collected all information relevant to FRA and, with the CIGRE, tried to provide a guide for the connection for FRA, such as an end-to-end open circuit, an end-to-end short circuit, capacitive interwinding measurement or inductive interwinding measurement. The FRA interpretation was also described, in which the low frequency range below 2 kHz corresponds to the core, the frequency from 2 kHz-20 kHz to interactions between windings, the frequency from 20 kHz to 1 MHz to the winding structure and the frequency above 1 MHz to the setup or connection of the FRA [41]. The appearance of resonances in each frequency

range was described. The phenomenon of residual magnetization was described, based on which it was claimed that due to the residual magnetization of the core, the results of the fingerprint and obtained data could be different even if no problem is present. The difference between phases in the transformer was shown, and the use of the same phases for reference during FRA was proposed. Even if a sister transformer can be used for the FRA test, a slight difference still exists.

As stated before, the axial displacement of a transformer is one of the main faults. Thus, to correctly identify this fault in the frequency response, Hashemnia et al. [40] proposed a 3D finite element model. In this model, the axial displacement and its effects on the transformer parameters and on the frequency response were analyzed. The results showed that the finite element model has better performance when it includes capacitance and inductance variation during axial displacement, as this helps emulate the axial displacement of the lumped model of the transformer more correctly. Additionally, the model showed that the leakage flux increases near the faulty section of the winding and has an asymmetrical distribution during axial displacement.

Hence, many scientists used SIs to interpret the frequency response, and Samimi et al. [42] tried to understand their behavior during different faults. A practical model of a transformer winding with a defined axial displacement, a defined radial deformation and different interdisk variations was created. These authors created 11 different cases of major faults and applied SIs to analyze the

results. The results showed that the SD and variance have a linear relationship with mechanical faults. The SSE has a parabolic relationship with mechanical faults. As the CC seems to produce false results for the situations in which the response shapes are identical but have different amplitudes, the authors proposed using the ASLE as the indicator, which overcomes all these issues. Moreover, due to its linearity and robust to uncertainties, the variance is also recommended as an SI for the detection of mechanical faults.

Wesley et al. [44] simulated an interturn winding short circuit on a 15 kVA cast-resin transformer using its taps to change the short circuit percentage. Their results showed that the ASLE is the most robust SI for FRA interpretation. Moreover, the ARA and CC exhibit linearity in response to mechanical faults only in the open circuit test, whereas they are not reliable in short circuit tests.

Samimi et al. [45] provided a review of the usage of numerical methods for interpretation purposes. The relative factor (R_{xy}) was shown to be a standard used by China for fault detection in transformers with the help of FRA. The ASLE method is the most accurate and tends to have 90% accuracy in fault detection. Additionally, the system based on neural networks and trained for FRA fault detection using numerical methods was reported to have an accuracy of 95%. In the end, the recommendation of numerical method usage was proposed. First, the extraction of all the values of the indices from the results is required to observe the linearity and basic trends. The same numbers of samples should be provided

for each method, a proper connection scheme for FRA should be selected, uncertainties in indices should be taken into account if they exist, and more than one index should be utilized.

CHAPTER 2 – METHODOLOGY AND EXPERIMENTAL SETUP

This chapter provides numerical indices that was chosen out of many available, based on the literature review and their sensitivity to our results. All numerical indices were given with formulas and description. The setup for FRA was shown and clearly described. The experiment required predefined fault on each transformer, thus, the rheostat parallel to transformer winding was connected. This fault emulated the inter-disk short circuit. With the help of voltage taps on transformers and variable resistance on rheostat, different fault values were obtained. Therefore, based on the results, which showed the linear effect of the resistance on the Frequency Response of the transformers, criteria identification could be obtained.

2.1 Methodology

In this section, various types of statistical indices, such as the correlation coefficient (CC), standard deviation (SD), sum squared error (SSE), absolute sum of logarithmic error (ASLE), absolute difference (DABS), root mean square error (RMSE), Euclidean distance (ED), complex distance (CD), comparative standard deviation (CSD), cross-correlation coefficient (CCF), maximum of difference (MAX), minimum-maximum ratio (MM), sum squared max-min ratio error (SSMMRE), sum squared ratio error (SSRE) and normalized correlation

coefficient (ρ), will be utilized. However, among all of these, the IEEE standard recommends the CC method for FRA interpretation [1], [5], [46], [47].

For the calculation of all the SIs, $X(i)$ and $Y(i)$ stand for the i -th sample of the reference and new measured data, respectively.

2.1.1 Euclidean Distance(ED)

The FRA response index was analyzed with the Euclidean distance (ED) in [47], which is given as

$$ED = \|X - Y\| = \sqrt{\sum_{i=1}^N (Y(i) - X(i))^2} \quad (1)$$

where N is the number of samples in the FRA spectrum. In [47], this statistical indicator was compared with other indicators: the CC, SSE, and maximum difference (MAX); the ED had more regular and linear changes due to axial and radial deformations [46].

2.1.2 Standard Deviation (SD)

In [34], the influence of changes in the moisture level and temperature on the FRA spectrum was examined. To interpret the results, the CC and SD were utilized in [33]. After several experiments that were done in [33], these indices were found to not be sufficiently accurate to distinguish winding deformation from temperature or moisture content variations. In [47], the axial displacement of a transformer winding was examined, and the SD was found to be sensitive to axial displacements. The SD can determine axial displacements of less than 1%.

Criteria for axial displacements of more than 1% were defined in [42], and this criterion of 1% was used as suggested in IEC 60076-5 [17]. The SD is given by (2).

$$SD = \sqrt{\frac{\sum_{i=1}^N (Y(i) - X(i))^2}{N-1}} \quad (2)$$

2.1.3 Absolute Sum of Logarithmic Error (ASLE)

In calculating the ASLE, the recorded spectra are compared on a logarithmic scale. According to [48], the ASLE is a more pertinent statistical indicator than the SSE or CC.

$$ASLE = \frac{\sum_{i=1}^N |20\log_{10} Y(i) - 20\log_{10} X(i)|}{N} \quad (3)$$

2.1.4 Absolute Difference (DABS)

In [44], the DABS was found to be less sensitive to the magnitude variation of FRA spectra. It is sensitive to new resonant frequencies and to shifts in resonant frequencies. The DABS will be zero if the response overlays well with the fingerprint [49].

$$DABS = \frac{\sum_{i=1}^N |Y(i) - X(i)|}{N} \quad (4)$$

2.1.5 Root Mean Square Error (RMSE)

The quality of the frequency response approximation can be measured using the RMSE, which is a rational function with minimal complexity for FRA trace comparisons [50]:

$$RMSE = \sqrt{\frac{1}{N} \sum_{i=1}^N \left(\frac{|Y(i)| - |X(i)|}{\frac{1}{N} \sum_{i=1}^N |X(i)|} \right)^2} \quad (5)$$

2.1.6 Correlation Coefficient (CC)

The degree of similarity between two frequency responses can be obtained using the CC [47], [49], [50]-[56]. If responses overlay well, then the result becomes one; otherwise, it will be zero, thus yielding a result between 0 and 1. This indicator is the normalization of the covariance; consequently, it is not sensitive to constant changes between two frequency responses [57].

$$CC = \frac{\sum_{i=1}^N X(i)Y(i)}{\sqrt{\sum_{i=1}^N [X(i)]^2 \sum_{i=1}^N [Y(i)]^2}} \quad (6)$$

2.1.7 Sum Squared Error (SSE)

The SSE suppresses small errors and magnifies large errors. The SSE result will be zero if the spectra are similar, and the variations less than one are compressed; however, differences of greater than one are magnified [46], [48] and [54]. The SSE result shows the difference between two spectra, and the SSE unnecessarily

enlarges or compresses the deviation. Considering the studies by [49] and [58], the SSE is very sensitive to large differences and not sensitive to differences less than 1.

$$SSE = \frac{\sum_{i=1}^N (Y(i) - X(i))^2}{N} \quad (7)$$

2.1.8 Complex Distance (CD)

The phases of the response change due to axial displacements, and transfer functions are a combination of real and imaginary numbers [43]. The ED calculates only variations in the magnitude of the frequency responses, and to also consider phase variations, a new index, the CD, is developed. The CD can determine phase and magnitude differences between two frequency responses. In [9], the index was determined to be more accurate and to improve the performance as it considers phase changes. The CD equation is given in (8).

$$CD = \sqrt{\sum_{i=1}^N \left(|X(i) \cos \varphi_x(i) - Y(i) \cos \varphi_y(i)|^2 + |X(i) \sin \varphi_x(i) - Y(i) \sin \varphi_y(i)|^2 \right)} \quad (8)$$

2.1.9 Comparative Standard Deviation (CSD)

The CSD is a modified version of the SD [47]. In the CSD, the variation of each sample with respect to its mean value is calculated, which is further used to obtain the comparative deviation. In the interpretation, if the CSD result is 0, then the two responses match well [47].

$$CSD = \sqrt{\frac{\sum_{i=1}^N [(Y(i) - \mu_Y) - (X(i) - \mu_X)]^2}{N - 1}} \quad (9)$$

where, μ_x and μ_y are average values of corresponding vectors.

2.1.10 Cross-correlation coefficient (CCF)

In [6], [55] and [58], for interpretation of transfer functions, the cross-correlation coefficient (CCF) was used, and in [55] some criteria for CCF values is given.

$$CCF = \frac{\sum_{i=1}^N (X(i) - \mu_X)(Y(i) - \mu_Y)}{\sqrt{\sum_{i=1}^N (X(i) - \mu_X)^2 \sum_{i=1}^N (Y(i) - \mu_Y)^2}} \quad (10)$$

2.1.11 Maximum of Difference (MAX)

The maximum value of the variance between the baseline and new response is calculated using the maximum difference (MAX) indicator [46], [52], given by (11).

$$MAX = \max(Y(i) - X(i)) \quad (11)$$

2.1.12 Minimum-Maximum Ratio (MM)

The MM is another statistical indicator that can be used to obtain the level of similarity between two data sets. According to the study results of [25], the MM is sensitive to frequency response shape changes caused by response amplitude changes and shifts in resonant frequencies. The MM results will approach 1 if the two compared results are similar [52].

$$MM = \frac{\sum_{i=1}^N \min(Y(i), X(i))}{\sum_{i=1}^N \max(Y(i), X(i))} \quad (12)$$

2.1.13 Normalized Correlation Coefficient (ρ)

The normalized CC is used to measure the similarity between two response progressions. For two frequency responses, the normalized CC is given by (13) [8].

$$\rho = \frac{\sum_{i=1}^N X^*(i)Y^*(i)}{\sqrt{\sum_{i=1}^N [X^*(i)]^2 \sum_{i=1}^N [Y^*(i)]^2}} \quad (13)$$

where,

$$X^*(i) = |X(i)| - \frac{1}{N} \sum_{i=1}^N X(i) \quad (14)$$

$$Y^*(i) = |Y(i)| - \frac{1}{N} \sum_{i=1}^N Y(i) \quad (15)$$

2.1.14 Sum squared ratio error (SSRE)

In [45], [52] and [53] SSRE is used, which is developed to normalize the SSE and the equation is as follows:

$$SSRE = \frac{\sum_{i=1}^N \left[\frac{Y(i)}{X(i)} - 1 \right]^2}{N} \quad (16)$$

2.1.15 *Sum squared max-min ratio error (SSMMRE)*

SSMMRE is the modified version of SSRE used in [52], which is as following:

$$SSMMRE = \frac{\sum_{i=1}^N \left(\frac{\max(Y(i), X(i))}{\min(Y(i), X(i))} - 1 \right)^2}{N} \quad (17)$$

2.2 *Experimental Setup*

To examine different statistical indicators, twelve single-phase and three-phase distribution transformers were examined. The first single-phase transformer was a 0.4 kVA, 220/5/12/24/36 V transformer, and the second and third were 0.4 kVA, 230/24 V sister transformers. The fourth single-phase transformer was a 0.63 kVA, 220/5/12/22/42/110/220 V transformer, and the fifth was a 0.63 kVA, 230/230 V transformer. The sixth was a 0.63 kVA, 230/220 V transformer, and the seventh single-phase transformer was a 0.75 kVA transformer with 230/53/200/400 V secondary windings and a 230/115/230 V tertiary winding. Finally, the eighth single-phase transformer was a 1 kVA, 230/5/12/24/36/110/220 V transformer. The three-phase transformers included three 350 VA sister transformers with a 230/400-230 V voltage rating: a 1.2 kVA, 220-24/42 V transformer; a 5 kVA, 230/380-42 V transformer; and 20 kVA and 40 kVA, 10 kV/400 V transformers. All the transformers have different accessible taps that assisted us in emulating disk-to-disk short circuit faults over the windings using a rheostat between the taps. According to IEEE Std C57.149-2012 [59], we used an end-to-end open circuit test for FRA measurements. The end-to-end short

circuit and capacitive and inductive connection tests were not performed in this study. The equipment for FRA measurement was well-established commercialized equipment, and only the low-voltage windings of the transformers were examined [33]-[35]. The frequency range was from 20 Hz to 2 MHz, with 975 logarithmically spaced data collection points. The two outputs of the FRANEO, the source and the reference, were connected together and input into one end of the winding, whereas the third output, which is the response, was connected to the other end of the winding. The connections were performed via 50 Ω wires, and the injection of 10 V V_{P-P} was carried out [60]. The rheostat was connected in parallel to each winding, and at each tap level, the resistance was set to 15 k Ω , then to 5 k Ω and gradually reduced by 500 Ω to 200 Ω . Finally, it was shorted (zero Ω) to emulate a real short circuit. Figure 1 shows the connection setup.

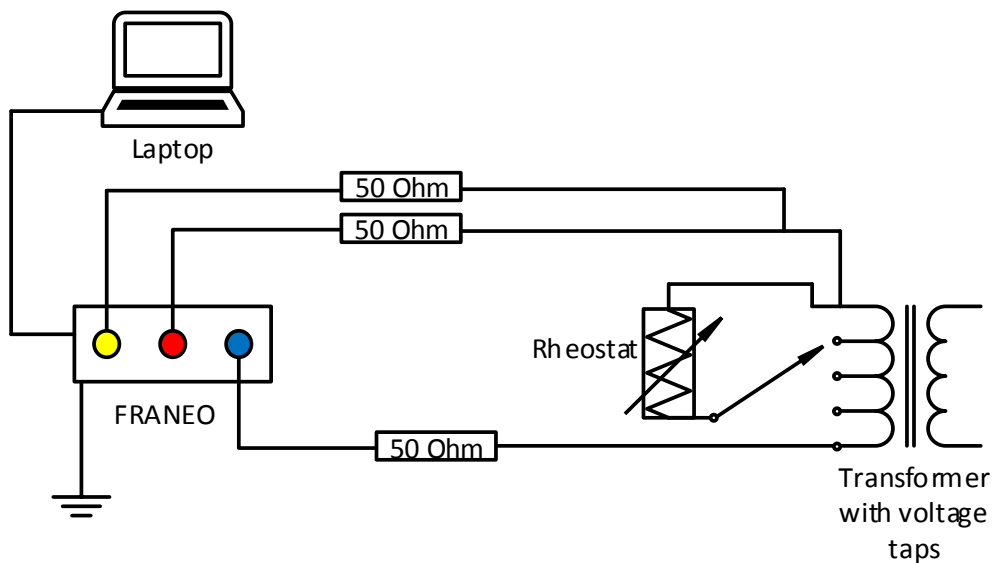


Figure 2.1. Experimental setup

The $15\text{k}\Omega$ resistance is significant and, for small transformers, could be considered an open circuit when connected parallel to the winding; see Figure 2.2. Furthermore, the $5\text{k}\Omega$ resistance could also be considered an open circuit or could pass some short circuit circulating current. The main idea of the experiment was to find the tolerable resistance of the short circuit. Figure 2.2 shows three experimental scenarios. In the first, the winding is an open circuit. In the second, the resistance is not significant, and a short circuit current slightly passes through the resistor. The last is a complete short circuit via the wire [61].

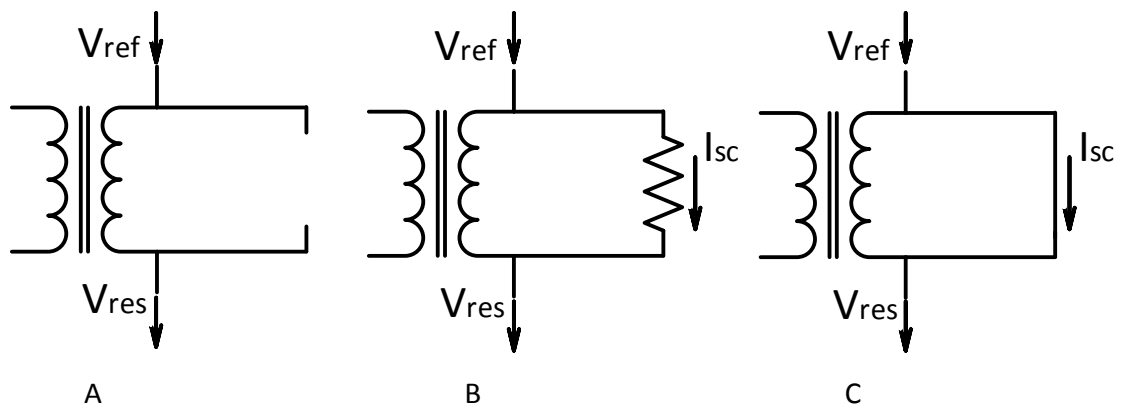


Figure 2.2. End-to-end open circuit FRA measurement. A) Open circuit. B) Partial short circuit via rheostat. C) Short circuit.

2.3 The effect of the rheostat connected in parallel to the transformer winding

As we can see in Figure 2b, during our FRA measurement with the rheostat, we have the resistance or rheostat parallel to the transformer. Thus, here, the circuit can be analyzed as a simple circuit with two parallel resistances or

impedances. In our case, the rheostat has a significant resistance, and the transformer has a significant impedance because the DC resistance of the transformer is small; however, due to the winding, tank and core, we have a very high impedance. Thus, when we perform the FRA test, our signal chooses the easiest path or the path of least resistance. Therefore, when the rheostat resistance is significant in comparison with the parallel impedance of the winding, the signal will pass through the winding, and when the resistance is equal to or smaller than the impedance, the signal will split between the two impedances or pass through the rheostat, respectively. Based on this concept, the significant resistance of the rheostat applied to a small portion of the winding in parallel, with the help of voltage taps, should not affect the frequency response, as the entire signal should bypass the rheostat. Despite the very large resistance, leakage of the signal could occur; however, its effect should be negligible or in a tolerable range.

The voltage taps of the transformers are used in our experiment in order to access different percentages of the winding. With the help of FRANEO, measuring the total impedance of the winding was possible; thus, the behavior under different resistances could be explained. To show that the voltage taps provide different winding percentages, which lead to different impedances, Figure 3 is provided below. In the figure, the 1 kVA transformer's impedance at different voltage taps is shown. The voltage taps are 5/12/24/36/110/220 V.

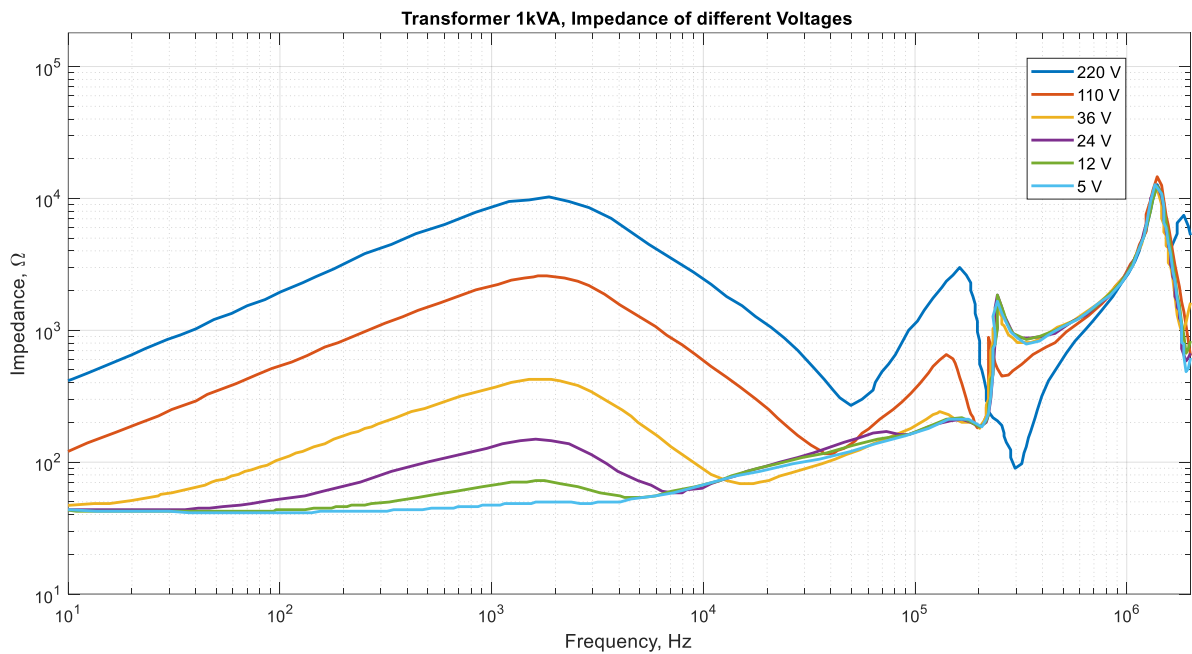


Figure 2.3. The total impedance at different voltage taps of 1kVA transformer

As can be seen, the higher the voltage is, the more winding is used and thus the higher the impedance. Moreover, the changing impedance value reveals the dependence of the resistance on the frequency. The majority of the impedance is contributed by the winding; thus, it is inductive, and at higher frequencies, the capacitance starts to influence the impedance.

CHAPTER 3 – RESULTS AND DISCUSSION

This chapter provides graphs of FR of different voltage taps of the transformer. At each voltage tap, the effect of different resistance values could be seen. Moreover, based on the FRA results, the tables with calculated statistical indices for each transformer under test were provided. Also, the transformers were energized and current flowing through the rheostat was measured at specific values. Based on figures, tables and current values two level of criteria for each index were provided.

3.1 Results of FR with calculated SIs

To visualize the effect of different resistances on different voltage taps, the frequency responses of the 1 kVA transformer are provided as an example below. The same data are available for each transformer and were analyzed.

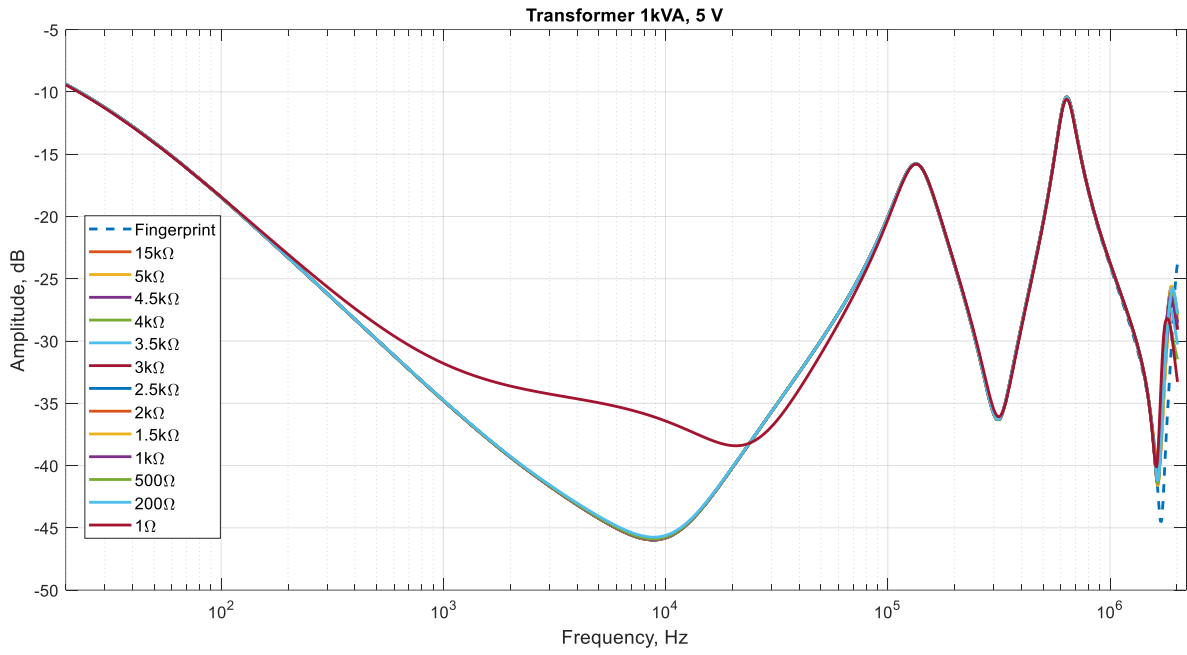


Figure 3.1. Frequency response of 5 V tap with different resistances.

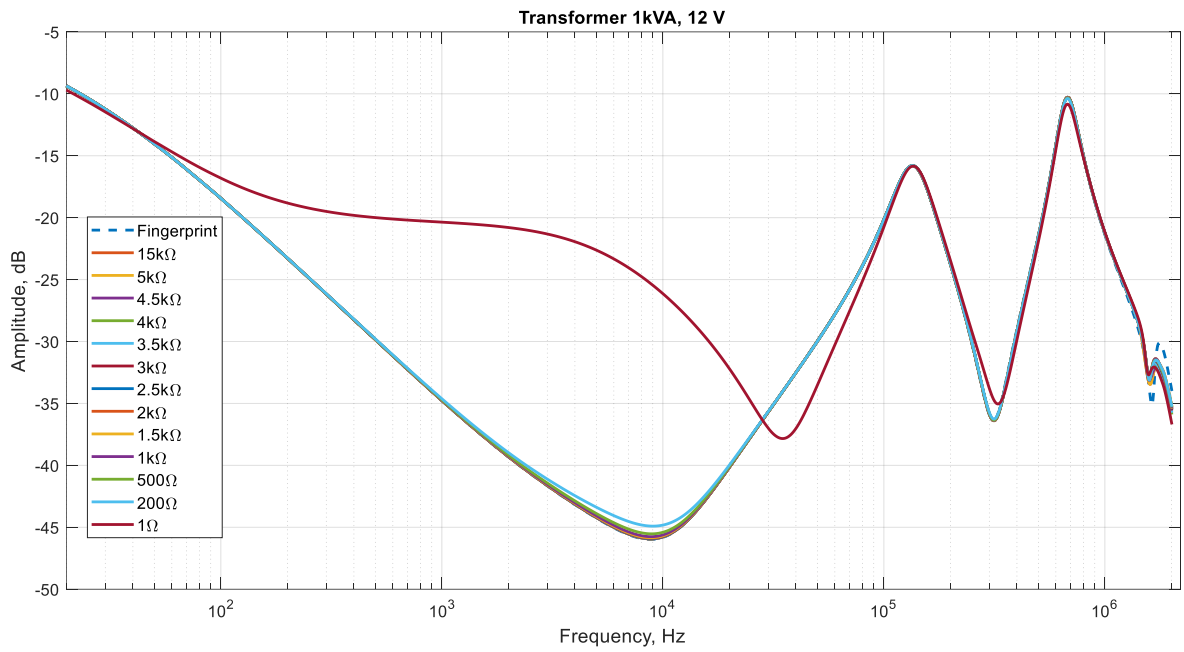


Figure 3.2. Frequency response of 12 V tap with different resistances

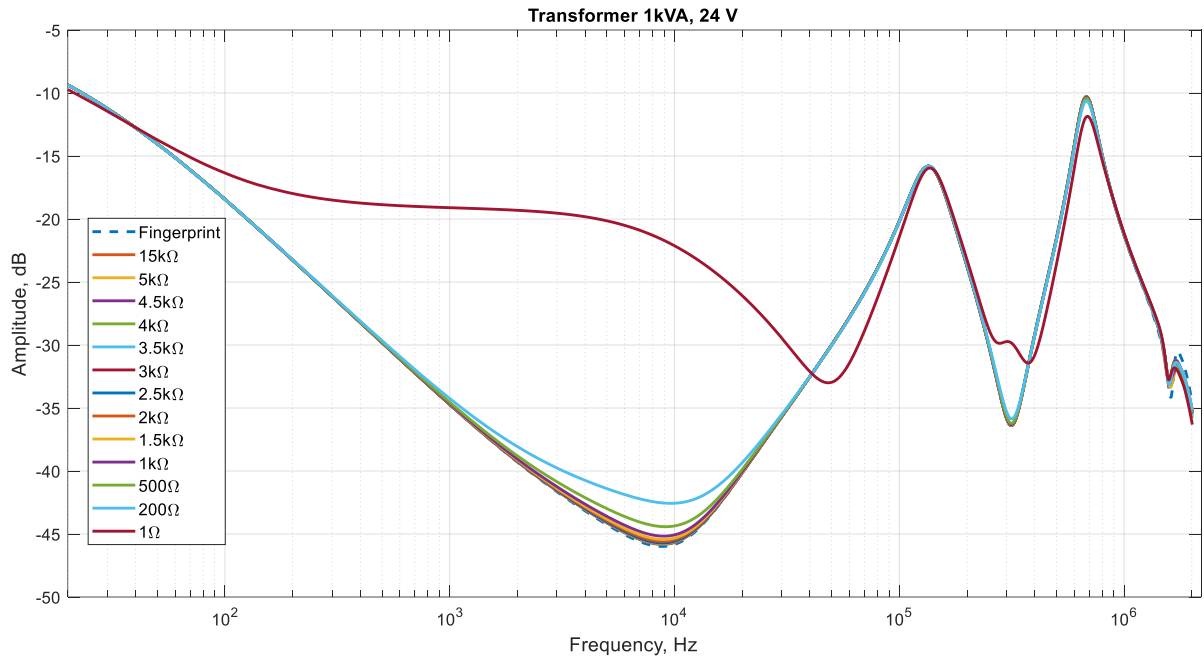


Figure 3.3. Frequency response of 24 V tap with different resistances

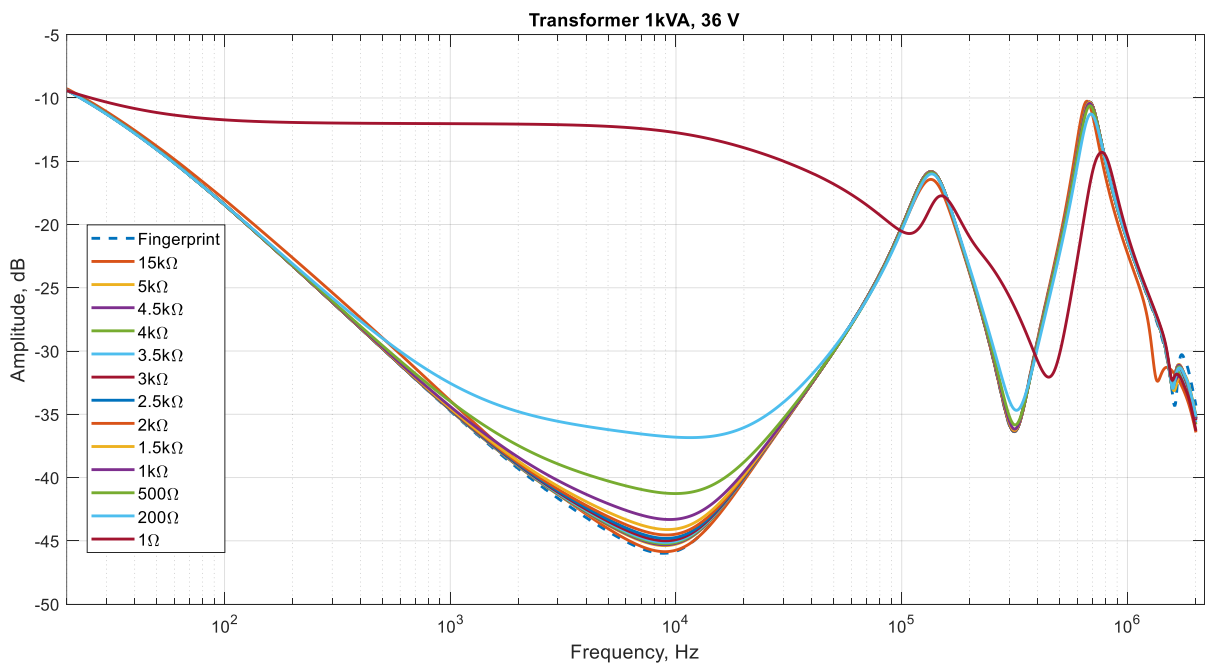


Figure 3.4. Frequency response of 36 V tap with different resistances

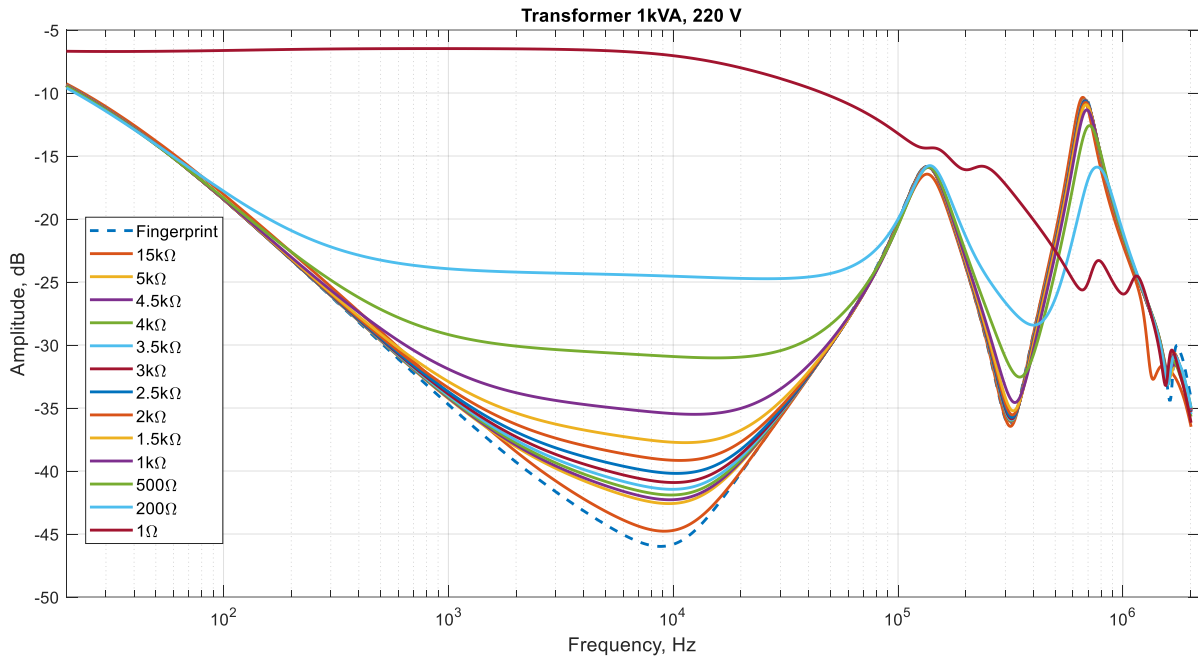


Figure 3.5. Frequency response of 110 V tap with different resistances

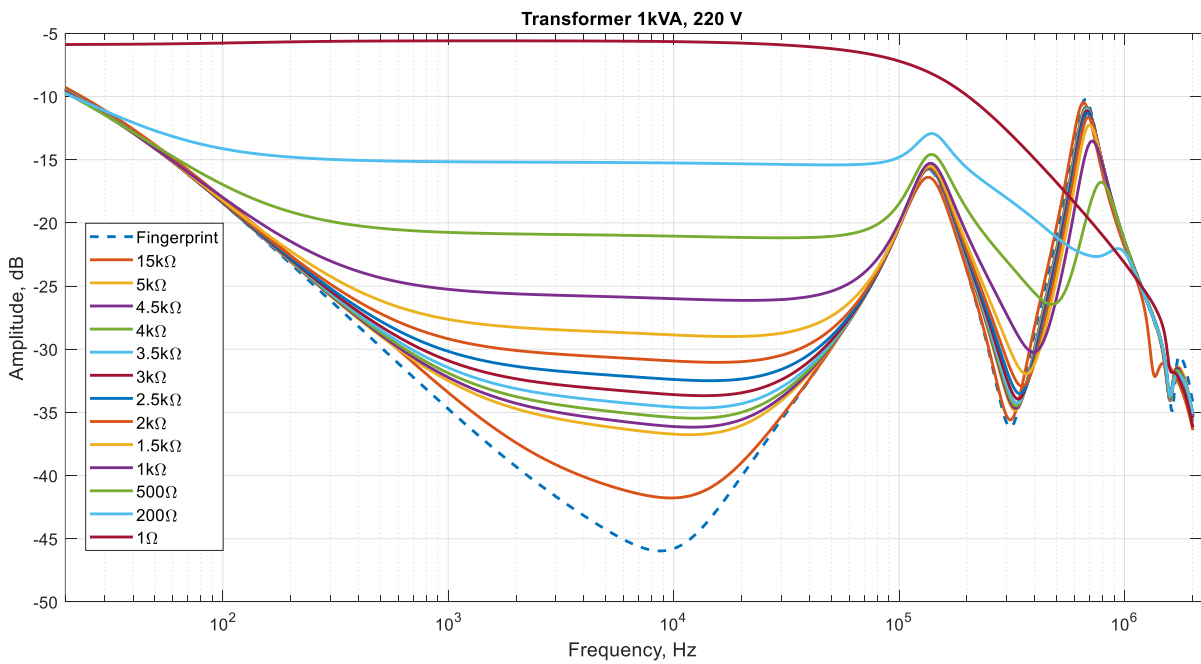


Figure 3.6 Frequency response of 220 V tap with different resistances

As shown in Figures 3.1-3.6, the effect of the same resistance is different for different voltage taps. The smaller the voltage tap level is, the smaller the resistance needed to affect the frequency response. For example, the effect of 5

$k\Omega$ on the 220 V tap is already observed. However, for voltage tap levels below 110 V, the response almost matches the fingerprint. This phenomenon is easily explained by our Figure 3, which shows that the 220 V tap has a $10\text{ k}\Omega$ resistance, which is greater than $5\text{ k}\Omega$, so the signal splits between the two impedances, and a visible effect on the frequency response appears. The large effect of the rheostat on higher frequencies above 1 MHz can be explained by the structure of the rheostat. The rheostat consists of wire that winds in the form of a helix around carbon pipe. Thus, at high frequencies, it can act as an inductor, and the wire would also have a series capacitance.

Table 3.1. The CC results for all transformers

CC	Wind. %	15k Ω	5k Ω	4.5k Ω	4k Ω	3.5k Ω	3k Ω	2.5k Ω	2k Ω	1.5k Ω	1k Ω	500 Ω	200 Ω	1 Ω
1 phase														
400VA														
T1 5V	13.89%	0.9998	0.9997	0.9998	0.9997	0.9997	0.9998	0.9999	0.9997	0.9998	0.9999	0.9998	0.9977	0.9045
T1 12V	33.33%	0.9998	0.9997	0.9997	0.9997	0.9998	0.9999	0.9997	0.9998	0.9997	0.9998	0.9997	0.9992	0.8983
T1 24V	66.67%	0.9997	0.9999	0.9999	0.9999	0.9999	0.9999	0.9999	0.9998	0.9998	0.9995	0.9985	0.9939	0.8985
T1 36V	100%	0.9997	0.9989	0.9985	0.9986	0.9989	0.9989	0.9989	0.9989	0.9987	0.9980	0.9949	0.9820	0.9008
T2 24V	100%	0.9999	1.0000	0.9999	0.9997	0.9998	0.9998	0.9999	0.9998	0.9997	0.9995	0.9984	0.9937	0.9385
T3 24V	100%	0.9986	0.9997	0.9999	0.9999	1.0000	0.9999	0.9999	0.9999	0.9998	0.9992	0.9981	0.9941	0.9454
630VA														
T4 5V	2.27%	0.9998	0.9998	0.9997	0.9998	0.9997	0.9997	0.9997	0.9997	0.9997	0.9997	0.9997	0.9998	0.9449
T4 12V	5.4%	0.9998	1.0000	0.9999	0.9999	0.9998	0.9999	0.9999	1.0000	0.9999	1.0000	1.0000	0.9999	0.8950
T4 22V	10%	0.9998	1.0000	1.0000	0.9999	1.0000	1.0000	1.0000	1.0000	1.0000	1.0000	0.9998	0.9992	0.8296
T4 42V	19.1%	0.9998	1.0000	1.0000	0.9997	0.9999	0.9999	0.9999	0.9999	0.9998	0.9996	0.9987	0.9953	0.7701
T4 110V	50%	0.9997	0.9993	0.9992	0.9984	0.9988	0.9985	0.9980	0.9973	0.9960	0.9933	0.9856	0.9659	0.7181
T4 220V	100%	0.9989	0.9951	0.9946	0.9936	0.9925	0.9911	0.9891	0.9862	0.9819	0.9726	0.9501	0.9030	0.6842
T5 230V	100%	0.9995	0.9967	0.9962	0.9957	0.9947	0.9936	0.9920	0.9895	0.9856	0.9778	0.9562	0.9079	0.6788
T6 220V	100%	0.9989	0.9954	0.9950	0.9943	0.9932	0.9917	0.9897	0.9869	0.9824	0.9735	0.9509	0.9019	0.6649
750kVA														
T7 53V	13.25%	1.0000	1.0000	0.9999	0.9998	0.9999	0.9999	0.9999	0.9998	0.9998	0.9996	0.9990	0.9967	0.8161
T7 200V	50%	0.9994	0.9983	0.9981	0.9976	0.9973	0.9967	0.9959	0.9947	0.9928	0.9893	0.9804	0.9611	0.7005
T7 400V	100%	0.9976	0.9912	0.9903	0.9890	0.9876	0.9858	0.9834	0.9800	0.9748	0.9659	0.9437	0.8947	0.6480
T7 115V	50%	0.9994	0.9996	0.9995	0.9992	0.9992	0.9990	0.9987	0.9982	0.9972	0.9953	0.9893	0.9739	0.7169
T7 230V	100%	0.9990	0.9965	0.9960	0.9952	0.9944	0.9933	0.9917	0.9893	0.9855	0.9783	0.9599	0.9186	0.7051
1kVA														
T8 5V	2.27%	0.9997	0.9997	0.9997	0.9998	0.9998	0.9997	0.9997	0.9997	0.9997	0.9997	0.9997	0.9997	0.9433
T8 12V	5.45%	0.9997	1.0000	0.9999	0.9999	0.9999	0.9999	0.9999	0.9999	0.9999	0.9999	0.9999	0.9999	0.8978
T8 24V	10.9%	0.9997	1.0000	1.0000	1.0000	1.0000	1.0000	1.0000	1.0000	1.0000	1.0000	0.9999	0.9996	0.8472
T8 36V	16.36%	0.9997	1.0000	1.0000	0.9999	0.9999	0.9999	0.9999	0.9999	0.9999	0.9997	0.9992	0.9966	0.7446
T8 110V	50%	0.9997	0.9996	0.9995	0.9994	0.9992	0.9990	0.9987	0.9982	0.9972	0.9952	0.9888	0.9716	0.7103
T8 220V	100%	0.9993	0.9964	0.9959	0.9951	0.9942	0.9930	0.9913	0.9889	0.9847	0.9769	0.9566	0.9143	0.7003
3 phase														
350VA														
T9 230V	57.5%	0.9993	0.9987	0.9984	0.9981	0.9975	0.9973	0.9967	0.9957	0.9940	0.9906	0.9818	0.9610	0.7048
T9 400V	100%	0.9980	0.9925	0.9914	0.9906	0.9885	0.9873	0.9851	0.9816	0.9762	0.9660	0.9409	0.8860	0.6531

T9 230V	57.5%	0.9994	0.9982	0.9978	0.9975	0.9966	0.9964	0.9955	0.9943	0.9922	0.9882	0.9782	0.9547	0.7276
T9 400V	100%	0.9976	0.9908	0.9897	0.9891	0.9864	0.9851	0.9826	0.9790	0.9733	0.9623	0.9340	0.8740	0.6224
T9 230V	57.5%	0.9986	0.9984	0.9979	0.9973	0.9970	0.9966	0.9959	0.9948	0.9929	0.9894	0.9805	0.9585	0.7313
T9 400V	100%	0.9971	0.9917	0.9910	0.9899	0.9886	0.9866	0.9842	0.9807	0.9755	0.9649	0.9382	0.8796	0.6217
1.2kVA														
T10 24V	57.1%	0.9993	0.9998	0.9998	0.9996	0.9997	0.9999	0.9999	0.9999	0.9999	0.9999	0.9999	0.9995	0.9650
T10 42V	100%	0.9993	0.9997	0.9996	0.9997	0.9998	0.9998	0.9998	0.9998	0.9998	0.9997	0.9993	0.9971	0.9655
5kVA														
T11	100%	0.9997	0.9997	0.9998	0.9997	0.9998	0.9997	0.9999	0.9997	0.9998	0.9997	0.9997	0.9996	0.9926
20kVA														
T12	100%	0.9998	0.9996	0.9995	0.9994	0.9992	0.9990	0.9985	0.9980	0.9969	0.9942	0.9854	0.9602	0.8029
40kVA														
T13	100%	1.0000	0.9998	0.9997	0.9997	0.9996	0.9994	0.9992	0.9987	0.9977	0.9956	0.9869	0.9616	0.8518

Table 3.2. The SD results for all transformers

SD	Wind.%	15kΩ	5kΩ	4.5kΩ	4kΩ	3.5kΩ	3kΩ	2.5kΩ	2kΩ	1.5kΩ	1kΩ	500 Ω	200Ω	1Ω
400VA														
T1 5V	13.89%	1.9155	1.0909	1.2691	1.3889	1.2881	1.2656	1.2555	1.2389	1.2299	1.2231	1.2013	1.1510	7.3829
T1 12V	33.33%	1.5758	0.4347	0.4793	0.7436	0.5391	0.5172	0.5368	0.5693	0.5319	0.5522	0.5710	0.8413	7.9023
T1 24V	66.67%	1.7833	0.2358	0.2296	0.2329	0.2280	0.2688	0.3117	0.3658	0.4546	0.6295	1.1410	2.3066	8.0404
T1 36V	100%	1.8683	0.8045	0.9343	0.9120	0.8123	0.8457	0.8411	0.8725	0.9869	1.2890	2.1480	3.9604	8.1097
T2 24V	100%	1.0823	0.1486	0.2086	0.4132	0.3278	0.2893	0.2919	0.3269	0.4029	0.5467	0.9656	1.8679	5.5971
T3 24V	100%	0.9851	0.4013	0.2717	0.2805	0.1922	0.2057	0.2505	0.2996	0.3884	0.6904	1.0527	1.9316	5.7617
630VA														
T4 5V	2.27%	1.5073	0.7353	0.8873	1.1266	1.0060	0.9403	0.9158	0.9182	0.9048	0.8908	0.8558	0.8155	13.4734
T4 12V	5.4%	0.9671	0.3009	0.4230	0.5836	0.6496	0.4962	0.4501	0.3779	0.4509	0.3938	0.3836	0.6671	17.6099
T4 22V	10%	0.6896	0.1531	0.1366	0.3957	0.1683	0.1744	0.1850	0.2282	0.2991	0.4425	0.8402	1.8462	21.5171
T4 42V	19.1%	0.8053	0.3275	0.3729	0.9581	0.5517	0.5625	0.6409	0.7823	0.9997	1.4217	2.4926	4.7789	24.3227
T4 110V	50%	1.1296	1.8060	1.9885	2.4665	2.4545	2.7461	3.1473	3.6806	4.5252	5.8298	8.6453	12.9662	26.5184
T4 220V	100%	2.3753	5.0946	5.4639	5.8977	6.3711	6.9895	7.7259	8.6937	10.0027	12.1303	15.7323	20.2274	27.9812
T5 230V	100%	1.5439	3.7722	4.0824	4.4456	4.8607	5.3891	6.0282	6.8715	8.0927	9.9603	13.3872	17.7117	25.4741
T6 220V	100%	2.7133	5.5370	5.9250	6.3823	6.8924	7.5535	8.4145	9.4550	10.9157	13.0983	16.8719	21.4771	29.4361
750kVA														
T7 53V	13.25%	1.2284	0.3756	0.4701	0.7068	0.6220	0.6554	0.6875	0.7636	0.9066	1.2005	2.0247	3.8615	23.6702
T7 200V	50%	1.4821	2.6520	2.8759	3.1717	3.4525	3.8331	4.3066	4.9697	5.8976	7.3439	10.3054	14.6924	28.0370
T7 400V	100%	3.3147	6.5141	6.9078	7.3847	7.9138	8.5458	9.3296	10.3398	11.7478	13.7327	17.3651	21.8443	29.6568

T7 115V	50%	1.2613	1.0876	1.2149	1.4007	1.5155	1.6876	1.9395	2.2892	2.8397	3.7443	5.7848	9.1918	22.0984
T7 230V	100%	1.7778	3.2189	3.4703	3.7817	4.1122	4.5449	5.0851	5.8148	6.8071	8.4061	11.3634	15.3106	22.7032
1kVA														
T8 5V	2.27%	1.6915	0.8001	0.9311	1.1314	1.0566	1.0270	0.9972	0.9969	0.9751	1.0096	0.9144	0.8958	12.1836
T8 12V	5.45%	0.8505	0.2705	0.3190	0.3866	0.3533	0.3341	0.3278	0.3217	0.3219	0.3262	0.3487	0.4691	15.3249
T8 24V	10.9%	0.8041	0.1589	0.2105	0.2621	0.2242	0.2067	0.2077	0.2158	0.2558	0.3167	0.5532	1.2126	18.2617
T8 36V	16.36%	0.8223	0.2705	0.3289	0.3905	0.3872	0.4085	0.4548	0.5337	0.6720	0.9466	1.7182	3.6340	22.5608
T8 110V	50%	0.9392	1.2121	1.3353	1.4864	1.6541	1.8647	2.1586	2.5938	3.2208	4.2863	6.6567	10.5490	23.8395
T8 220V	100%	1.7207	3.6678	3.9533	4.3025	4.7056	5.2044	5.8340	6.6358	7.8225	9.5934	12.9520	17.2109	24.6815
3 phase														
350VA														
T9 230V	57.5%	1.3588	2.0661	2.2899	2.5262	2.8270	3.0376	3.4139	3.9480	4.7573	6.0289	8.6177	12.5667	25.3161
T9 400V	100%	2.6345	5.3258	5.7085	6.1028	6.6009	7.1175	7.7878	8.6939	9.9266	11.7935	15.0269	19.1271	26.5609
T9 230V	57.5%	1.6583	3.3274	3.6302	3.9560	4.4189	4.7753	5.3703	6.1249	7.2640	9.0559	12.3979	17.1420	29.8035
T9 400V	100%	4.0382	8.0685	8.5223	9.0781	9.7669	10.4703	11.4089	12.5345	14.0434	16.3493	20.3257	25.0254	33.0743
T9 230V	57.5%	2.4682	3.2512	3.8008	4.2478	4.5161	4.8808	5.4448	6.2144	7.3297	9.0691	12.3490	17.1627	29.6813
T9 400V	100%	4.4731	8.0612	8.5321	9.1646	9.7741	10.4900	11.3559	12.5368	14.1339	16.3897	20.3054	25.0108	32.9953
1.2kVA														
T10 24V	57.1%	0.6415	0.2872	0.3602	0.4427	0.4029	0.2827	0.2552	0.2379	0.2259	0.2275	0.2926	0.5453	4.1345
T10 42V	100%	0.6850	0.3784	0.4741	0.4539	0.3697	0.3571	0.3516	0.3689	0.3872	0.4755	0.6798	1.2844	4.1964
5kVA														
T11	100%	1.0015	0.4527	0.5743	0.6792	0.6299	0.5799	0.6146	0.5222	0.4724	0.4434	0.4445	0.5237	1.7993
20kVA														
T12	100%	0.4422	0.5629	0.7873	0.8604	0.9538	1.0757	1.2210	1.5135	1.7866	2.2320	3.0274	4.7851	7.6503
40kVA														
T13	100%	0.1256	0.4326	0.4811	0.5329	0.6054	0.7047	0.8354	1.0373	1.3644	1.8979	3.2081	5.4009	10.5056

Table 3.3. The SSE results for all transformers

SSE	Wind.%	15k Ω	5k Ω	4.5k Ω	4k Ω	3.5k Ω	3k Ω	2.5k Ω	2k Ω	1.5k Ω	1k Ω	500 Ω	200 Ω	1 Ω
400VA														
T1 5V	13.89%	3.6654	1.1887	1.6090	1.9271	1.6574	1.6002	1.5748	1.5334	1.5110	1.4946	1.4417	1.3234	54.4520
T1 12V	33.33%	2.4806	0.1888	0.2295	0.5524	0.2903	0.2672	0.2878	0.3238	0.2826	0.3046	0.3257	0.7070	62.3822
T1 24V	66.67%	3.1767	0.0556	0.0527	0.0542	0.0519	0.0722	0.0970	0.1337	0.2064	0.3958	1.3006	5.3148	64.5812
T1 36V	100%	3.4868	0.6466	0.8721	0.8309	0.6591	0.7145	0.7066	0.7605	0.9729	1.6597	4.6094	15.6687	65.6998
T2 24V	100%	1.1702	0.0221	0.0434	0.1705	0.1073	0.0836	0.0851	0.1068	0.1622	0.2985	0.9315	3.4856	31.2951
T3 24V	100%	0.9693	0.1609	0.0738	0.0786	0.0369	0.0423	0.0627	0.0896	0.1507	0.4761	1.1070	3.7271	33.1633

630VA														
T4 5V	2.27%	2.270	0.540	0.787	1.268	1.011	0.883	0.838	0.842	0.818	0.793	0.732	0.664	181.346
T4 12V	5.4%	0.934	0.090	0.179	0.340	0.422	0.246	0.202	0.143	0.203	0.155	0.147	0.445	309.791
T4 22V	10%	0.475	0.023	0.019	0.157	0.028	0.030	0.034	0.052	0.089	0.196	0.705	3.405	462.512
T4 42V	19.1%	0.648	0.107	0.139	0.917	0.304	0.316	0.410	0.611	0.998	2.019	6.207	22.814	590.987
T4 110V	50%	1.275	3.258	3.950	6.077	6.019	7.533	9.895	13.533	20.457	33.952	74.665	167.950	702.502
T4 220V	100%	5.636	25.928	29.824	34.747	40.550	48.803	59.629	75.502	99.951	146.995	247.252	408.727	782.144
T5 230V	100%	2.381	14.215	16.649	19.743	23.602	29.013	36.301	47.169	65.425	99.106	179.033	313.382	648.263
T6 220V	100%	7.354	30.627	35.070	40.692	47.456	56.997	70.731	89.305	119.029	171.390	284.370	460.791	865.598
750kVA														
T7 53V	13.25%	1.5073	0.1409	0.2208	0.4991	0.3865	0.4292	0.4722	0.5824	0.8211	1.4398	4.0951	14.8961	559.7025
T7 200V	50%	2.1943	7.0257	8.2622	10.0496	11.9072	14.6774	18.5277	24.6721	34.7454	53.8769	106.0923	215.6455	785.2688
T7 400V	100%	10.976	42.390	47.669	54.479	62.565	72.957	86.952	106.802	137.868	188.395	301.236	476.684	878.625
T7 115V	50%	1.589	1.182	1.475	1.960	2.294	2.845	3.758	5.235	8.056	14.006	33.430	84.403	487.838
T7 230V	100%	3.157	10.351	12.031	14.287	16.893	20.635	25.832	33.778	46.290	70.590	128.995	234.173	514.905
1kVA														
T8 5V	2.27%	2.8581	0.6395	0.8661	1.2788	1.1153	1.0536	0.9933	0.9928	0.9499	1.0183	0.8352	0.8017	148.2868
T8 12V	5.45%	0.7227	0.0731	0.1017	0.1493	0.1247	0.1115	0.1073	0.1034	0.1035	0.1063	0.1215	0.2198	234.6104
T8 24V	10.9%	0.6460	0.0252	0.0443	0.0686	0.0502	0.0427	0.0431	0.0465	0.0654	0.1002	0.3057	1.4690	333.1492
T8 36V	16.36%	0.6755	0.0731	0.1081	0.1524	0.1498	0.1667	0.2067	0.2845	0.4511	0.8951	2.9491	13.1923	508.4678
T8 110V	50%	0.8813	1.4678	1.7812	2.2072	2.7333	3.4736	4.6549	6.7210	10.3632	18.3531	44.2657	111.1672	567.7382
T8 220V	100%	2.9578	13.4389	15.6128	18.4925	22.1199	27.0582	34.0006	43.9883	61.1280	91.9388	167.5825	295.9126	608.5494
3 phase														
350VA														
T9 230V	57.5%	1.8443	4.2643	5.2384	6.3751	7.9837	9.2173	11.6431	15.5707	22.6089	36.3103	74.1889	157.7593	640.2470
T9 400V	100%	6.9333	28.335	32.554	37.207	43.527	50.608	60.587	75.506	98.437	138.94	225.58	365.47	704.76
T9 230V	57.5%	2.7472	11.060	13.165	15.634	19.507	22.780	28.810	37.476	52.712	81.93	153.55	293.55	887.34
T9 400V	100%	16.2902	65.035	72.556	82.328	95.294	109.514	130.030	156.953	197.016	267.02	412.71	625.63	1092.80
T9 230V	57.5%	6.0858	10.559	14.431	18.025	20.374	23.798	29.615	38.580	53.670	82.16	152.34	294.26	880.07
T9 400V	100%	19.9884	64.917	72.722	83.903	95.434	109.927	128.824	157.011	199.563	268.35	411.89	624.90	1087.60
1.2kVA														
T10 24V	57.1%	0.4111	0.0824	0.1296	0.1958	0.1622	0.0799	0.0651	0.0565	0.0510	0.0517	0.0855	0.2971	17.076
T10 42V	100%	0.4687	0.1431	0.2245	0.2059	0.1365	0.1274	0.1235	0.1359	0.1498	0.2259	0.4617	1.6481	17.592
5kVA														
T11	100%	1.0020	0.2047	0.3295	0.4609	0.3964	0.3359	0.3773	0.2724	0.2229	0.1964	0.1974	0.2740	3.234
20kVA														
T12	100%	0.1953	0.6191	0.7395	0.9089	1.1559	1.4893	2.2883	3.1886	4.9768	9.1559	22.8740	58.4675	207.7306

T9 230V	57.5%	0.1020	0.1730	0.1984	0.2264	0.2539	0.2812	0.3248	0.3973	0.5153	0.7266	1.2536	2.3194	9.474
T9 400V	100%	0.2555	0.6158	0.6856	0.7579	0.8443	0.9473	1.0831	1.2824	1.5826	2.0955	3.1752	4.9813	10.930
T9 230V	57.5%	0.1749	0.3605	0.4043	0.4495	0.5027	0.5588	0.6493	0.7656	0.9569	1.2892	2.0253	3.3092	9.341
T9 400V	100%	0.4857	1.1279	1.2197	1.3430	1.4834	1.6419	1.8594	2.1377	2.5410	3.2297	4.6400	6.7619	13.145
T9 230V	57.5%	0.2377	0.3651	0.4547	0.5148	0.5504	0.6031	0.6884	0.8120	1.0030	1.3324	2.0556	3.3635	9.294
T9 400V	100%	0.5495	1.1520	1.2560	1.3933	1.5229	1.6734	1.8713	2.1649	2.6033	3.2713	4.6552	6.7727	13.061
1.2kVA														
T10 24V	57.1%	0.0631	0.0365	0.0419	0.0490	0.0488	0.0391	0.0386	0.0408	0.0444	0.0552	0.0913	0.1928	2.708
T10 42V	100%	0.0710	0.0542	0.0629	0.0646	0.0637	0.0659	0.0715	0.0822	0.0976	0.1353	0.2276	0.4769	2.777
5kVA														
T11	100%	0.0907	0.0467	0.0569	0.0619	0.0613	0.0572	0.0620	0.0564	0.0584	0.0654	0.0939	0.1694	1.256
20kVA														
T12	100%	0.0858	0.1642	0.1826	0.1999	0.2318	0.2705	0.4075	0.4784	0.6125	0.8685	1.5419	2.9579	9.172
40kVA														
T13	100%	0.0307	0.1010	0.1148	0.1279	0.1432	0.1663	0.1994	0.2509	0.3352	0.4798	0.8784	1.7367	6.386

Table 3.5. The DABS results for all transformers

DABS	Wind.%	15kΩ	5kΩ	4.5kΩ	4kΩ	3.5kΩ	3kΩ	2.5kΩ	2kΩ	1.5kΩ	1kΩ	500 Ω	200Ω	1Ω
400VA														
T1 5V	13.89%	0.6280	0.2293	0.2502	0.2619	0.2441	0.2390	0.2369	0.2345	0.2345	0.2377	0.2470	0.2759	4.8870
T1 12V	33.33%	0.5736	0.1161	0.1251	0.1703	0.1393	0.1388	0.1470	0.1602	0.1643	0.1905	0.2565	0.4501	5.3124
T1 24V	66.67%	0.6051	0.1037	0.1063	0.1089	0.1140	0.1332	0.1544	0.1825	0.2295	0.3190	0.5908	1.2599	5.4784
T1 36V	100%	0.6349	0.2986	0.3319	0.3302	0.3282	0.3599	0.3920	0.4408	0.5260	0.7047	1.1902	2.3275	5.5998
T2 24V	100%	0.4476	0.0928	0.1141	0.1569	0.1551	0.1593	0.1749	0.2042	0.2567	0.3522	0.6220	1.2245	4.3398
T3 24V	100%	0.2294	0.1429	0.1294	0.1448	0.1257	0.1386	0.1677	0.1982	0.2528	0.4067	0.6739	1.2854	4.3946
630VA														
T4 5V	2.27%	0.4150	0.2234	0.2577	0.3000	0.2740	0.2588	0.2535	0.2539	0.2536	0.2530	0.2590	0.2794	9.8658
T4 12V	5.4%	0.2459	0.1065	0.1362	0.1620	0.1807	0.1454	0.1388	0.1285	0.1554	0.1614	0.2104	0.3917	13.2379
T4 22V	10%	0.1767	0.0820	0.0834	0.1325	0.0920	0.0990	0.1069	0.1263	0.1647	0.2378	0.4564	1.0357	16.8557
T4 42V	19.1%	0.2383	0.1964	0.2269	0.3129	0.3122	0.3234	0.3644	0.4422	0.5651	0.7962	1.4389	2.9666	19.4608
T4 110V	50%	0.5493	1.0447	1.1725	1.3676	1.4658	1.6473	1.9112	2.2649	2.8690	3.8281	6.1194	9.9553	22.4322
T4 220V	100%	1.4501	3.2995	3.5913	3.9527	4.2965	4.8159	5.4149	6.2536	7.4337	9.3707	12.7978	17.1467	24.3385
T5 230V	100%	0.9783	2.4586	2.6864	2.9380	3.2674	3.6768	4.1917	4.8905	5.9207	7.5661	10.7425	14.8505	21.9115
T6 220V	100%	1.8889	3.9243	4.2743	4.6735	5.0692	5.5937	6.3161	7.2081	8.5088	10.4854	14.0649	18.4375	25.5776
750kVA														
T7 53V	13.25%	0.3851	0.1471	0.1721	0.2183	0.2177	0.2376	0.2614	0.3030	0.3759	0.5161	0.9218	1.9644	17.9490

T7 200V	50%	0.6915	1.2846	1.4139	1.5890	1.7540	1.9808	2.2787	2.7110	3.3516	4.4126	6.7933	10.6565	22.5893
T7 400V	100%	1.8046	3.7217	4.0249	4.4047	4.7966	5.2812	5.9069	6.7406	7.9492	9.7282	13.1885	17.5729	25.0576
T7 115V	50%	0.5284	0.4955	0.5610	0.6465	0.7094	0.7958	0.9292	1.1177	1.4311	1.9864	3.3885	6.1082	18.1382
T7 230V	100%	0.9421	1.6564	1.8238	2.0369	2.2439	2.5270	2.8989	3.4242	4.1798	5.4771	8.0828	11.8344	19.0058
1kVA														
T8 5V	2.27%	0.7294	0.1584	0.1781	0.2048	0.1931	0.1882	0.1836	0.1838	0.1813	0.1894	0.1846	0.2037	9.0657
T8 12V	5.45%	0.5344	0.0884	0.1000	0.1150	0.1101	0.1053	0.1067	0.1085	0.1131	0.1269	0.1633	0.2684	11.4946
T8 24V	10.9%	0.5138	0.0679	0.0816	0.0951	0.0902	0.0902	0.0967	0.1082	0.1337	0.1757	0.3132	0.6858	14.1035
T8 36V	16.36%	0.5248	0.1507	0.1752	0.1987	0.2075	0.2256	0.2550	0.3024	0.3828	0.5411	0.9946	2.2280	18.5204
T8 110V	50%	0.6770	0.6996	0.7740	0.8651	0.9603	1.0829	1.2631	1.5383	1.9491	2.6894	4.4845	7.7862	20.3332
T8 220V	100%	1.2378	2.2523	2.4551	2.7095	2.9934	3.3565	3.8312	4.4591	5.4262	6.9533	10.0429	14.1643	21.3515
3 phase														
350VA														
T9 230V	57.5%	0.5142	0.9001	1.0310	1.1679	1.3067	1.4251	1.6222	1.9456	2.4494	3.3007	5.2048	8.4217	19.710
T9 400V	100%	1.2789	2.8609	3.1579	3.4435	3.7869	4.1545	4.6369	5.3221	6.3008	7.8334	10.6070	14.2458	20.720
T9 230V	57.5%	0.9285	1.9736	2.2021	2.4290	2.7077	2.9720	3.4061	3.9433	4.7976	6.1959	8.9911	13.1024	23.635
T9 400V	100%	2.5588	5.5091	5.9013	6.4045	6.9828	7.5786	8.3811	9.3689	10.7237	12.8528	16.6136	21.0461	28.167
T9 230V	57.5%	1.1625	1.9673	2.3871	2.6682	2.8620	3.1293	3.5440	4.1200	4.9738	6.3603	9.1070	13.2996	23.572
T9 400V	100%	2.8308	5.5933	6.0274	6.5861	7.0978	7.6766	8.4112	9.4561	10.9335	12.9776	16.6586	21.0940	28.071
1.2kVA														
T10 24V	57.1%	0.1968	0.1026	0.1204	0.1434	0.1373	0.1024	0.0955	0.0943	0.0965	0.1093	0.1606	0.3024	2.692
T10 42V	100%	0.2176	0.1399	0.1623	0.1673	0.1540	0.1501	0.1548	0.1693	0.1884	0.2459	0.3626	0.6935	2.779
5kVA														
T11	100%	0.2883	0.1404	0.1744	0.1933	0.1846	0.1663	0.1773	0.1530	0.1447	0.1478	0.1783	0.2583	1.063
20kVA														
T12	100%	0.2545	0.4616	0.5112	0.5581	0.6396	0.7377	1.0571	1.2380	1.5567	2.1448	3.5520	6.0422	12.401
40kVA														
T13	100%	0.0743	0.2439	0.2743	0.3046	0.3420	0.3958	0.4700	0.5865	0.7745	1.0877	1.8997	3.4207	8.130

Table 3.6. The RMSE results for all transformers

RMSE	Wind. %	15k Ω	5k Ω	4.5k Ω	4k Ω	3.5k Ω	3k Ω	2.5k Ω	2k Ω	1.5k Ω	1k Ω	500 Ω	200 Ω	1 Ω
400VA														
T1 5V	13.89%	0.1282	0.0730	0.0850	0.0930	0.0862	0.0847	0.0840	0.0829	0.0823	0.0819	0.0804	0.0770	0.4942
T1 12V	33.33%	0.1051	0.0290	0.0320	0.0496	0.0359	0.0345	0.0358	0.0380	0.0355	0.0368	0.0381	0.0561	0.5269
T1 24V	66.67%	0.1191	0.0157	0.0153	0.0156	0.0152	0.0179	0.0208	0.0244	0.0304	0.0420	0.0762	0.1540	0.5370
T1 36V	100%	0.1245	0.0536	0.0623	0.0608	0.0541	0.0564	0.0560	0.0581	0.0658	0.0859	0.1431	0.2639	0.5404

T2 24V	100%	0.0815	0.0112	0.0157	0.0311	0.0247	0.0218	0.0220	0.0246	0.0303	0.0412	0.0727	0.1407	0.4215
T3 24V	100%	0.0675	0.0275	0.0186	0.0192	0.0132	0.0141	0.0172	0.0205	0.0266	0.0473	0.0721	0.1323	0.3947
630VA														
T4 5V	2.27%	0.0439	0.0214	0.0258	0.0328	0.0293	0.0274	0.0266	0.0267	0.0263	0.0259	0.0249	0.0237	0.3921
T4 12V	5.4%	0.0282	0.0088	0.0124	0.0170	0.0190	0.0145	0.0131	0.0110	0.0132	0.0115	0.0112	0.0195	0.5143
T4 22V	10%	0.0202	0.0045	0.0040	0.0116	0.0049	0.0051	0.0054	0.0067	0.0088	0.0129	0.0246	0.0540	0.6296
T4 42V	19.1%	0.0235	0.0096	0.0109	0.0280	0.0161	0.0164	0.0187	0.0228	0.0292	0.0415	0.0728	0.1396	0.7104
T4 110V	50%	0.0329	0.0527	0.0580	0.0719	0.0716	0.0801	0.0918	0.1073	0.1320	0.1700	0.2521	0.3781	0.7734
T4 220V	100%	0.0693	0.1487	0.1595	0.1722	0.1860	0.2040	0.2255	0.2538	0.2920	0.3541	0.4592	0.5905	0.8168
T5 230V	100%	0.0490	0.1198	0.1296	0.1412	0.1543	0.1711	0.1914	0.2182	0.2570	0.3163	0.4251	0.5624	0.8088
T6 220V	100%	0.0760	0.1550	0.1659	0.1787	0.1929	0.2114	0.2356	0.2647	0.3056	0.3667	0.4723	0.6012	0.8240
750kVA														
T7 53V	13.25%	0.0364	0.0111	0.0139	0.0210	0.0184	0.0194	0.0204	0.0226	0.0269	0.0356	0.0600	0.1145	0.7019
T7 200V	50%	0.0439	0.0786	0.0852	0.0940	0.1023	0.1136	0.1276	0.1473	0.1748	0.2177	0.3054	0.4355	0.8310
T7 400V	100%	0.0984	0.1933	0.2050	0.2192	0.2349	0.2536	0.2769	0.3069	0.3487	0.4076	0.5154	0.6483	0.8802
T7 115V	50%	0.0453	0.0390	0.0436	0.0503	0.0544	0.0606	0.0696	0.0822	0.1019	0.1344	0.2077	0.3300	0.7933
T7 230V	100%	0.0638	0.1156	0.1246	0.1358	0.1476	0.1632	0.1826	0.2088	0.2444	0.3018	0.4080	0.5497	0.8151
1kVA														
T8 5V	2.27%	0.0554	0.0262	0.0305	0.0371	0.0346	0.0337	0.0327	0.0327	0.0320	0.0331	0.0300	0.0294	0.3992
T8 12V	5.45%	0.0282	0.0090	0.0106	0.0128	0.0117	0.0111	0.0109	0.0107	0.0107	0.0108	0.0116	0.0156	0.5082
T8 24V	10.9%	0.0267	0.0053	0.0070	0.0087	0.0074	0.0069	0.0069	0.0072	0.0085	0.0105	0.0183	0.0402	0.6057
T8 36V	16.36%	0.0273	0.0090	0.0109	0.0130	0.0128	0.0136	0.0151	0.0177	0.0223	0.0314	0.0570	0.1206	0.7485
T8 110V	50%	0.0312	0.0402	0.0443	0.0493	0.0549	0.0619	0.0716	0.0860	0.1068	0.1422	0.2208	0.3499	0.7908
T8 220V	100%	0.0571	0.1218	0.1313	0.1429	0.1563	0.1728	0.1938	0.2204	0.2598	0.3186	0.4302	0.5716	0.8197
3 phase														
350VA														
T9 230V	57.5%	0.0438	0.0665	0.0737	0.0813	0.0910	0.0978	0.1099	0.1271	0.1532	0.1941	0.2775	0.4046	0.8152
T9 400V	100%	0.0847	0.1713	0.1836	0.1963	0.2123	0.2290	0.2505	0.2797	0.3193	0.3794	0.4834	0.6153	0.8549
T9 230V	57.5%	0.0434	0.0870	0.0949	0.1035	0.1156	0.1249	0.1405	0.1602	0.1900	0.2368	0.3243	0.4483	0.7807
T9 400V	100%	0.1055	0.2109	0.2227	0.2372	0.2552	0.2736	0.2982	0.3276	0.3670	0.4273	0.5312	0.6540	0.8645
T9 230V	57.5%	0.0645	0.0849	0.0993	0.1110	0.1180	0.1275	0.1422	0.1623	0.1915	0.2369	0.3226	0.4483	0.7753
T9 400V	100%	0.1169	0.2107	0.2230	0.2396	0.2555	0.2742	0.2968	0.3277	0.3695	0.4284	0.5308	0.6538	0.8625
1.2kVA														
T10 24V	57.1%	0.0486	0.0218	0.0273	0.0335	0.0305	0.0214	0.0193	0.0180	0.0171	0.0172	0.0222	0.0413	0.3133
T10 42V	100%	0.0519	0.0287	0.0359	0.0344	0.0280	0.0271	0.0266	0.0280	0.0293	0.0360	0.0515	0.0973	0.3180
5kVA														
T11	100%	0.0865	0.0391	0.0496	0.0586	0.0544	0.0501	0.0531	0.0451	0.0408	0.0383	0.0384	0.0452	0.1553

20kVA														
T12	100%	0.0217	0.0386	0.0422	0.0468	0.0528	0.0599	0.0743	0.0877	0.1095	0.1486	0.2348	0.3755	0.708
40kVA														
T13	100%	0.0080	0.0276	0.0307	0.0340	0.0386	0.0450	0.0533	0.0662	0.0871	0.1211	0.2048	0.3447	0.6706

Table 3.7. The ED results for all transformers

ED	Wind.%	15kΩ	5kΩ	4.5kΩ	4kΩ	3.5kΩ	3kΩ	2.5kΩ	2kΩ	1.5kΩ	1kΩ	500 Ω	200Ω	1Ω
400VA														
T1 5V	13.89%	59.781	34.044	39.608	43.347	40.199	39.499	39.184	38.666	38.383	38.173	37.492	35.921	230.414
T1 12V	33.33%	49.179	13.567	14.957	23.207	16.824	16.140	16.753	17.769	16.600	17.234	17.819	26.255	246.622
T1 24V	66.67%	55.654	7.360	7.165	7.268	7.116	8.388	9.727	11.418	14.187	19.645	35.610	71.986	250.932
T1 36V	100%	58.307	25.109	29.159	28.463	25.350	26.395	26.248	27.231	30.799	40.227	67.038	123.600	253.095
T2 24V	100%	33.779	4.637	6.509	12.895	10.229	9.030	9.110	10.203	12.574	17.061	30.136	58.296	174.679
T3 24V	100%	30.743	12.524	8.480	8.754	5.997	6.421	7.817	9.349	12.123	21.546	32.853	60.282	179.817
630VA														
T4 5V	2.27%	47.042	22.949	27.692	35.159	31.397	29.346	28.580	28.656	28.237	27.801	26.708	25.451	420.490
T4 12V	5.4%	30.183	9.390	13.201	18.213	20.272	15.487	14.047	11.793	14.073	12.292	11.970	20.820	549.587
T4 22V	10%	21.521	4.779	4.263	12.351	5.252	5.443	5.775	7.120	9.334	13.810	26.222	57.619	671.527
T4 42V	19.1%	25.131	10.220	11.637	29.902	17.217	17.554	20.003	24.415	31.199	44.369	77.792	149.144	759.086
T4 110V	50%	35.252	56.363	62.061	76.977	76.603	85.701	98.225	114.869	141.228	181.942	269.812	404.662	827.611
T4 220V	100%	74.130	158.997	170.523	184.060	198.836	218.136	241.119	271.321	312.173	378.576	490.990	631.275	873.264
T5 230V	100%	48.185	117.727	127.409	138.743	151.697	168.189	188.133	214.451	252.566	310.851	417.801	552.763	795.020
T6 220V	100%	84.679	172.805	184.914	199.186	215.104	235.737	262.608	295.080	340.667	408.785	526.556	670.277	918.672
750kVA														
T7 53V	13.25%	38.336	11.723	14.673	22.059	19.413	20.456	21.457	23.830	28.295	37.467	63.188	120.514	738.722
T7 200V	50%	46.254	82.765	89.753	98.987	107.748	119.626	134.404	155.098	184.057	229.194	321.621	458.535	875.007
T7 400V	100%	103.450	203.299	215.586	230.470	246.983	266.707	291.167	322.695	366.636	428.585	541.946	681.738	925.559
T7 115V	50%	39.364	33.943	37.917	43.714	47.296	52.667	60.530	71.442	88.624	116.857	180.539	286.868	689.668
T7 230V	100%	55.484	100.459	108.306	118.023	128.336	141.843	158.702	181.475	212.444	262.346	354.641	477.827	708.542
1kVA														
T8 5V	2.27%	52.7891	24.9702	29.0594	35.3110	32.9758	32.0507	31.1202	31.1126	30.4330	31.5090	28.5363	27.9585	380.2363
T8 12V	5.45%	26.5440	8.4422	9.9553	12.0666	11.0275	10.4265	10.2289	10.0407	10.0447	10.1801	10.8831	14.6396	478.2731
T8 24V	10.9%	25.096	4.959	6.571	8.179	6.998	6.451	6.481	6.736	7.983	9.885	17.263	37.845	569.930
T8 36V	16.36%	25.663	8.441	10.265	12.188	12.084	12.749	14.195	16.655	20.972	29.541	53.622	113.413	704.100
T8 110V	50%	29.313	37.829	41.674	46.390	51.623	58.196	67.369	80.951	100.519	133.770	207.748	329.223	744.006
T8 220V	100%	123.3945	122.922	131.318	141.783	153.747	168.736	187.533	212.028	248.340	302.890	406.938	540.111	774.7858

3 phase														
350VA														
T9 230V	57.5%	42.405	64.480	71.466	78.840	88.228	94.799	106.55	123.21	148.47	188.16	268.95	392.19	790.09
T9 400V	100%	82.219	166.21	178.16	190.46	206.01	222.13	243.05	271.33	309.80	368.06	468.97	596.94	828.94
T9 230V	57.5%	51.755	103.85	113.29	123.46	137.91	149.03	167.60	191.15	226.70	282.63	386.93	534.99	930.14
T9 400V	100%	126.03	251.81	265.97	283.32	304.81	326.77	356.06	391.19	438.28	510.24	634.34	781.02	1032.2
T9 230V	57.5%	77.030	101.47	118.62	132.57	140.94	152.33	169.93	193.95	228.75	283.04	385.40	535.63	926.32
T9 400V	100%	139.60	251.58	266.28	286.02	305.04	327.38	354.41	391.26	441.11	511.51	633.71	780.56	1029.7
1.2kVA														
T10 24V	57.1%	20.020	8.9636	11.241	13.815	12.575	8.8236	7.9657	7.4232	7.0515	7.0996	9.1307	17.019	129.03
T10 42V	100%	21.378	11.811	14.796	14.167	11.537	11.146	10.972	11.513	12.086	14.840	21.216	40.086	130.97
5kVA														
T11	100%	31.257	14.129	17.925	21.198	19.659	18.097	19.180	16.297	14.743	13.838	13.872	16.345	56.155
20kVA														
T12	100%	13.799	24.570	26.853	29.769	33.572	38.107	47.235	55.758	69.659	94.483	149.34	238.76	450.04
40kVA														
T13	100%	3.9209	13.500	15.016	16.630	18.894	21.991	26.071	32.374	42.583	59.232	100.12	168.56	327.87

Table 3.8. The CD results for all transformers

CD	Wind.%	15kΩ	5kΩ	4.5kΩ	4kΩ	3.5kΩ	3kΩ	2.5kΩ	2kΩ	1.5kΩ	1kΩ	500 Ω	200Ω	1Ω
400VA														
T1 5V	13.89%	480.71	440.88	411.67	413.71	417.52	407.90	404.13	396.55	384.00	389.36	442.29	567.36	693.38
T1 12V	33.33%	467.66	411.61	424.34	432.71	412.82	432.67	430.97	474.21	517.21	609.32	704.34	633.11	711.75
T1 24V	66.67%	484.66	569.90	562.97	579.12	599.91	619.49	666.61	676.75	628.59	588.18	639.27	632.09	716.29
T1 36V	100%	571.88	720.07	720.81	680.70	663.05	620.83	615.16	630.02	628.96	613.83	580.50	617.54	686.31
T2 24V	100%	421.26	400.17	380.15	389.85	402.90	410.77	429.44	436.06	439.18	507.10	531.85	449.78	469.28
T3 24V	100%	482.96	493.52	420.55	452.48	494.49	424.16	429.82	367.75	354.34	576.04	572.51	535.25	588.45
630VA														
T4 5V	2.27%	761.22	572.50	584.94	595.81	644.27	614.02	582.30	577.34	590.39	596.30	665.53	951.73	1336.70
T4 12V	5.4%	667.47	476.74	494.47	506.16	545.77	522.07	539.48	587.44	701.13	943.92	1440.20	1469.40	1299.60
T4 22V	10%	594.56	754.70	751.22	849.25	918.43	997.15	1146.90	1294.70	1484.00	1550.70	1421.20	1445.90	1234.50
T4 42V	19.1%	895.90	1574.40	1581.40	1591.80	1578.30	1510.90	1449.90	1409.70	1369.90	1544.10	1441.10	1373.90	1247.30
T4 110V	50%	1602.80	1453.90	1563.30	1577.10	1474.10	1487.00	1521.30	1420.30	1510.70	1442.70	1407.50	1350.60	1176.20
T4 220V	100%	1635.70	1422.80	1521.20	1462.30	1398.40	1493.20	1389.60	1422.50	1389.40	1353.20	1289.70	1208.50	1165.50
T5 230V	100%	1374.10	1242.60	1262.70	1398.80	1318.80	1279.10	1359.20	1287.00	1252.50	1265.00	1179.40	1156.80	1092.40
T6 220V	100%	1506.00	1380.80	1404.20	1502.90	1639.20	1552.10	1349.40	1494.40	1394.70	1376.30	1288.90	1288.70	1189.60

750kVA														
T7 53V	13.25%	894.63	1553.50	1562.00	1542.00	1485.10	1414.30	1376.70	1518.00	1591.20	1565.60	1526.90	1464.80	1231.80
T7 200V	50%	1624.30	1550.60	1490.30	1515.20	1529.70	1488.40	1505.60	1477.50	1472.70	1449.00	1329.50	1354.30	1188.30
T7 400V	100%	1573.30	1426.90	1413.50	1437.60	1417.50	1389.40	1447.90	1321.80	1417.60	1238.10	1222.40	1244.30	1167.50
T7 115V	50%	1266.10	1204.00	1281.70	1297.00	1216.20	1216.80	1259.40	1169.60	1174.40	1182.10	1180.10	1127.40	987.74
T7 230V	100%	1357.70	1227.30	1217.70	1192.90	1209.20	1205.40	1171.00	1181.90	1118.30	1077.30	1059.80	1057.30	1011.20
1kVA														
T8 5V	2.27%	588.86	374.15	354.33	348.98	353.86	350.48	337.56	338.37	345.29	379.97	374.9	546.21	1300
T8 12V	5.45%	575.22	460.34	464.3	451.27	488.05	501.04	499.5	506.49	541.09	624.32	948.74	1450.2	1219.5
T8 24V	10.9%	543.58	513.79	539.45	569.66	635.43	690.86	762.95	887.84	1087.6	1340.7	1393.2	1419	1176.3
T8 36V	16.36%	619.90	1182.3	1239.8	1317.8	1399	1451.1	1473	1433.3	1357.6	1306	1232.2	1285.6	1135.2
T8 110V	50%	1460.8	1391.9	1444.9	1394	1256.3	1302.2	1407.3	1289.7	1365.5	1362.9	1273.6	1204.1	1089.1
T8 220V	100%	1392.8	1262.3	1262	1366.9	1278.9	1302.7	1292.9	1278.7	1249.2	1234.8	1176.5	1138.3	1053.1
3 phase														
350VA														
T9 230V	57.5%	1436.3	1420.6	1437.0	1380.9	1433.2	1402.5	1350.6	1354.3	1359.9	1306.6	1293.3	1205.2	1119.6
T9 400V	100%	1444.3	1386.0	1353.6	1321.2	1380.1	1359.3	1276.9	1350.4	1235.3	1308.0	1218.7	1081.5	1117.3
T9 230V	57.5%	1722.8	1730.1	1734.1	1659.2	1715.1	1685.1	1650.9	1678.2	1653.2	1558.6	1572.9	1436.8	1334.0
T9 400V	100%	1720.5	1629.1	1572.8	1564.8	1629.8	1588.1	1539.5	1568.1	1464.5	1480.5	1435.8	1340.6	1299.0
T9 230V	57.5%	1665.9	1738.0	1731.9	1676.2	1705.8	1700.9	1656.9	1725.4	1669.2	1575.4	1601.1	1446.8	1282.0
T9 400V	100%	1658.0	1600.3	1578.0	1594.6	1606.0	1574.9	1590.0	1571.3	1514.1	1482.8	1459.0	1343.6	1291.5
1.2kVA														
T10 24V	57.1%	452.76	437.53	384.64	427.17	420.63	490.97	427.86	411.31	409.77	409.25	496.73	441.33	533.22
T10 42V	100%	454.03	443.43	417.29	410.04	453.16	491.17	429.33	456.39	499.53	469.28	433.15	471.49	522.83
5kVA														
T11	100%	441.03	409.92	389.03	392.47	381.65	476.48	441.73	373.49	379.36	366.99	408.21	469.87	378.81
20kVA														
T12	100%	987.16	908.01	921.87	949.04	947.38	971.50	986.65	884.78	908.67	873.93	890.79	853.09	732.50
40kVA														
T13	100%	527.70	788.37	777.46	761.17	735.49	666.38	609.65	616.32	691.94	637.93	624.49	733.05	617.28

Table 3.9. The CSD results for all transformers

CSD	Wind.%	15kΩ	5kΩ	4.5kΩ	4kΩ	3.5kΩ	3kΩ	2.5kΩ	2kΩ	1.5kΩ	1kΩ	500 Ω	200Ω	1Ω
400VA														
T1 5V	13.89%	1.8973	1.0908	1.2691	1.3889	1.2880	1.2656	1.2555	1.2388	1.2297	1.2230	1.2009	1.1494	6.5474
T1 12V	33.33%	1.5640	0.4322	0.4764	0.7410	0.5352	0.5128	0.5319	0.5638	0.5244	0.5411	0.5449	0.7648	6.2932

T1 24V	66.67%	1.7719	0.2316	0.2220	0.2212	0.2136	0.2522	0.2914	0.3401	0.4191	0.5753	1.0334	2.0509	6.1523
T1 36V	100%	1.8604	0.7978	0.9254	0.8995	0.7950	0.8228	0.8073	0.8223	0.9111	1.1642	1.8937	3.3885	6.0690
T2 24V	100%	1.0522	0.1346	0.1955	0.4059	0.3139	0.2672	0.2615	0.2880	0.3516	0.4741	0.8296	1.5722	4.2368
T3 24V	100%	0.9604	0.4009	0.2673	0.2536	0.1674	0.1799	0.2264	0.2585	0.3379	0.6576	0.9603	1.6680	4.0972
630VA														
T4 5V	2.27%	1.4533	0.7108	0.8581	1.1004	0.9746	0.9110	0.8871	0.8891	0.8757	0.8625	0.8256	0.7760	10.113
T4 12V	5.4%	0.9358	0.2830	0.4020	0.5671	0.6252	0.4757	0.4296	0.3570	0.4250	0.3617	0.3247	0.5475	12.609
T4 22V	10%	0.6687	0.1481	0.1126	0.3821	0.1482	0.1475	0.1604	0.1963	0.2564	0.3860	0.7160	1.5743	14.745
T4 42V	19.1%	0.7765	0.2752	0.3057	0.9347	0.4646	0.4701	0.5377	0.6568	0.8385	1.1962	2.0739	3.8423	15.673
T4 110V	50%	1.0380	1.5058	1.6470	2.1480	2.0173	2.2480	2.5636	2.9796	3.6109	4.5708	6.4590	9.0404	15.810
T4 220V	100%	1.9448	3.9683	4.2042	4.5167	4.8507	5.2572	5.7482	6.3652	7.1449	8.3738	10.204	12.015	14.925
T5 230V	100%	1.2498	2.9955	3.2237	3.4547	3.7669	4.1340	4.5758	5.1448	5.9195	7.0502	8.9891	11.093	14.451
T6 220V	100%	1.9857	4.0199	4.2297	4.5021	4.8448	5.2805	5.8076	6.4263	7.2444	8.4269	10.264	12.161	15.611
750kVA														
T7 53V	13.25%	1.2284	0.3553	0.4486	0.6902	0.5977	0.6263	0.6493	0.7137	0.8383	1.0999	1.8166	3.3494	16.468
T7 200V	50%	1.4493	2.3541	2.5448	2.8049	3.0304	3.3382	3.7178	4.2388	4.9451	5.9958	7.9592	10.505	17.713
T7 400V	100%	3.0060	5.4219	5.7039	6.0540	6.4167	6.8445	7.3630	8.0088	8.8664	10.004	11.889	13.935	17.223
T7 115V	50%	1.2572	0.9838	1.0993	1.2799	1.3702	1.5161	1.7318	2.0296	2.4944	3.2355	4.8007	7.1085	14.042
T7 230V	100%	1.6925	2.8051	3.0069	3.2667	3.5229	3.8574	4.2693	4.8108	5.5181	6.5876	8.3638	10.351	13.449
1kVA														
T8 5V	2.27%	0.6399	0.7888	0.9202	0.8237	0.9472	0.8162	0.9859	0.9855	0.9638	0.998	0.9011	0.8781	9.31
T8 12V	5.45%	0.8487	0.2705	0.319	0.3866	0.3533	0.3339	0.3274	0.321	0.3207	0.3236	0.3402	0.4316	11.400
T8 24V	10.9%	0.8027	0.1577	0.2093	0.2611	0.2222	0.2028	0.2013	0.2056	0.2407	0.289	0.489	1.0441	13.001
T8 36V	16.36%	0.8204	0.2583	0.316	0.3778	0.3682	0.3816	0.4185	0.4837	0.6011	0.8343	1.4796	3.0127	14.767
T8 110V	50%	0.911	1.0618	1.1676	1.2994	1.4351	1.6068	1.8469	2.1993	2.6991	3.5247	5.2494	7.7887	14.705
T8 220V	100%	1.4854	3.0432	3.2633	3.534	3.8336	4.2001	4.6534	5.2161	6.019	7.1487	9.0646	10.992	13.778
3 phase														
350VA														
T9 230V	57.5%	1.3039	1.8936	2.1067	2.2975	2.5982	2.7436	3.0564	3.4988	4.1540	5.1479	7.0324	9.6381	17.017
T9 400V	100%	2.3784	4.5997	4.9141	5.1790	5.6160	5.9574	6.4371	7.0778	7.9239	9.1579	11.162	13.5209	17.334
T9 230V	57.5%	1.4736	2.7641	3.0195	3.2265	3.6845	3.8775	4.3131	4.8365	5.6244	6.8097	8.8586	11.542	18.745
T9 400V	100%	3.2411	6.1019	6.4079	6.6855	7.2317	7.6032	8.1498	8.8027	9.6552	10.913	12.939	15.110	18.656
T9 230V	57.5%	2.1958	2.6333	3.0130	3.3656	3.5612	3.8230	4.2234	4.7609	5.5185	6.6397	8.6219	11.324	18.670
T9 400V	100%	3.4898	5.9587	6.2138	6.5752	6.9527	7.4232	7.9550	8.6393	9.4995	10.759	12.764	14.947	18.731
1.2kVA														
T10 24V	57.1%	0.6198	0.2817	0.3516	0.4354	0.3895	0.2717	0.2430	0.2252	0.2133	0.2100	0.2671	0.4978	3.4025
T10 42V	100%	0.6509	0.3657	0.4532	0.4275	0.3412	0.3303	0.3231	0.3375	0.3517	0.4270	0.6097	1.1490	3.2154

5kVA														
T11	100%	0.9595	0.4313	0.5480	0.6526	0.6032	0.5565	0.5897	0.5008	0.4527	0.4225	0.4165	0.4783	1.4902
20kVA														
T12	100%	0.4039	0.6875	0.7539	0.8367	0.9325	1.0462	1.2692	1.4895	1.8327	2.4450	3.6945	5.4299	7.8475
40kVA														
T13	100%	0.1217	0.4035	0.4504	0.4971	0.5640	0.6564	0.7766	0.9656	1.2643	1.7498	2.9264	4.7362	6.9818

Table 3.10. The CCF results for all transformers

CCF	Wind.%	15kΩ	5kΩ	4.5kΩ	4kΩ	3.5kΩ	3kΩ	2.5kΩ	2kΩ	1.5kΩ	1kΩ	500 Ω	200Ω	1Ω
400VA														
T1 5V	13.89%	0.9725	0.9911	0.9880	0.9856	0.9876	0.9881	0.9882	0.9886	0.9887	0.9888	0.9892	0.9900	0.6697
T1 12V	33.33%	0.9813	0.9986	0.9983	0.9958	0.9978	0.9980	0.9979	0.9976	0.9980	0.9979	0.9980	0.9967	0.6864
T1 24V	66.67%	0.9760	0.9996	0.9997	0.9997	0.9997	0.9996	0.9995	0.9993	0.9990	0.9981	0.9939	0.9737	0.6952
T1 36V	100%	0.9742	0.9953	0.9937	0.9940	0.9953	0.9950	0.9953	0.9953	0.9946	0.9917	0.9786	0.9197	0.7045
T2 24V	100%	0.9998	0.9998	0.9995	0.9980	0.9988	0.9992	0.9992	0.9991	0.9986	0.9973	0.9915	0.9685	0.7519
T3 24V	100%	0.9954	0.9990	0.9995	0.9997	0.9998	0.9998	0.9996	0.9995	0.9991	0.9970	0.9932	0.9791	0.8895
630VA														
T4 5V	2.27%	0.9889	0.9974	0.9961	0.9937	0.9950	0.9957	0.9959	0.9959	0.9960	0.9961	0.9964	0.9969	0.4351
T4 12V	5.4%	0.9997	0.9996	0.9992	0.9983	0.9980	0.9988	0.9990	0.9994	0.9991	0.9994	0.9996	0.9993	0.2115
T4 22V	10%	0.9976	0.9999	1.0000	0.9992	0.9999	0.9999	0.9999	0.9999	0.9999	0.9996	0.9989	0.9938	-0.090
T4 42V	19.1%	0.9969	0.9998	0.9998	0.9955	0.9993	0.9995	0.9993	0.9990	0.9984	0.9968	0.9896	0.9571	-0.229
T4 110V	50%	0.9954	0.9947	0.9937	0.9823	0.9906	0.9884	0.9845	0.9780	0.9660	0.9359	0.8166	0.3815	-0.312
T4 220V	100%	0.9905	0.9562	0.9508	0.9391	0.9266	0.9105	0.8798	0.8319	0.7486	0.5280	0.1195	-0.120	-0.250
T5 230V	100%	0.9965	0.9697	0.9635	0.9600	0.9480	0.9345	0.9124	0.8756	0.8059	0.6419	0.2058	-0.142	-0.317
T6 220V	100%	0.9863	0.9554	0.9522	0.9459	0.9306	0.9075	0.8731	0.8142	0.6910	0.3762	-0.157	-0.363	-0.478
750kVA														
T7 53V	13.25%	0.9998	0.9997	0.9994	0.9986	0.9990	0.9989	0.9989	0.9988	0.9984	0.9975	0.9940	0.9801	-0.472
T7 200V	50%	0.9975	0.9903	0.9886	0.9858	0.9837	0.9803	0.9757	0.9686	0.9571	0.9355	0.8710	0.6393	-0.482
T7 400V	100%	0.9925	0.9479	0.9423	0.9339	0.9248	0.9126	0.8954	0.8692	0.8221	0.7183	0.3426	-0.161	-0.462
T7 115V	50%	0.9994	0.9975	0.9968	0.9951	0.9948	0.9938	0.9921	0.9892	0.9835	0.9714	0.9277	0.7512	-0.297
T7 230V	100%	0.9958	0.9786	0.9754	0.9702	0.9650	0.9571	0.9454	0.9261	0.8922	0.8100	0.5258	0.0874	-0.216
1kVA														
T8 5V	2.27%	0.9980	0.9975	0.9987	0.9991	0.9984	0.9993	0.9987	0.9985	0.9984	0.9987	0.9981	0.9977	0.4907
T8 12V	5.45%	0.9994	0.9996	0.9995	0.9992	0.9993	0.9994	0.9994	0.9995	0.9995	0.9995	0.9994	0.9993	0.3002
T8 24V	10.9%	0.9989	0.9999	0.9998	0.9996	0.9997	0.9998	0.9998	0.9998	0.9998	0.9997	0.9993	0.9973	0.0779
T8 36V	16.36%	0.9997	0.9997	0.9996	0.9994	0.9994	0.9995	0.9994	0.9993	0.999	0.9982	0.9946	0.9767	-0.293

T8 110V	50%	0.9975	0.9971	0.9964	0.9955	0.9946	0.9934	0.9913	0.9876	0.9809	0.9655	0.907	0.6491	-0.345
T8 220V	100%	0.9927	0.9747	0.9701	0.9636	0.9561	0.9455	0.9296	0.9045	0.8545	0.7403	0.3567	-0.085	-0.275
3 phase														
350VA														
T9 230V	57.5%	0.9957	0.9930	0.9908	0.9896	0.9854	0.9853	0.9821	0.9764	0.9662	0.9456	0.8839	0.7108	-0.078
T9 400V	100%	0.9890	0.9570	0.9488	0.9461	0.9297	0.9233	0.9083	0.8831	0.8406	0.7542	0.5443	0.2409	-0.068
T9 230V	57.5%	0.9948	0.9854	0.9814	0.9807	0.9695	0.9702	0.9625	0.9529	0.9328	0.8892	0.7523	0.3830	-0.403
T9 400V	100%	0.9825	0.9173	0.9042	0.9038	0.8636	0.8516	0.8193	0.7676	0.6775	0.4941	0.1344	-0.142	-0.340
T9 230V	57.5%	0.9845	0.9879	0.9829	0.9765	0.9756	0.9733	0.9684	0.9599	0.9447	0.9131	0.8009	0.3567	-0.485
T9 400V	100%	0.9745	0.9346	0.9313	0.9229	0.9101	0.8888	0.8592	0.8106	0.7286	0.4994	0.0231	-0.277	-0.423
1.2kVA														
T10 24V	57.1%	0.9976	0.9994	0.9991	0.9986	0.9990	0.9995	0.9997	0.9997	0.9997	0.9997	0.9995	0.9981	0.9172
T10 42V	100%	0.9979	0.9991	0.9988	0.9991	0.9995	0.9995	0.9995	0.9994	0.9993	0.9989	0.9972	0.9891	0.9248
5kVA														
T11	100%	0.9958	0.9992	0.9988	0.9981	0.9984	0.9985	0.9983	0.9988	0.9990	0.9992	0.9992	0.9988	0.9852
20kVA														
T12	100%	0.9986	0.9964	0.9956	0.9946	0.9933	0.9917	0.9870	0.9817	0.9714	0.9445	0.8516	0.6410	0.3500
40kVA														
T13	100%	0.9999	0.9989	0.9986	0.9983	0.9978	0.9970	0.9959	0.9935	0.9886	0.9774	0.9293	0.7800	0.4655

Table 3.11. The MAX results for all transformers

MAX	Wind.%	15kΩ	5kΩ	4.5kΩ	4kΩ	3.5kΩ	3kΩ	2.5kΩ	2kΩ	1.5kΩ	1kΩ	500 Ω	200Ω	1Ω
400VA														
T1 5V	13.89%	5.3204	12.071	15.770	19.382	19.120	18.820	18.352	17.967	18.187	17.833	16.932	15.626	8.3403
T1 12V	33.33%	5.0514	4.7699	5.2724	10.166	7.1520	6.5987	6.8928	7.5221	6.6361	6.7617	5.7491	3.3797	2.0212
T1 24V	66.67%	4.7957	1.8511	1.5830	2.4367	1.9370	2.2359	2.2179	2.0910	1.7137	0.7652	0.4241	0.8112	0.0612
T1 36V	100%	5.1675	9.4418	10.198	11.866	10.600	11.308	9.9822	8.2777	6.6603	4.5597	0.7425	1.1819	-0.025
T2 24V	100%	0.8691	0.8385	1.4942	3.6328	2.517	1.6638	1.1868	1.0146	0.9921	0.8883	0.7996	1.4568	1.0497
T3 24V	100%	0.0668	6.3115	3.5395	0.1874	0.2124	0.2466	1.1541	0.3534	0.4585	8.4954	7.4047	3.2599	2.2415
630VA														
T4 5V	2.27%	0.0593	3.4458	3.5635	11.167	2.9682	1.9032	1.8403	1.8091	2.0323	3.0457	3.0485	3.0113	7.3078
T4 12V	5.4%	0.0438	0.0351	0.0372	6.9242	0.0322	0.0331	0.0332	0.0353	0.0347	0.0321	0.0484	0.1021	6.7166
T4 22V	10%	0.0621	0.9001	0.5136	7.4513	2.2410	0.0522	0.0955	0.0642	0.0538	0.4932	0.1206	0.7302	5.6654
T4 42V	19.1%	0.0626	0.2161	0.1988	22.215	0.2049	0.0719	0.0816	0.0963	0.1215	0.1714	0.2950	0.8113	6.2747
T4 110V	50%	0.9219	1.0596	2.4451	31.230	3.2485	0.8230	0.5268	0.7032	1.0712	1.8077	3.9623	8.3798	15.375
T4 220V	100%	0.9139	0.7507	0.7380	5.3806	1.2449	1.6802	2.1680	3.0827	4.4046	7.0630	11.703	11.388	9.3348

T10 24V	57.1%	1.0151	1.0078	1.0092	1.0110	1.0105	1.0078	1.0073	1.0072	1.0074	1.0084	1.0123	1.0234	1.2523
T10 42V	100%	1.0168	1.0107	1.0125	1.0128	1.0118	1.0115	1.0119	1.0130	1.0145	1.0190	1.0282	1.0552	1.2659
5kVA														
T11	100%	1.0255	1.0123	1.0153	1.0170	1.0162	1.0146	1.0155	1.0134	1.0127	1.0129	1.0156	1.0228	1.1008
20kVA														
T12	100%	1.0126	1.0231	1.0257	1.0281	1.0323	1.0375	1.0544	1.0643	1.0822	1.1166	1.2081	1.4124	2.5275
40kVA														
T13	100%	1.0048	1.0158	1.0178	1.0198	1.0222	1.0258	1.0308	1.0386	1.0516	1.0738	1.1352	1.2704	2.0599

Table 3.13. The SSRE results for all transformers

SSRE	Wind.%	15kΩ	5kΩ	4.5kΩ	4kΩ	3.5kΩ	3kΩ	2.5kΩ	2kΩ	1.5kΩ	1kΩ	500 Ω	200Ω	1Ω
400VA														
T1 5V	13.89%	0.0005	0.0010	0.0014	0.0016	0.0013	0.0012	0.0012	0.0012	0.0011	0.0011	0.0011	0.0010	0.1586
T1 12V	33.33%	0.0005	0.0001	0.0002	0.0004	0.0002	0.0002	0.0002	0.0002	0.0002	0.0002	0.0003	0.0012	0.1734
T1 24V	66.67%	0.0004	0.0001	0.0001	0.0001	0.0001	0.0001	0.0002	0.0002	0.0004	0.0008	0.0026	0.0105	0.1804
T1 36V	100%	0.0004	0.0005	0.0007	0.0007	0.0006	0.0007	0.0009	0.0011	0.0017	0.0031	0.0092	0.0320	0.1844
T2 24V	100%	0.0000	0.0001	0.0001	0.0003	0.0002	0.0002	0.0003	0.0004	0.0007	0.0014	0.0044	0.0171	0.1656
T3 24V	100%	0.0005	0.0001	0.0001	0.0001	0.0002	0.0002	0.0003	0.0004	0.0007	0.0016	0.0048	0.0184	0.1754
630VA														
T4 5V	2.27%	0.0012	0.0003	0.0004	0.0007	0.0005	0.0005	0.0004	0.0005	0.0004	0.0004	0.0004	0.0004	0.1154
T4 12V	5.4%	0.0005	0.0001	0.0001	0.0002	0.0002	0.0001	0.0001	0.0001	0.0001	0.0001	0.0001	0.0002	0.2097
T4 22V	10%	0.0003	0.0000	0.0000	0.0001	0.0000	0.0000	0.0000	0.0000	0.0000	0.0001	0.0003	0.0015	0.3036
T4 42V	19.1%	0.0004	0.0001	0.0001	0.0004	0.0001	0.0001	0.0002	0.0003	0.0004	0.0009	0.0027	0.0105	0.3797
T4 110V	50%	0.0006	0.0014	0.0018	0.0028	0.0027	0.0034	0.0045	0.0061	0.0094	0.0161	0.0381	0.0959	0.4805
T4 220V	100%	0.0027	0.0121	0.0140	0.0165	0.0194	0.0237	0.0295	0.0383	0.0527	0.0827	0.1539	0.2639	0.5369
T5 230V	100%	0.0014	0.0081	0.0095	0.0114	0.0137	0.0171	0.0218	0.0291	0.0418	0.0673	0.1355	0.2453	0.5179
T6 220V	100%	0.0041	0.0147	0.0170	0.0199	0.0234	0.0284	0.0357	0.0459	0.0629	0.0945	0.1672	0.2777	0.5386
750kVA														
T7 53V	13.25%	0.0001	0.0001	0.0001	0.0004	0.0003	0.0003	0.0003	0.0003	0.0004	0.0006	0.0014	0.0052	0.2845
T7 200V	50%	0.0003	0.0025	0.0029	0.0037	0.0043	0.0053	0.0067	0.0090	0.0128	0.0206	0.0436	0.0987	0.4307
T7 400V	100%	0.0033	0.0157	0.0178	0.0207	0.0241	0.0285	0.0347	0.0438	0.0588	0.0853	0.1533	0.2739	0.5328
T7 115V	50%	0.0001	0.0006	0.0008	0.0011	0.0012	0.0014	0.0019	0.0026	0.0041	0.0073	0.0187	0.0534	0.4343
T7 230V	100%	0.0001	0.0053	0.0062	0.0076	0.0090	0.0111	0.0142	0.0190	0.0270	0.0437	0.0895	0.1852	0.4343
1kVA														
T8 5V	2.27%	0.0007	0.0005	0.0006	0.0007	0.0006	0.0006	0.0007	0.0007	0.0007	0.0007	0.0006	0.0006	0.1148
T8 12V	5.45%	0.0007	0.0001	0.0001	0.0002	0.0001	0.0001	0.0001	0.0001	0.0001	0.0001	0.0001	0.0002	0.1958

T8 24V	10.9%	0.0006	0.0000	0.0000	0.0001	0.0001	0.0000	0.0000	0.0000	0.0001	0.0001	0.0002	0.0008	0.274
T8 36V	16.36%	0.0005	0.0001	0.0001	0.0001	0.0001	0.0001	0.0001	0.0002	0.0003	0.0005	0.0016	0.0073	0.4106
T8 110V	50%	0.0007	0.0008	0.0010	0.0012	0.0015	0.0019	0.0025	0.0036	0.0057	0.0103	0.0268	0.0772	0.4811
T8 220V	100%	0.0021	0.0074	0.0087	0.0103	0.0125	0.0154	0.0197	0.026	0.0375	0.0599	0.1243	0.234	0.5124
3 phase														
350VA														
T9 230V	57.5%	0.0008	0.0015	0.0019	0.0023	0.0029	0.0034	0.0043	0.0058	0.0087	0.0146	0.0325	0.0786	0.4434
T9 400V	100%	0.0026	0.0111	0.0129	0.0150	0.0178	0.0211	0.0258	0.0332	0.0450	0.0676	0.1217	0.2220	0.4734
T9 230V	57.5%	0.0011	0.0038	0.0045	0.0054	0.0069	0.0080	0.0102	0.0134	0.0192	0.0308	0.0611	0.1241	0.4022
T9 400V	100%	0.0058	0.0242	0.0273	0.0313	0.0367	0.0427	0.0517	0.0638	0.0827	0.1180	0.1990	0.3156	0.5595
T9 230V	57.5%	0.0030	0.0037	0.0054	0.0069	0.0075	0.0087	0.0108	0.0141	0.0199	0.0313	0.0612	0.1255	0.4003
T9 400V	100%	0.0077	0.0243	0.0276	0.0324	0.0372	0.0432	0.0515	0.0643	0.0847	0.1200	0.2009	0.3169	0.5571
1.2kVA														
T10 24V	57.1%	0.0004	0.0001	0.0001	0.0002	0.0002	0.0001	0.0001	0.0001	0.0001	0.0001	0.0003	0.0013	0.1056
T10 42V	100%	0.0005	0.0002	0.0003	0.0002	0.0002	0.0002	0.0002	0.0003	0.0003	0.0006	0.0019	0.0074	0.1062
5kVA														
T11	100%	0.0011	0.0002	0.0004	0.0004	0.0004	0.0004	0.0004	0.0003	0.0003	0.0003	0.0004	0.0011	0.0377
20kVA														
T12	100%	0.0002	0.0008	0.0009	0.0011	0.0015	0.0019	0.0032	0.0044	0.0071	0.0136	0.0378	0.1124	0.4241
40kVA														
T13	100%	0.0000	0.0003	0.0004	0.0005	0.0006	0.0008	0.0012	0.0019	0.0033	0.0068	0.0223	0.0684	0.2763

Table 3.14. The SSMMRE results for all transformers

SSMMRE	Wind. %	15k Ω	5k Ω	4.5k Ω	4k Ω	3.5k Ω	3k Ω	2.5k Ω	2k Ω	1.5k Ω	1k Ω	500 Ω	200 Ω	1 Ω
400VA														
T1 5V	13.89%	0.0005	0.0007	0.0009	0.0009	0.0008	0.0008	0.0007	0.0007	0.0007	0.0007	0.0007	0.0007	0.1422
T1 12V	33.33%	0.0004	0.0001	0.0001	0.0003	0.0002	0.0002	0.0002	0.0002	0.0002	0.0002	0.0003	0.0012	0.1729
T1 24V	66.67%	0.0004	0.0001	0.0001	0.0001	0.0001	0.0001	0.0002	0.0002	0.0004	0.0008	0.0025	0.0105	0.1804
T1 36V	100%	0.0004	0.0005	0.0006	0.0006	0.0006	0.0007	0.0008	0.0011	0.0016	0.0031	0.0091	0.0317	0.1844
T2 24V	100%	0.0000	0.0001	0.0001	0.0002	0.0002	0.0002	0.0003	0.0004	0.0007	0.0013	0.0043	0.0165	0.1654
T3 24V	100%	0.0005	0.0001	0.0001	0.0001	0.0002	0.0002	0.0003	0.0004	0.0007	0.0015	0.0046	0.0174	0.1741
630VA														
T4 5V	2.27%	0.0012	0.0003	0.0004	0.0007	0.0005	0.0005	0.0004	0.0005	0.0004	0.0004	0.0004	0.0004	0.1150
T4 12V	5.4%	0.0005	0.0001	0.0001	0.0002	0.0002	0.0001	0.0001	0.0001	0.0001	0.0001	0.0001	0.0002	0.2093
T4 22V	10%	0.0003	0.0000	0.0000	0.0001	0.0000	0.0000	0.0000	0.0000	0.0000	0.0001	0.0003	0.0015	0.3019
T4 42V	19.1%	0.0004	0.0001	0.0001	0.0003	0.0001	0.0001	0.0002	0.0003	0.0004	0.0009	0.0027	0.0105	0.3781

T4 110V	50%	0.0006	0.0014	0.0018	0.0024	0.0027	0.0034	0.0045	0.0061	0.0094	0.0161	0.0375	0.0915	0.4594
T4 220V	100%	0.0026	0.0121	0.0140	0.0164	0.0194	0.0236	0.0293	0.0380	0.0518	0.0798	0.1434	0.2536	0.5310
T5 230V	100%	0.0014	0.0080	0.0095	0.0113	0.0136	0.0170	0.0215	0.0286	0.0407	0.0640	0.1228	0.2279	0.5076
T6 220V	100%	0.0041	0.0147	0.0170	0.0199	0.0234	0.0283	0.0356	0.0456	0.0621	0.0922	0.1602	0.2716	0.5350
750kVA														
T7 53V	13.25%	0.0001	0.0001	0.0001	0.0003	0.0003	0.0003	0.0003	0.0003	0.0004	0.0006	0.0014	0.0052	0.2838
T7 200V	50%	0.0003	0.0024	0.0029	0.0036	0.0043	0.0052	0.0067	0.0089	0.0128	0.0205	0.0435	0.0982	0.4297
T7 400V	100%	0.0033	0.0157	0.0178	0.0207	0.0240	0.0285	0.0346	0.0437	0.0585	0.0843	0.1480	0.2586	0.5270
T7 115V	50%	0.0001	0.0006	0.0007	0.0010	0.0012	0.0014	0.0019	0.0026	0.0041	0.0073	0.0187	0.0530	0.4261
T7 230V	100%	0.0009	0.0053	0.0062	0.0075	0.0090	0.0111	0.0141	0.0190	0.0269	0.0434	0.0880	0.1807	0.4688
1kVA														
T8 5V	2.27%	0.0007	0.0005	0.0006	0.0005	0.0004	0.0005	0.0006	0.0006	0.0007	0.0007	0.0006	0.0006	0.1138
T8 12V	5.45%	0.0006	0.0001	0.0001	0.0001	0.0001	0.0001	0.0001	0.0001	0.0001	0.0001	0.0001	0.0002	0.1953
T8 24V	10.9%	0.0007	0.0000	0.0000	0.0001	0.0000	0.0000	0.0000	0.0000	0.0001	0.0001	0.0002	0.0008	0.2732
T8 36V	16.36%	0.0007	0.0001	0.0001	0.0001	0.0001	0.0001	0.0001	0.0002	0.0003	0.0005	0.0016	0.0073	0.3973
T8 110V	50%	0.0007	0.0008	0.0010	0.0012	0.0015	0.0019	0.0025	0.0036	0.0057	0.0103	0.0262	0.0713	0.4534
T8 220V	100%	0.002	0.0074	0.0086	0.0103	0.0124	0.0153	0.0195	0.0257	0.0368	0.0576	0.1129	0.2155	0.5027
3 phase														
350VA														
T9 230V	57.5%	0.0007	0.0015	0.0019	0.0023	0.0028	0.0033	0.0043	0.0058	0.0087	0.0146	0.0324	0.0778	0.4183
T9 400V	100%	0.0025	0.0111	0.0129	0.0149	0.0177	0.0210	0.0258	0.0331	0.0448	0.0670	0.1191	0.2129	0.4669
T9 230V	57.5%	0.0010	0.0038	0.0045	0.0054	0.0067	0.0079	0.0101	0.0134	0.0192	0.0308	0.0608	0.1233	0.4015
T9 400V	100%	0.0057	0.0242	0.0272	0.0312	0.0364	0.0425	0.0514	0.0633	0.0816	0.1150	0.1886	0.3008	0.5515
T9 230V	57.5%	0.0030	0.0037	0.0054	0.0069	0.0075	0.0087	0.0108	0.0141	0.0199	0.0312	0.0608	0.1243	0.3990
T9 400V	100%	0.0077	0.0243	0.0275	0.0323	0.0371	0.0431	0.0512	0.0637	0.0833	0.1163	0.1889	0.3009	0.5479
1.2kVA														
T10 24V	57.1%	0.0004	0.0001	0.0001	0.0002	0.0002	0.0001	0.0001	0.0001	0.0001	0.0001	0.0003	0.0013	0.1030
T10 42V	100%	0.0005	0.0002	0.0003	0.0002	0.0002	0.0002	0.0002	0.0003	0.0003	0.0006	0.0019	0.0074	0.1062
5kVA														
T11	100%	0.0011	0.0002	0.0004	0.0004	0.0004	0.0004	0.0004	0.0003	0.0003	0.0003	0.0004	0.0011	0.0377
20kVA														
T12	100%	0.0002	0.0008	0.0009	0.0011	0.0015	0.0019	0.0032	0.0044	0.0069	0.0132	0.0350	0.0974	0.4132
40kVA														
T13	100%	0.0000	0.0003	0.0004	0.0005	0.0006	0.0008	0.0012	0.0018	0.0032	0.0063	0.0183	0.0525	0.2727

Table 3.15. The ρ results for all transformers

ρ	Wind. %	15k Ω	5k Ω	4.5k Ω	4k Ω	3.5k Ω	3k Ω	2.5k Ω	2k Ω	1.5k Ω	1k Ω	500 Ω	200 Ω	1 Ω
400VA														
T1 5V	13.89%	0.9998	0.9994	0.9992	0.9990	0.9991	0.9992	0.9992	0.9992	0.9992	0.9992	0.9992	0.9993	0.9717
T1 12V	33.33%	0.9998	0.9999	0.9999	0.9997	0.9999	0.9999	0.9999	0.9998	0.9999	0.9999	0.9999	0.9998	0.9672
T1 24V	66.67%	0.9998	1.0000	1.0000	1.0000	1.0000	1.0000	1.0000	0.9999	0.9999	0.9999	0.9995	0.9982	0.9672
T1 36V	100%	0.9998	0.9997	0.9996	0.9996	0.9997	0.9997	0.9997	0.9997	0.9996	0.9994	0.9985	0.9946	0.9673
T2 24V	100%	1.0000	1.0000	1.0000	0.9999	0.9999	1.0000	1.0000	0.9999	0.9999	0.9999	0.9995	0.9981	0.9785
T3 24V	100%	0.9996	0.9999	1.0000	1.0000	1.0000	1.0000	1.0000	1.0000	0.9999	0.9997	0.9994	0.9981	0.9797
630VA														
T4 5V	2.27%	0.9998	0.9999	0.9999	0.9999	0.9999	0.9999	0.9999	0.9999	0.9999	0.9999	0.9999	0.9999	0.9851
T4 12V	5.4%	0.9999	1.0000	1.0000	1.0000	1.0000	1.0000	1.0000	1.0000	1.0000	1.0000	1.0000	1.0000	0.9706
T4 22V	10%	1.0000	1.0000	1.0000	1.0000	1.0000	1.0000	1.0000	1.0000	1.0000	1.0000	1.0000	0.9998	0.9508
T4 42V	19.1%	0.9999	1.0000	1.0000	0.9999	1.0000	1.0000	1.0000	1.0000	0.9999	0.9999	0.9996	0.9988	0.9308
T4 110V	50%	0.9999	0.9998	0.9998	0.9996	0.9997	0.9996	0.9995	0.9993	0.9989	0.9982	0.9962	0.9911	0.9115
T4 220V	100%	0.9997	0.9987	0.9985	0.9983	0.9980	0.9976	0.9971	0.9964	0.9952	0.9928	0.9869	0.9740	0.8954
T5 230V	100%	0.9999	0.9991	0.9990	0.9988	0.9986	0.9983	0.9979	0.9972	0.9962	0.9942	0.9885	0.9755	0.8946
T6 220V	100%	0.9997	0.9988	0.9987	0.9985	0.9982	0.9978	0.9973	0.9966	0.9954	0.9931	0.9873	0.9741	0.8906
750kVA														
T7 53V	13.25%	1.0000	1.0000	1.0000	1.0000	1.0000	1.0000	1.0000	1.0000	0.9999	0.9999	0.9997	0.9991	0.9488
T7 200V	50%	0.9999	0.9995	0.9995	0.9993	0.9992	0.9991	0.9988	0.9985	0.9980	0.9970	0.9946	0.9894	0.9109
T7 400V	100%	0.9994	0.9976	0.9973	0.9969	0.9966	0.9961	0.9954	0.9945	0.9931	0.9907	0.9848	0.9716	0.8881
T7 115V	50%	1.0000	0.9999	0.9998	0.9998	0.9998	0.9997	0.9996	0.9995	0.9992	0.9987	0.9971	0.9930	0.9126
T7 230V	100%	0.9998	0.9990	0.9989	0.9987	0.9985	0.9981	0.9977	0.9971	0.9960	0.9941	0.9892	0.9782	0.9060
1kVA														
T8 5V	2.27%	1	0.9999	0.9999	0.9998	0.9999	0.9999	0.9999	0.9999	0.9999	0.9999	0.9999	0.9999	0.9849
T8 12V	5.45%	1	1	1	1	1	1	1	1	1	1	1	1	0.9727
T8 24V	10.9%	1	1	1	1	1	1	1	1	1	1	1	0.9999	0.9576
T8 36V	16.36%	1	1	1	1	1	1	1	1	1	0.9999	0.9998	0.9991	0.9252
T8 110V	50%	1	0.9999	0.9998	0.9998	0.9998	0.9997	0.9996	0.9995	0.9992	0.9987	0.997	0.9924	0.9128
T8 220V	100%	0.9998	0.999	0.9989	0.9987	0.9984	0.9981	0.9976	0.997	0.9959	0.9938	0.9885	0.9772	0.9072
3 phase														
350VA														
T9 230V	57.5%	0.9998	0.9996	0.9995	0.9995	0.9993	0.9992	0.9991	0.9988	0.9983	0.9973	0.9949	0.9891	0.9046
T9 400V	100%	0.9994	0.9979	0.9975	0.9973	0.9967	0.9964	0.9958	0.9948	0.9933	0.9905	0.9836	0.9679	0.8797
T9 230V	57.5%	0.9998	0.9995	0.9994	0.9993	0.9991	0.9990	0.9988	0.9985	0.9979	0.9968	0.9942	0.9880	0.9180

T9 400V	100%	0.9993	0.9975	0.9972	0.9971	0.9963	0.9960	0.9953	0.9944	0.9929	0.9900	0.9825	0.9656	0.8709
T9 230V	57.5%	0.9996	0.9996	0.9994	0.9993	0.9992	0.9991	0.9989	0.9986	0.9981	0.9971	0.9948	0.9890	0.9203
T9 400V	100%	0.9992	0.9977	0.9976	0.9973	0.9969	0.9964	0.9958	0.9948	0.9935	0.9907	0.9837	0.9676	0.8729
1.2kVA														
T10 24V	57.1%	0.9998	1.0000	0.9999	0.9999	0.9999	1.0000	1.0000	1.0000	1.0000	1.0000	1.0000	0.9998	0.9875
T10 42V	100%	0.9998	0.9999	0.9999	0.9999	0.9999	0.9999	0.9999	0.9999	0.9999	0.9999	0.9998	0.9991	0.9874
5kVA														
T11	100%	0.9994	0.9999	0.9998	0.9997	0.9998	0.9998	0.9998	0.9998	0.9999	0.9999	0.9999	0.9999	0.9972
20kVA														
T12	100%	1.0000	0.9999	0.9999	0.9998	0.9998	0.9997	0.9996	0.9994	0.9992	0.9984	0.9961	0.9892	0.9341
40kVA														
T13	100%	1.0000	0.9999	0.9999	0.9999	0.9999	0.9998	0.9998	0.9996	0.9993	0.9987	0.9962	0.9889	0.9527

Table 3.16. The results of current flowing through the rheostat

	Wind.%	15k Ω	5k Ω	4.5k Ω	4k Ω	3.5k Ω	3k Ω	2.5k Ω	2k Ω	1.5k Ω	1k Ω	500 Ω	200 Ω	1 Ω
T8 5V	2.27%	0	0	0	0	0	0	0	0	0	0	0	0	-
T8 12V	5.45%	0	0	0	0	0	0	0	0	0	0	0	0	-
T8 24V	10.90%	0	0	0	0	0	0	0	0	0	0	0	0.022	-
T8 36V	16.36%	0	0	0	0	0	0	0	0	0	0	0.027	0.215	-
T8 110V	50%	0	0.021	0.022	0.025	0.029	0.035	0.042	-	-	-	-	-	-
T8 220V	100%	0.025	0.048	0.057	0.064	0.085	-	-	-	-	-	-	-	-
T7 5V	2.27%	0	0	0	0	0	0	0	0	0	0	0	0	-
T7 12V	5.45%	0	0	0	0	0	0	0	0	0	0	0	0	-
T7 22V	10%	0	0	0	0	0	0	0	0	0	0	0	0.022	-
T7 42V	19.1%	0	0	0	0	0	0	0	0	0	0.027	0.041	0.218	-
T7 110V	50%	0	0.024	0.027	0.029	0.035	0.043	0.055	-	-	-	-	-	-

3.2 Criteria for each SIs

The results of the CC method for all transformers can be found in Table 3.1. Among the transformers, the 1 kVA transformer test results for all statistical indices were analyzed as an example. However, the results for the other transformers were taken into account when proposing the criteria. This transformer had different voltage taps; thus, different percentages of the winding could be evaluated. If the tap with the 5 V rating is used, then, based on the total value of 220 V, the 5 V tap would be 2.2% of the entire winding or 2.2% of the entire winding turns. With this ratio in mind, the 5/12/24/36/110/220 V winding taps were examined. These taps are 2.2%/5.4%/11%/16%/50%/100% of the winding, respectively.

Table 3.1 shows the calculated values for the CCs of all transformers. For each voltage rating, the test was conducted with each resistance value; finding the critical value for the CC was possible. Then, using this value as a reference, the critical values for the other methods were found. Tables 3.1-3.15 show all the statistical indices for the transformers. Although the results of the 1 kVA transformer were taken as an example, the results of the other transformers were taken into account.

Based on Table 3.1, the CC method results and the FRA traces, for a winding percentage below 10%, all the rheostat values act as an open circuit. Only the total winding short circuit had a significant effect on the FRA trace and on the

CC value, which means that a total short circuit of even 2.2% of the winding is not tolerable. It was said before that FRA interpretation is visually interpreted by an experts. Thus, to overcome this the current that flows through the rheostat was measured. In emulation of disk-to-disk fault with the help of rheostat, the current values that will pass through the rheostat will create the trace difference in Frequency Response. That happens, because only current value is changing when resistance is varying, not the structure or winding position. Therefore, the current is the only thing that affects the Frequency Response. In that case, in order to find criteria for interpretation the current that flows through the resistor should be analyzed. Based on Table 3.16, where current values are presented we could see that at different voltage levels the current appears at different resistances. The higher the voltage level at higher resistances current starts to flow. It could be seen that for 1kVA transformer the current appears at 200 Ω at 24 V, at 500 Ω of 36 V, at 5 k Ω of 110 V and flows from 15 k Ω of 220 V. Using this information as a reference for criteria the next step was to check these values at different SIs. Thus, looking at the table of CC at the voltage and resistance levels of 1 kVA transformer that told before. It could be seen that the values of CC before the 200 Ω of 24 V, 500 Ω of 36 V, and 5 k Ω of 110 V all greater or equal to 0.9997. Moreover, all that values of resistance at their voltage level were analyzed visually also. And the Frequency Responses of the resistances mentioned above deviates from the fingerprints more significantly than the rest of the Responses. Thus, it could be said that proposed criteria was found with the help of current value,

proven by SIs and checked on FR. To find the critical value for the CC, the 36 V and 110 V ratings of the 1 kVA transformer were used, as they have a definite declining trend based on the decreasing resistance and this was the largest transformer under test that would be energized. However, the proposed critical values were also tested for the other transformers. In Figure 3.4, starting from 500 Ω , a significant deviation of the traces from the fingerprint can be observed. The same significant deviation can be seen on Figure 3.5 starting from the 5 k Ω trace. Thus, the values of the CC at these resistances were used as a boundary for the critical value, which is 0.9996. Moreover, to verify this value, the other resistances and their CC values were used.

Based on the fact that 15 k Ω is a significant resistance for 5.4% of the winding of the 1 kVA transformer, it would act as an open circuit, and hence, the value of the CC at this resistance is definitely in the range of the critical value. Thus, the CC value of 0.9997 is in the range. Moreover, to prove this, the setup shown in Figure 2.1 was used. The short circuit current that should flow through the rheostat during resistance variation was measured. The I_{sc} for 15 k Ω at this voltage level was zero. At 500 Ω for 36 V and 5 k Ω for 110 V, the I_{sc} started to change from zero to 0.022 A, and thus, these circuits were not open circuits. The short circuit current values of several transformer can be found in Table 3.16. With the help of this testing of all the transformers and Table 3.1, for all CC values above 0.9997, I_{sc} was found to be zero. This result means that our critical value

for the CC is 0.9997. Moreover, based on a comparison with the critical value for the CC from Nirgude et al. [34], which is 0.9998, it can be concluded that the proposed value is reliable. Thus, for our case, the critical value for the CC was chosen as 0.9997, which is close to Nirgude's value. This critical value was chosen as a reference for the detection of the critical values of other SIs. The same resistance values at 36 V and 110 V for the 1 kVA transformer were also used for the other methods. The results of these methods enable us to propose the boundaries for the critical value range, and short circuit monitoring during resistance variation helps us clearly find the boundary for an open circuit. Table 3.17 provides all the statistical indices critical for examining faults in transformers. They can be used to determine whether the transformer is healthy.

Table 3.17. The critical values of SIs for fault detection

Index	CC	SD	SSE	ASLE	DABS	RMSE	ED	ρ
Value	<0.9997	>1	>1	>0.125	>0.6	>0.04	>30	<0.9999
Index	CD	CSD	CCF	MAX	MM	SSRE	SSMMRE	
Value	invalid	>1	<0.9975	invalid	>1.0233	>0.0007	>0.0007	

Based on the above table, the CD and MAX cannot act as criteria because their behavior is not linear and cannot be described by certain trends. Therefore, these two indices should not be used for our fault detection criteria. The other indicators had a linear behavior and followed a certain trend, so we can relate them to each other and, based on the CC value as the reference, create criteria for them.

These values help us identify whether a fault is present, which is why they should be called critical values. Moreover, all values in the critical value ranges are in the safe zone or green zone. However, sometimes, the transformer continues to operate with some small fault, and in this situation, the term yellow zone should be used. This is the zone in which the transformer can be used even with a fault because the fault is not severe; however, for better exploitation, the fault should be fixed. Otherwise, a severe fault or even damage that would take the transformer out of service could occur.

To find the boundary values for the yellow zone, we used the idea that some level of fault should be accepted and that the SI value for this level should then be calculated as a reference for the yellow zone boundary. If for the critical value or the green zone, we do not allow any current to flow through the resistor, then the main contributor to changes in the frequency response is the short circuit current. For the yellow zone, current flow or leakage should be allowed to some extent. To identify this value, we refer to the differential relay used for transformers. The differential relay compares the input and output currents of the transformer and monitors the difference between them because it should be in a specific range at all times. A change in the current value indicates that some fault has occurred that resulted in an increase of current that could further damage the transformer. Thus, to prevent damage of equipment, differential relay trips and transformers should be checked and repaired. As the differential relay usually

trips during severe faults, its current values cannot be used for our yellow boundary case. However, if we make an analogy with the differential relay but for smaller current values, then the principle for yellow boundary identification can be found. The ABB company advises [62] to use for their differential relay 5% of the nominal current as the tolerable range of current values during input/output current monitoring. This means that even if the values of the currents should be the same, some uncertainties or processes that affect the current could occur. However, if the current variation is below 5%, it could be tolerated by the differential relay. For our yellow boundary case, 10% of the suggested 5% percent is taken for the current value; 5% of the nominal current is for severe faults, so if we use 10% of this 5%, we reduce the severity of the fault significantly. At this rate, which is 0.5% of the nominal current, the clear identification of the fault would occur; however, due to its low value, the severity of the fault is not significant, which describes our yellow zone. The fault is present, but the transformer can operate in normal conditions; however, check-up is advised.

For the 630 VA transformer, the nominal current was 2.86 A, and for the 1 kVA transformer, it was 4.54 A. Therefore, the values of 0.0143 A and 0.0227 A were used. Both of these current values were tested on the full winding percentage of 220 V. Now, the current value was known, but the resistor value at which the needed current flows through the rheostat was unknown. With the help of an ammeter connected in series to the rheostat, we adjusted the current and measured

the rheostat value at this current. Therefore, for the FRA test, the needed resistance was known.

During leakage or flow through the resistor of 0.005% of the nominal current, the following CC values for this case were obtained.

Table 3.18. The results of CC during 0.005% of nominal current flow through the rheostat

Transformer	Current value	Resistor Value	CC
400VA	0.055A	4.6k Ω	0.9990
630VA	0.0143A	15.4k Ω	0.9991
1kVA	0.0227A	10.5k Ω	0.9989

Using Table 3.18 for CC analysis, we could state that a CC value of 0.9990 can be taken as a boundary for the yellow zone. This small difference can occur due to uncertainties in the ammeter or ohmmeter or even small connection deviations.

Using the frequency response results used for Table 18 for the other SI value calculations, the obtained results for the yellow boundary values are presented below.

Table 3.19. The SIs values for yellow border.

Index	CC	SD	SSE	ASLE	DABS	RMSE	ED	ρ
Value	<0.9990	>2.1	>4.4	>0.245	>1.12	>0.07	>67	<0.9995
Index	CD	CSD	CCF	MAX	MM	SSRE	SSMMRE	
Value	invalid	>1.3	<0.9968	invalid	>1.0354	>0.0009	>0.0009	

Again, the MAX and CD were not used, as their values were not even considered in determining the critical value for the green zone. The obtained results suggest that, considering the two levels of critical values, which describe the no-fault zone and the operation with a small fault zone, the SI values below the yellow zone should be considered in the red zone and an indicator of a severe fault that would lead to equipment failure.

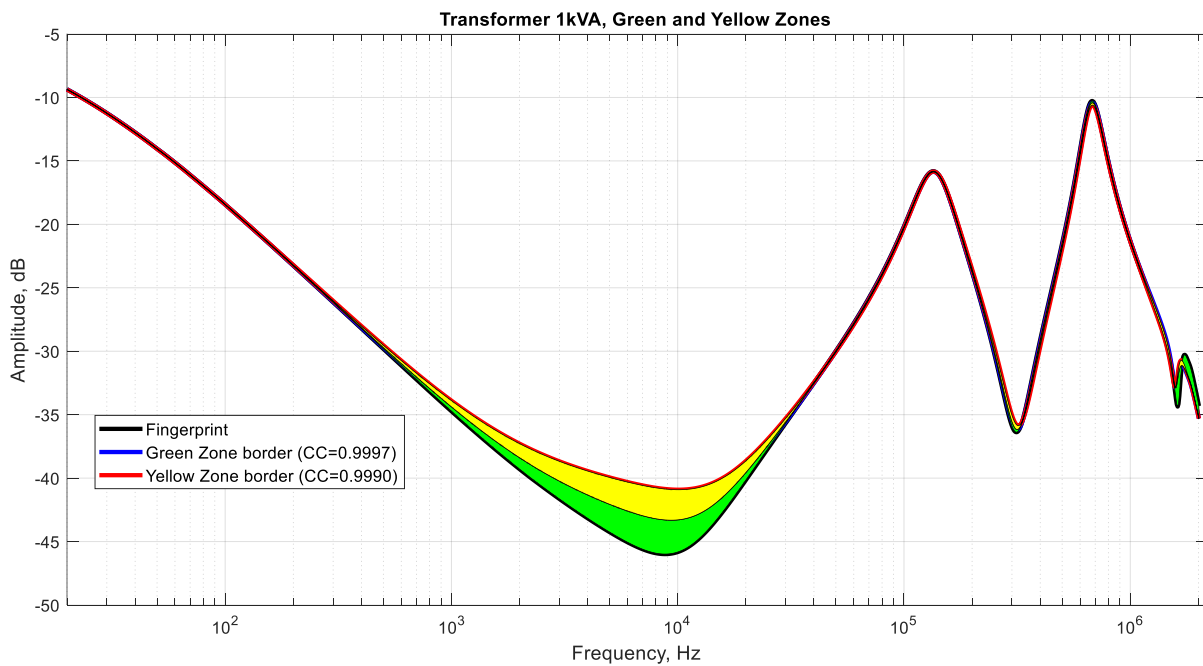


Figure 3.7. The criteria zone separation for 1kVA transformer

Figure 3.7 represents the outcomes of the research, where three zones could be seen. For further use of these criteria shown by zones, it is needed to obtain the frequency response of the equipment under test and compare its numerical index with the tables given above. Based on the value, it will lie in range of green zone, yellow or red. Based on the zone the current equipment status would be defined. Using Figure 3.7, it could be said that all FR that would lie in green zone, would have CC more than 0.9997 and would represent healthy transformer. The FRs that have CC between 0.9997 and 0.9990 would lie in yellow zone and signal that transformer has some sort of damage or improper operation. Everything above the yellow zone considered as unhealthy transformer, and requires in proper inspection. Figure 3.7 is given only for

visual understanding of the research outcome, however if the fault occurs in the higher range of frequency, from 1-2MHz, the criteria will still be applicable.

CHAPTER 4 – CONCLUSION

It can be concluded that FRA analysis is a convenient way to identify the mechanical defects of the transformer without opening transformer tank. It gives an opportunity to determine the transformer condition in fast and convenient way. The interpretation of healthy and unhealthy transformer frequency responses could be done with the help of SIs. From this study, it is summarized that if statistical indices would be standardized and their threshold values for comparison is determined, the FRA spectra can be interpreted more accurately. This study collected fifteen statistical indices and after practical measurement on different transformers, the criteria for CC, ASLE, SD, SSE, DABS, RMSE, ED, CSD, CCF, MM, SSRE, SSMMRE and ρ was obtained. Unfortunately, there are no criteria for CD and MM, hence it could not be used for interpretations. These critical values will be useful for unexperienced personnel to interpret the frequency response of a transformer. The two level of critical values or zone separation would allow to monitor the transformer life more accurately. The criteria was made only based on the emulated disk-to-disk short circuit, which leads to the weakness such as credibility of the criteria during other faults. The strong point for the first criteria based on the current appearance is that it clearly measures the factor that affects the FR, however, the ability of sensing only current higher than 0.022 A is a drawback. Also the percentage chosen for the second level is subjective.

For the future work, the different faults should be simulated, axial and radial displacement, real turn-to-turn and disk-to-disk faults. And for those cases the criteria should be tested, moreover, the transformers higher than 1kVA power should be energized.

References

- [1] M. Bagheri, M. Salay Naderi, T. Blackburn, and T. Phung, "Frequency Response Analysis and Short-Circuit Impedance Measurement in Detection of Winding Deformation Within Power Transformers," *IEEE Electrical Insulation Magazine*, vol. 29, no. 3, pp. 33-40, 2013.
- [2] V. Behjat and M. Mahvi, "Statistical approach for interpretation of power transformers frequency response analysis results," *IET Science, Measurement & Technology*, vol. 9, no. 3, pp. 367-375, 2015.
- [3] N. Wesley, S. Bhandari et. al "Evaluation of Statistical Interpretation Methods for Frequency Response Analysis based Winding Fault Detection of Transformers," *IEEE ICSET*, pp. 36-41, 2016.
- [4] Gomez-Luna, E., Aponte Mayor, G., Gonzalez-Garcia, C., et al.: 'Current status and future trends in frequency-response analysis with a transformer in service', *IEEE Trans. Power Deliv.*, 2013, 28, (2), pp. 1024–1031
- [5] M. Bagheri, M. S. Naderi, and T. Blackburn, "Advanced transformer winding deformation diagnosis: moving from off-line to on-line," *IEEE Transactions on Dielectrics and Electrical Insulation*, vol. 19, no. 6, pp. 1860-1870, 2012.
- [6] G. M. Kennedy, A. J. McGrail, and J.A. Lapworth, "Transformer sweep frequency response analysis (SFRA)," *Energize*, pp. 28-33, 2007
- [7] E. Rahimpour and S. Tenbohlen, "Experimental and theoretical investigation of disc space variation in real high-voltage windings using transfer function method," *IET Electric Power Applications*, vol. 4, no. 6, pp. 451-461, 2010.
- [8] E. Rahimpour, M. Jabbari, and S. Tenbohlen, "Mathematical comparison methods to assess transfer functions of transformers to detect different types of mechanical faults," *IEEE Transactions on Power Delivery*, vol. 25, no. 4, pp. 2544-2555, 2010.
- [9] M. Samimi and S. Tenbohlen, "FRA interpretation using numerical indices: State-of-the-art," *Elsevier EPES*, pp. 115-125, 2017.
- [10] A. Kraetge, M. Kruger, and P. Fong, "Frequency Response Analysis - Status of the worldwide standardization activities," *IEEE International Conference on Condition Monitoring and Diagnosis*, Beijing, China, pp. 651-654, 2008.
- [11] E. P. Dick and C. C. Erven, "Transformer diagnostic testing by frequency response analysis," *IEEE Transactions on Power Apparatus and Systems*, vol. PAS-97, pp. 2144-2153, 1978.
- [12] M. Gutten, M. Brandt, R. Polansky, and P. Prosr, "SFRA Method – Frequency Analysis of Transformers", *MEASUREMENT International Conference*, 2009.
- [13] C. Sweetser and T. McGrail, "Sweep Frequency Response Analysis Transformer Applications", *Doble Engineering*, 2003.
- [14] CIGRE SC 12 Transformer Colloquium: Summary on behalf of Study Committee 12, Budapest, 1999

- [15] S. Birlasekaran, Y Xingzhou., F. Fetherstone, ‘Diagnosis and identification of transformer faults from frequency response data’, *IEEE Power Eng. Rev.*, vol. 3, pp. 2251–2253, 2000.
- [16] A. Kraetge, M. Kruger, J. Velasquez, H. Viljoen, and A. Dierks, “Aspects of the Practical Application of Sweep Frequency Response Analysis (SFRA) on Power Transformers”, *CIGRE*, 2009.
- [17] IEEE C 57.149, “Guide for the Application and Interpretation of Frequency Response Analysis for Oil Immersed Transformer”, 2013.
- [18] IEC Standard 60076-18, “Measurement of Frequency Response”, Edition 1.0, 2012.
- [19] Bagheri, Mehdi, et al. "FRA vs. short circuit impedance measurement in detection of mechanical defects within large power transformer." *Electrical Insulation (ISEI), Conference Record of the 2012 IEEE International Symposium on*. IEEE, 2012.
- [20] S. V. Kulkarni and S. A. Khaparde, “Transformer Engineering Design and Practice,” Marcel Dekker Inc., USA, 2004.
- [21] G. Bertagnolli, “The ABB Approach to Short-circuit Duty of Power Transformers”, 3rd ed., ABB Ltd., Switzerland, 1996.
- [22] Jurisic, Bruno, et al. "High frequency transformer model derived from limited information about the transformer geometry." *International Journal of Electrical Power & Energy Systems* 94 (2018): 300-310.
- [23] Ryder, Simon A. "Diagnosing transformer faults using frequency response analysis." *IEEE Electrical Insulation Magazine* 19.2 (2003): 16-22.
- [24] Bagheri, Mehdi, B. T. Phung, and Trevor Blackburn. "Transformer frequency response analysis: mathematical and practical approach to interpret mid-frequency oscillations." *IEEE transactions on Dielectrics and Electrical Insulation* 20.6 (2013): 1962-1970.
- [25] Wang, Zhongdong, Jie Li, and Dahlina M. Sofian. "Interpretation of transformer FRA responses—Part I: Influence of winding structure." *IEEE Transactions on power delivery* 24.2 (2009): 703-710.
- [26] Wang, M., Vandermaar, A.J. and Srivastava, K.D., 2004. “Transformer winding movement monitoring in service-key factors affecting FRA measurements.” *IEEE Electrical Insulation Magazine*, 20(5), pp.5-12.
- [27] Bagheri, Mehdi, et al. "Case study on FRA capability in detection of mechanical defects within a 400MVA transformer." *CIGRE, Paris, France*. 2012.
- [28] Marks, J., Vitolina, S. and Liepniece, R., 2017, October. Modelling of vibrations caused by magnetostriction in magnetic core of large power transformers. In *Power and Electrical Engineering of Riga Technical University (RTUCON), 2017 IEEE 58th International Scientific Conference on* (pp. 1-5). IEEE.
- [29] Bagheri, M., Zollanvari, A. and Nezhivenko, S., 2018. Transformer Fault Condition Prognosis Using Vibration Signals over Cloud Environment. *IEEE Access*.

- [30] Bagheri, Mehdi, et al. "Bushing characteristic impacts on on-line frequency response analysis of transformer winding." *Power and Energy (PECon), 2012 IEEE International Conference on*. IEEE, 2012.
- [31] Setayeshmehr, A., Akbari, A., Borsi, H., Gockenbach, E. and Fofana, I., 2007, August. Winding Diagnostic by On-line Transfer Function Determination via Power Transformer Bushing Tap. In *15th International Symposium on High Voltage Engineering, Ljubljana, Slovenia*.
- [32] Bhardwaj, M., Choudhury, S., Xue, V. and Akin, B., 2014, March. Online LCL filter compensation using embedded FRA. In *Applied Power Electronics Conference and Exposition (APEC), 2014 Twenty-Ninth Annual IEEE* (pp. 3186-3191). IEEE.
- [33] M.H. Samimi, et al. "Effect of different connection schemes, terminating resistors and measurement impedances on the sensitivity of the FRA method." *IEEE Transactions on Power Delivery*, vol 32, no. 4, pp. 1713-1720, 2017
- [34] P. Nirgude, D. Ashokraju, A. Rajkumar, and B. Singh, "Application of numerical evaluation techniques for interpreting frequency response measurements in power transformers", *IET Science, Measurement & Technology*, vol. 2, no. 5, pp. 275-285, 2008
- [35] A.S. Murthy et al. "Investigation of the Effect of Winding Clamping Structure on Frequency Response Signature of 11 kV Distribution Transformer." *Energies*, vol. 11, no. 9, pp. 1-13, 2018
- [36] R. K. Senobari and H. B. Javad Sadeh, "Frequency response analysis (FRA) of transformers as a tool for fault detection and location: A review." *Electric Power Systems Research*, vol. 155, pp. 172-183, 2018
- [37] J. A. S. B. Jayasinghe, Z. D. Wang, P. N. Jarman, and A. W. Darwin, "Winding movement in power transformers: a comparison of FRA measurement connection methods," *IEEE Trans. Dielectr. Electr. Insul.*, Vol. 13, pp. 1342-1349, 2006.
- [38] Y. Liu, S. Ji, F. Yang, Y. Cui, L. Zhu, Z. Rao, C. Ke, and X. Yang, "A study of the sweep frequency impedance method and its application in the detection of internal winding short circuit faults in power transformers," *IEEE Trans. Dielectr. Electr. Insul.*, Vol. 22, pp. 2046-2056, 2015
- [39] P. Picher, et al., "Current state of transformer FRA interpretation: On behalf of CIGRE WG A2.53." *Procedia engineering*, vol. 202, pp. 3-12, 2017
- [40] N. Hashemnia, A. Abu-Siada, and S. Islam, "Improved power transformer winding fault detection using FRA diagnostics—part 1: axial displacement simulation." *IEEE transactions on dielectrics and Electrical insulation*, vol. 22, no. 1, pp. 556-563, 2015.
- [41] A. Abu-Siada, N. Hashemnia, S. Islam, and M. A. S. Masoum, "Understanding power transformer frequency response analysis signatures," *IEEE Electr. Insul. Mag.*, Vol. 29, pp. 48-56, 2013.
- [42] M. H. Samimi, S. Tenbohlen, A. A. S. Akmal, and H. Mohseni, "Evaluation of numerical indices for the assessment of transformer frequency response." *IET Generation, Transmission & Distribution*, vol.11 no.1, pp. 218-227, 2017.

- [43] Samimi, M.H., Tenbohlen, S., Shayegani-Akmal, A.A., et al.: ‘Using the complex values of the frequency response to improve power transformer diagnostics’. 24th Iranian Conf. on Electrical Engineering (ICEE2016), Shiraz, Iran, May 2016
- [44] N. K. Wesley, S. Bhandari, A. Subramaniam, M. Bagheri, and S. K. Panda, “Evaluation of statistical interpretation methods for frequency response analysis based winding fault detection of transformers”. *Sustainable Energy Technologies (ICSET), 2016 IEEE International Conference*, pp. 36-41, 2016.
- [45] M. H. Samimi, and S. Tenbohlen, “The Numerical Indices Proposed for the Interpretation of the FRA Results: a Review.” *VDE High Voltage Technology 2016, ETG-Symposium*, pp. 1-7, 2016.
- [46] M. Bagheri, B. Phung, and T. Blackburn, “Influence of temperature and moisture content on frequency response analysis of transformer winding”, *IEEE Transactions on Dielectrics and Electrical Insulation*, vol 21, no. 3, pp. 1393-1404, 2014.
- [47] K. P. Badgajar, M. Maoyafikuddin, and S. Kulkarni, “Alternative statistical techniques for aiding SFRA diagnostics in transformers”, *IET Generation, Transmission & Distribution*, vol. 6, pp. 189-198, 2012.
- [48] J. Secue and E. Mombello, “Sweep frequency response analysis (SFRA) for the assessment of winding displacements and deformation in power transformers’, *Electric Power Systems Research*, vol. 78, no. 6, pp. 1119-1128, 2008.
- [49] M. Heindl, S. Tenbohlen, A. Kraetge, M. Kruger, and J. Velasquez, “Algorithmic determination of pole-zero representations of power transformers transfer functions for interpretation of FRA data”, *16th International Symposium on High Voltage Engineering*, 2009.
- [50] E. Rahimpour, and D. Gorzin, “A new method for comparing the transfer function of transformers in order to detect the location and amount of winding faults’, *Electrical Engineering*, vol. 88, no. 5, pp. 411-416, 2006.
- [51] A. J. Ghanizadeh and G. B. Gharehpetian, “ANN and cross-correlation based features for discrimination between electrical and mechanical defects and their localization in transformer winding”, *IEEE Trans.on Dielectrics and Electrical Insulation*, vol. 21, no. 5, pp. 2374-2382, 2014
- [52] J. W. Kim, B. Park, S. C. Jeong, S. W. Kim, and P. Park, “Fault diagnosis of a power transformer using an improved frequency-response analysis”, *IEEE Transactions on Power Delivery*, vol. 20, no. 1, pp. 169-178, 2005.
- [53] R. Wimmer , S. Tenbohlen, M. Heindl, A. Kraetge, M. Kruger, and J. Christian, “Development of algorithms to assess the FRA”, *15th International Symposium on High Voltage Engineering*, 2007.
- [54] W. Tang, A. Shintemirov, and Q. Wu, “Detection of minor winding deformation fault in high frequency range for power transformer”, *IEEE PES general meeting*, pp. 1-6, 2010.
- [55] T. Ji, W. Tang, Q. Wu, “Detection of power transformer winding deformation and variation of measurement connections using a hybrid winding model”, *Electric Power Systems Research*, vol. 87, pp. 39-46, 2012.

- [56] J. Bak-Jensen, B. Bak-Jensen, and S. Mikkelsen, "Detection of faults and ageing phenomena in transformers by transfer functions", *IEEE Transactions on Power Delivery*, vol. 10, no. 1, pp. 308-314, 1995.
- [57] A. Islam, S. I. Khan, and A. Hoque, "Detection of mechanical deformation in old aged power transformer using cross correlation co-efficient analysis method", *Scientific Research EPE*, pp. 585-591, 2011.
- [58] G. M. Kennedy, A. J. McGrail, and J.A. Lapworth, "Using cross-correlation coefficients to analyze transformer sweep frequency response analysis (SFRA) traces", *IEEE Power Engineering Society Conference and Exposition in Africa - PowerAfrica*, 2007.
- [59] *IEEE Guide for the Application and Interpretation of Frequency Response Analysis for Oil-Immersed Transformers*, IEEE Std. C57.149-2012, pp. 1-72, 2013
- [60] Wimmer, R., Tenbohlen, S., Feser, K., et al.: 'The influence of connection and grounding technique on the repeatability of FRA-results'. Proc. 15th Int. Symp. on High Voltage Engineering, Ljubljana, Slovenia, August 2007, T7-522
- [61] V. Behjat, M. Mahvi and E. Rahimpour, "New statistical approach to interpret power transformer frequency response analysis: non-parametric statistical methods." *IET Science, Measurement & Technology*, vol. 10, no. 4, pp. 364-369, 2016
- [62] ABB 1MRS 755916, "Differential Protection RET 54_/Diff6T function", Application and Setting Guide, ver. A/17.08.2005, 2005

Appendix

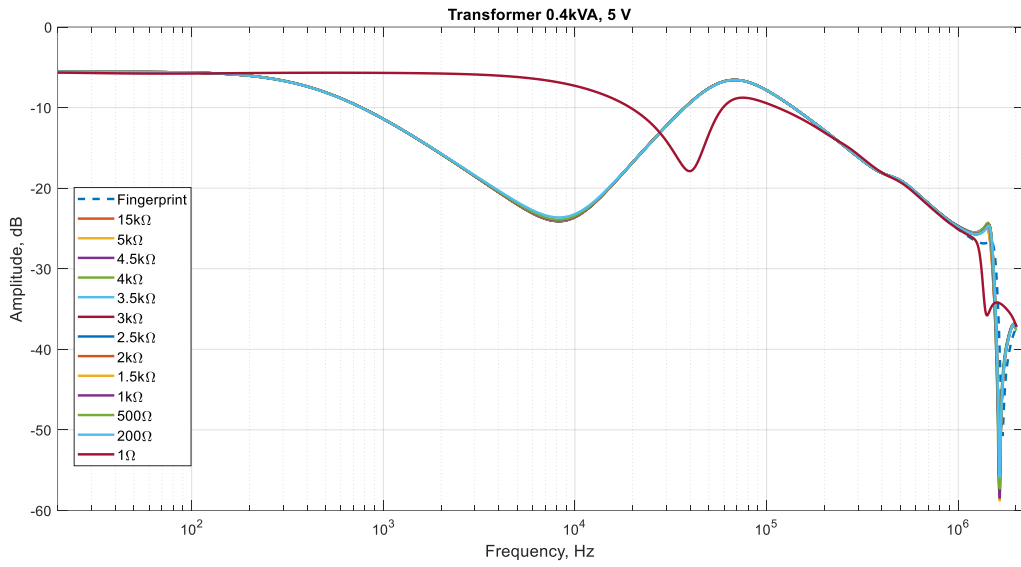


Figure 1A. Transformer 0.4kVA 5 V

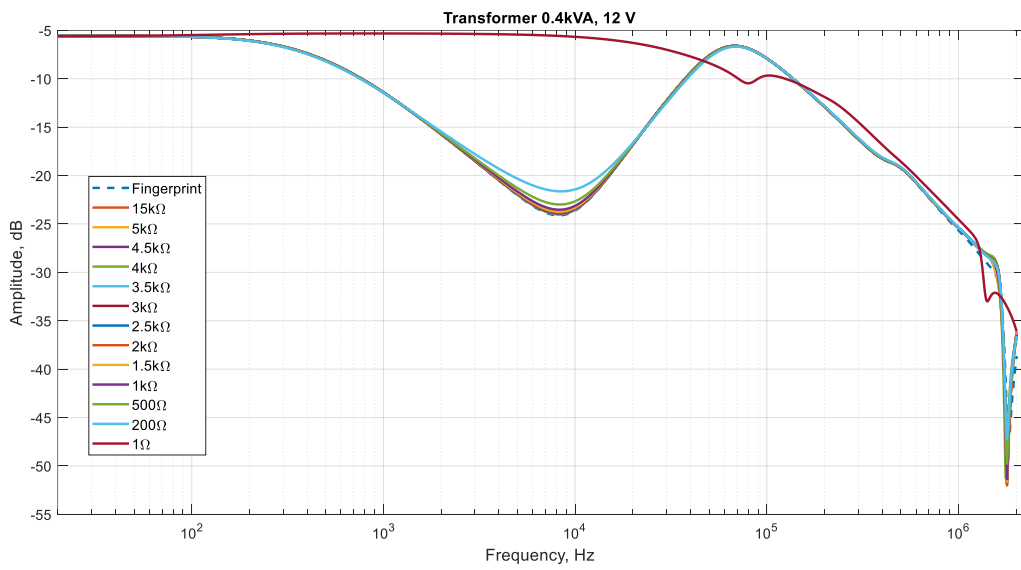


Figure 2A. Transformer 0.4kVA 12 V

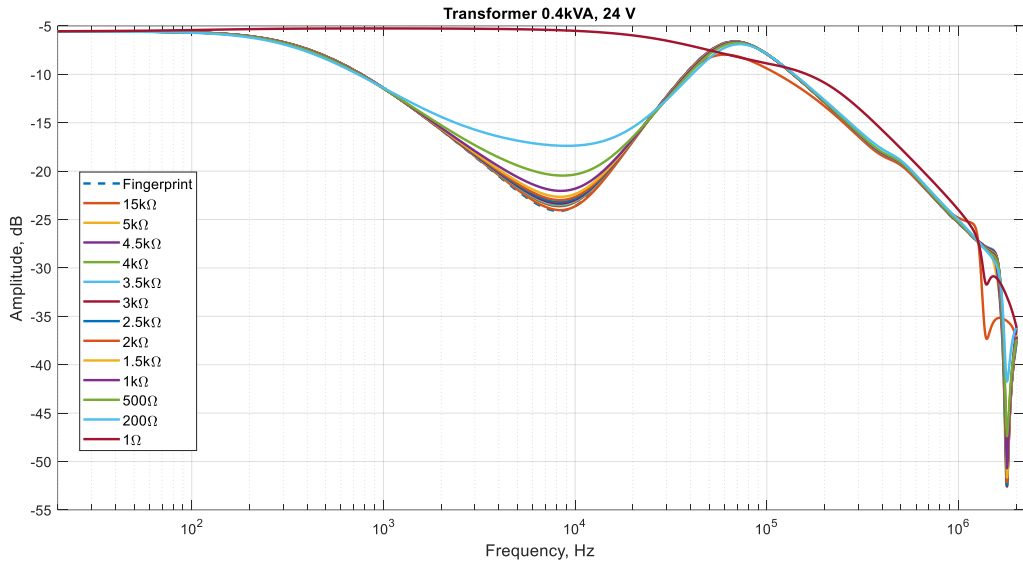


Figure 3A. Transformer 0.4kVA 24 V

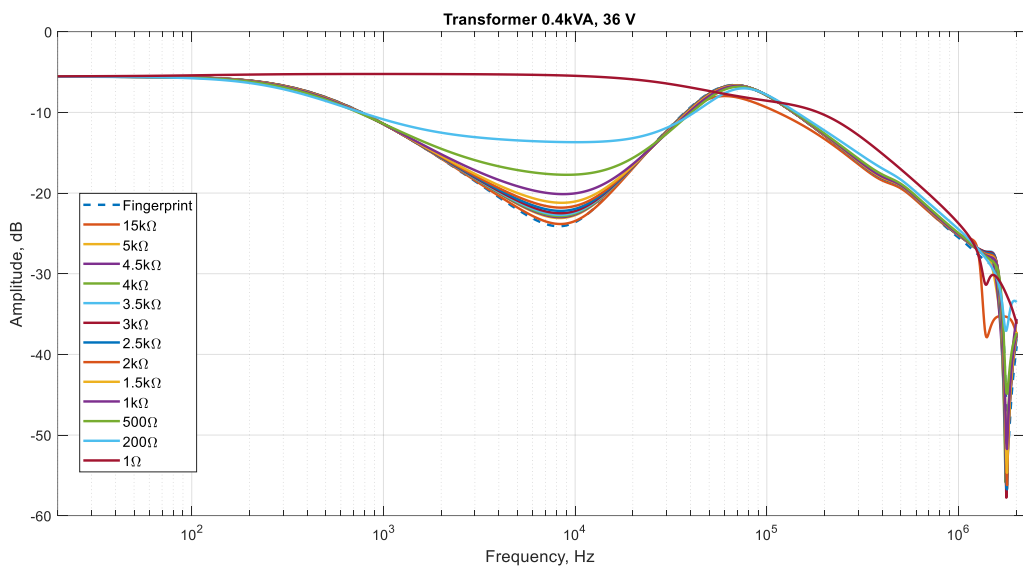


Figure 4A. Transformer 0.4kVA 36 V

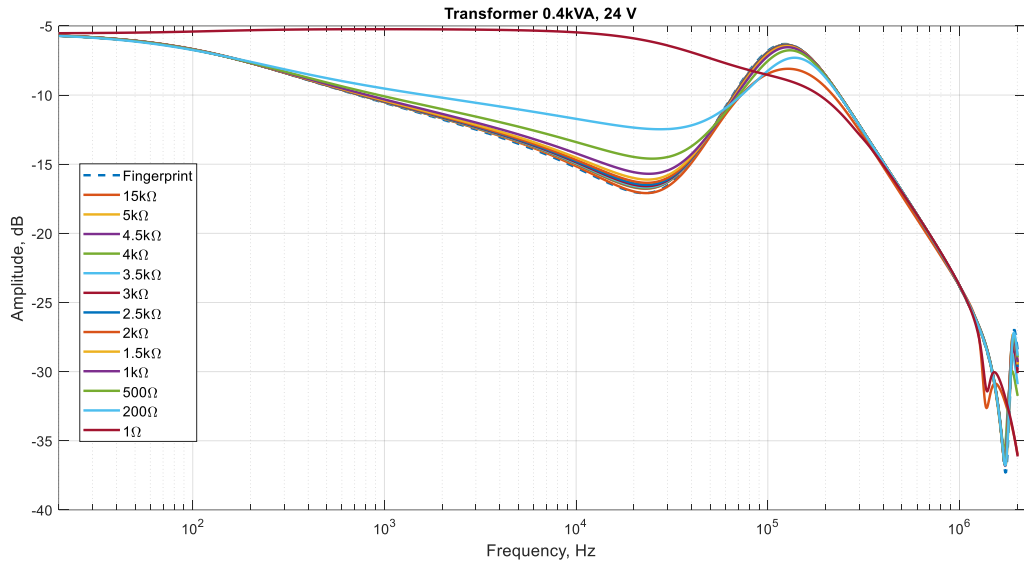


Figure 5A. Transformer 0.4kVA 24 V

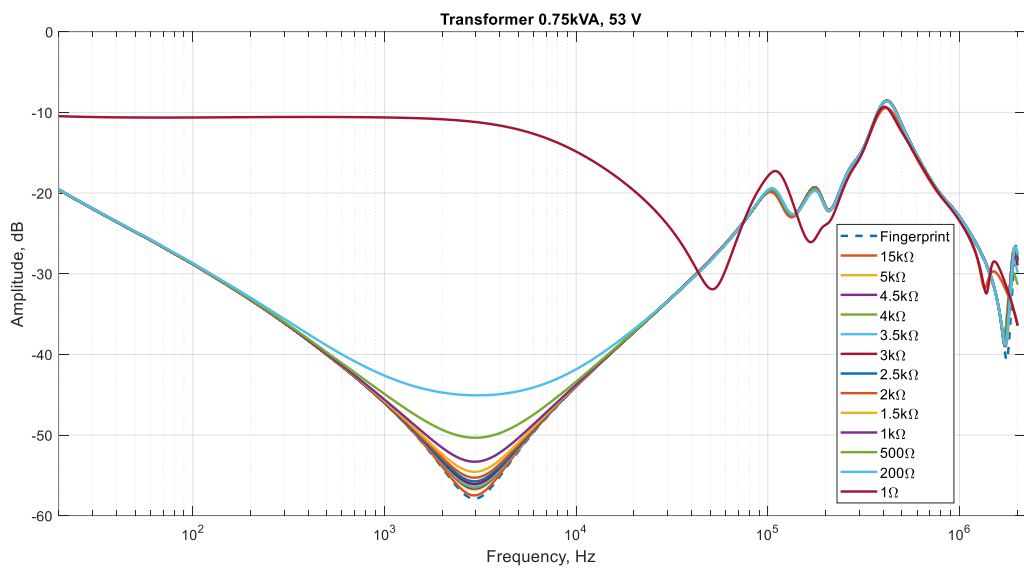


Figure 6A. Transformer 0.75kVA 53 V

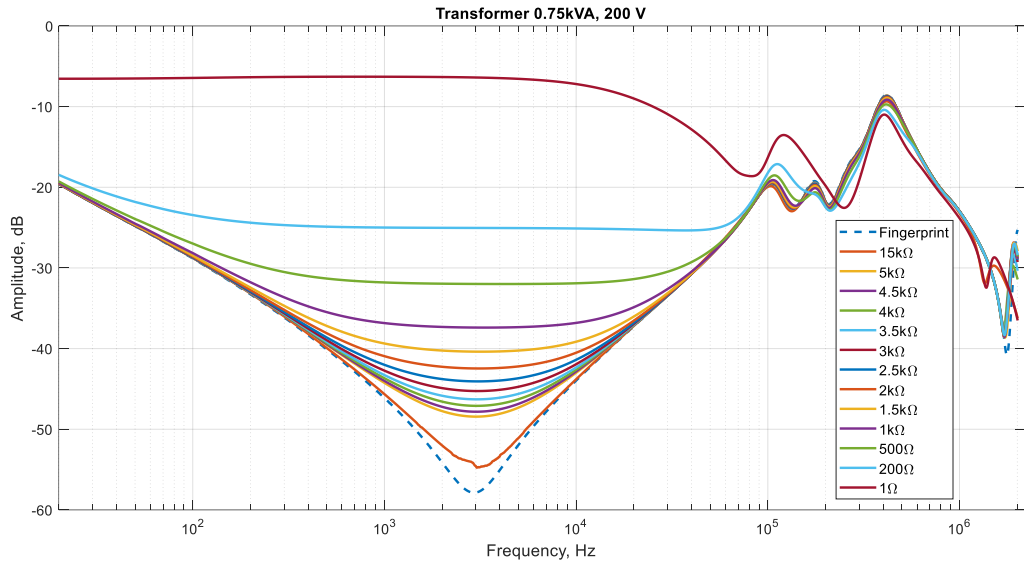


Figure 7A. Transformer 0.75kVA 200 V

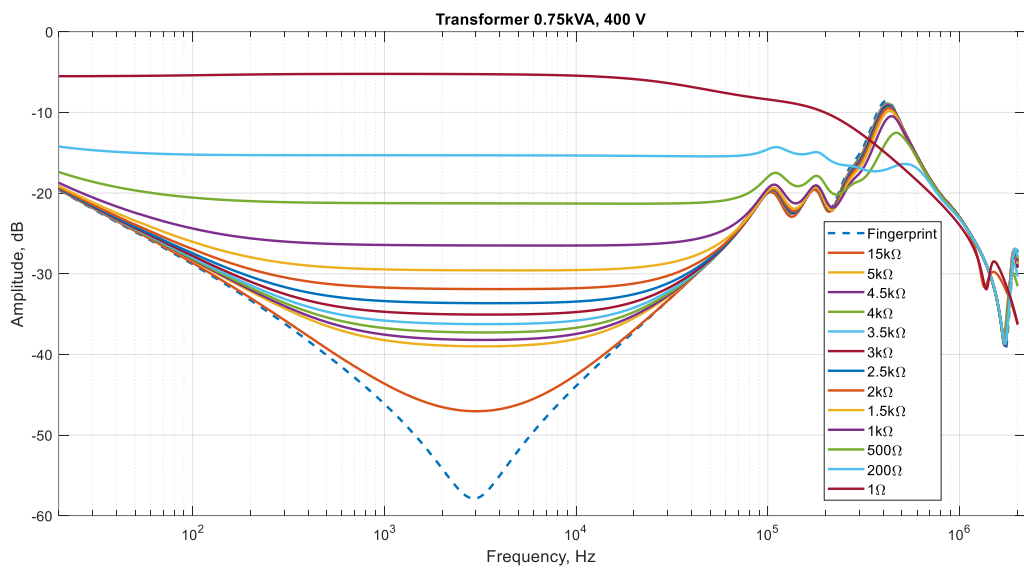


Figure 8A. Transformer 0.75kVA 400 V

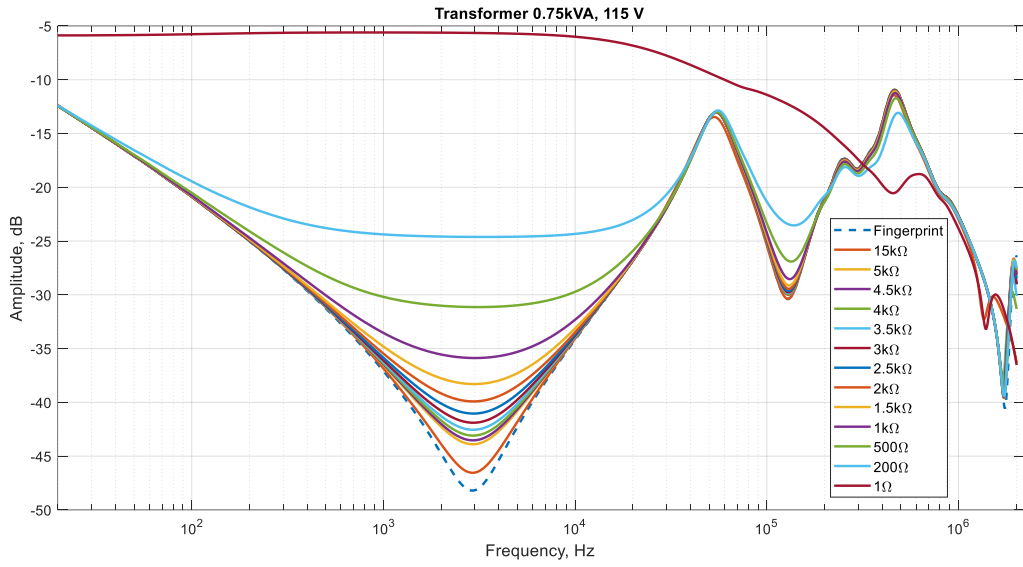


Figure 9A. Transformer 0.75kVA 115 V

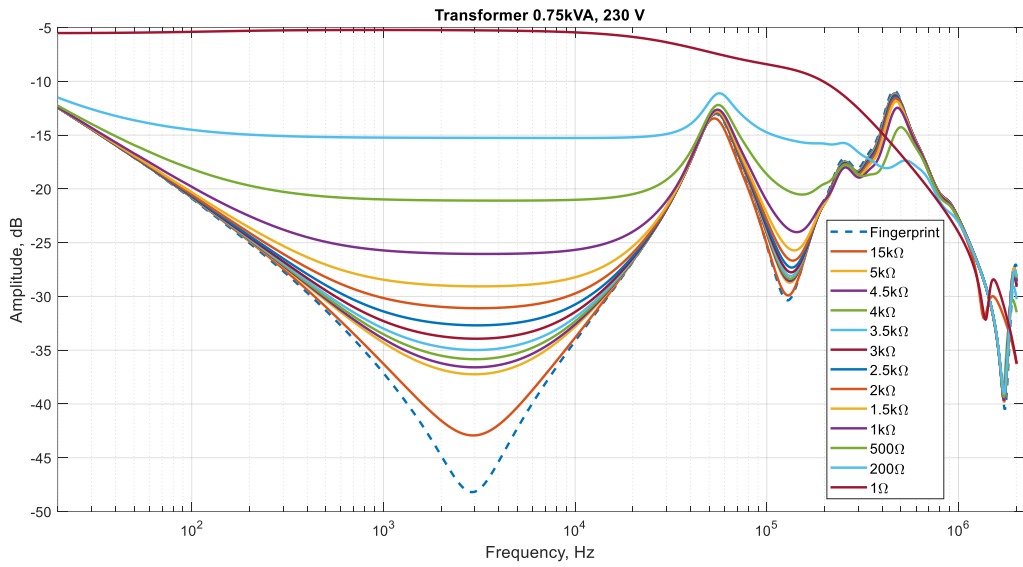


Figure 10A. Transformer 0.75kVA 230 V

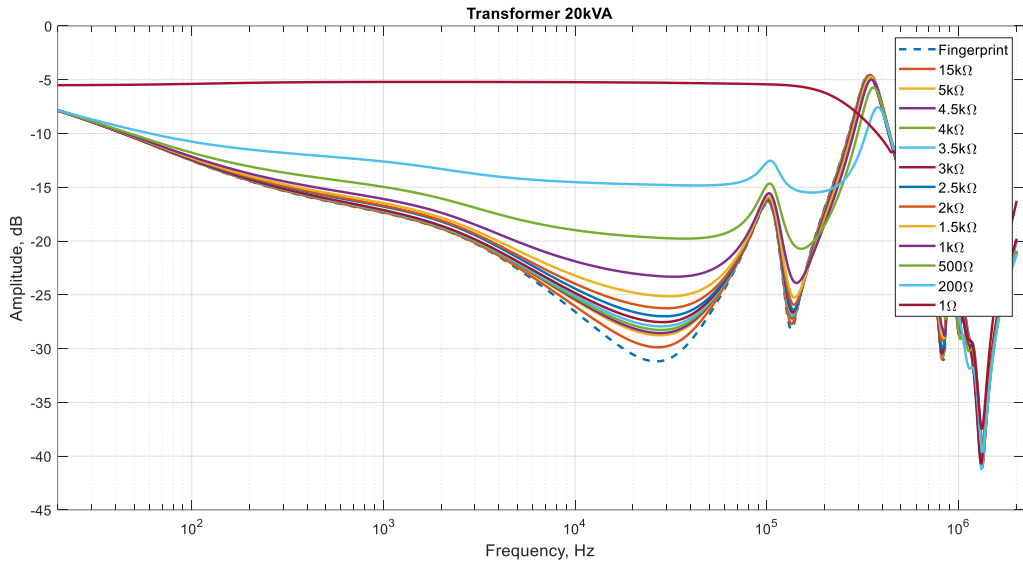


Figure 11A. Transformer 20kVA

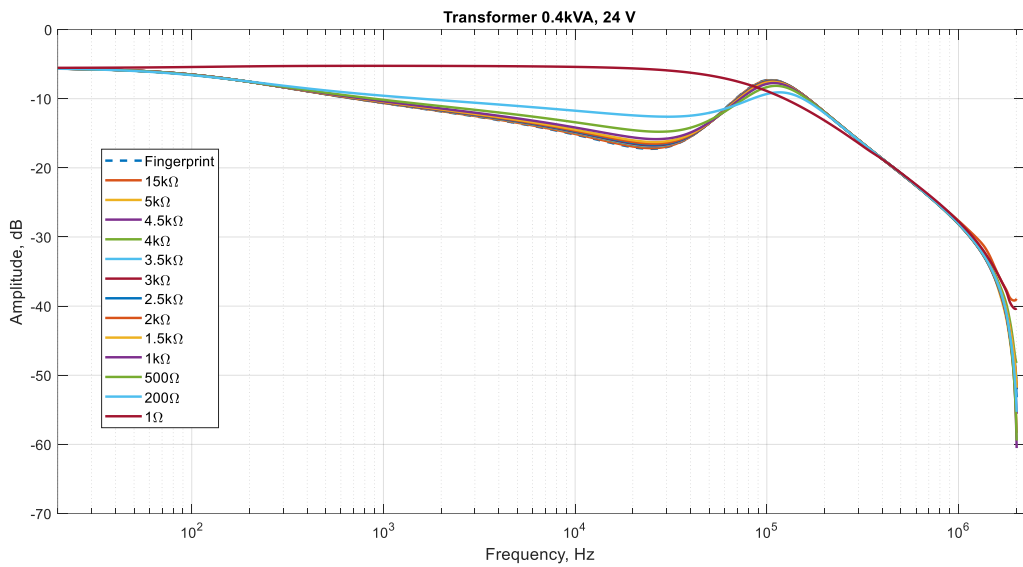


Figure 12A. Transformer 0.4kVA 24 V

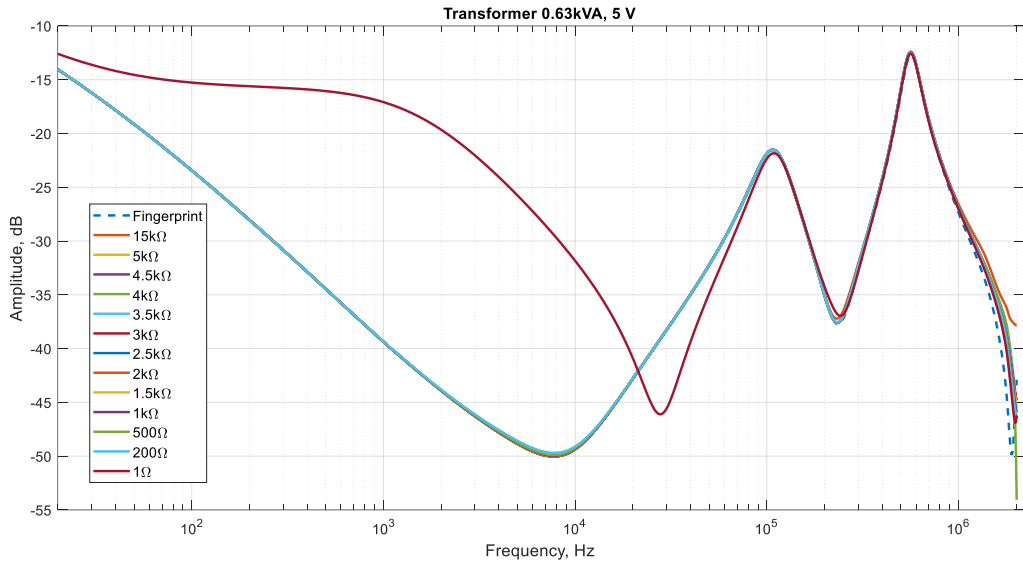


Figure 13A. Transformer 0.63kVA 5 V

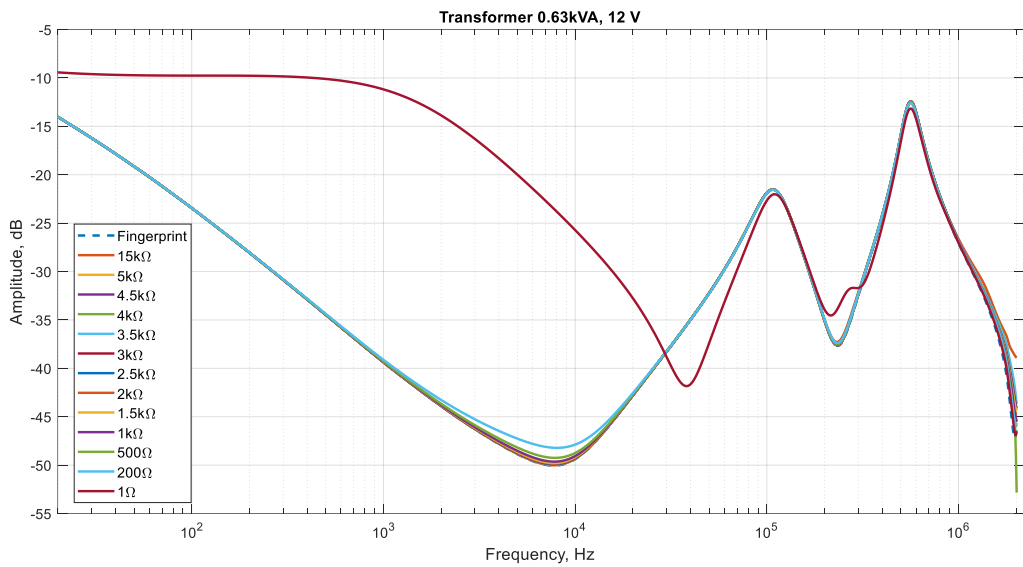


Figure 14A. Transformer 0.63kVA 12 V

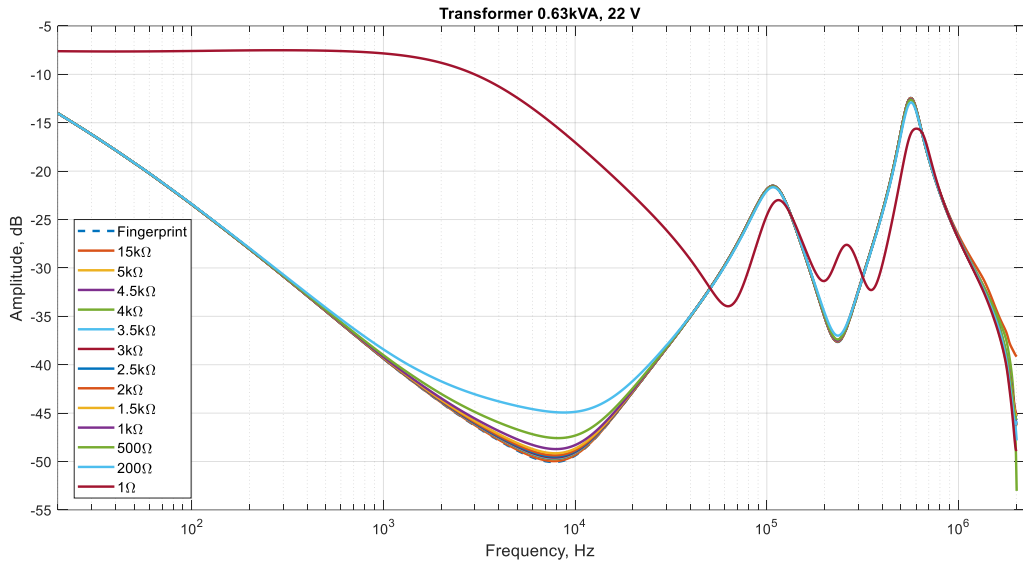


Figure 15A. Transformer 0.63kVA 22 V

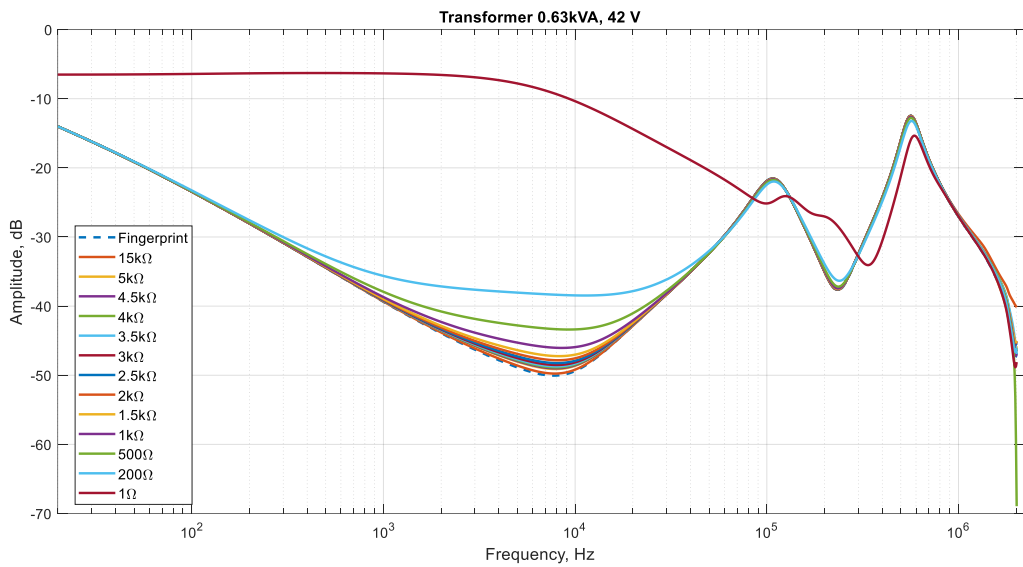


Figure 16A. Transformer 0.63kVA 42 V

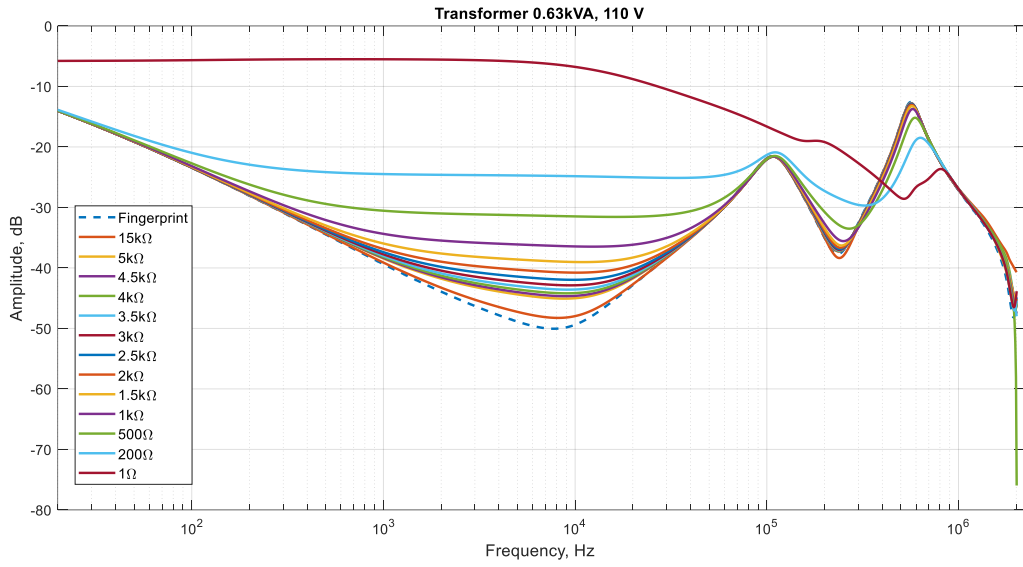


Figure 17A. Transformer 0.63kVA 110 V

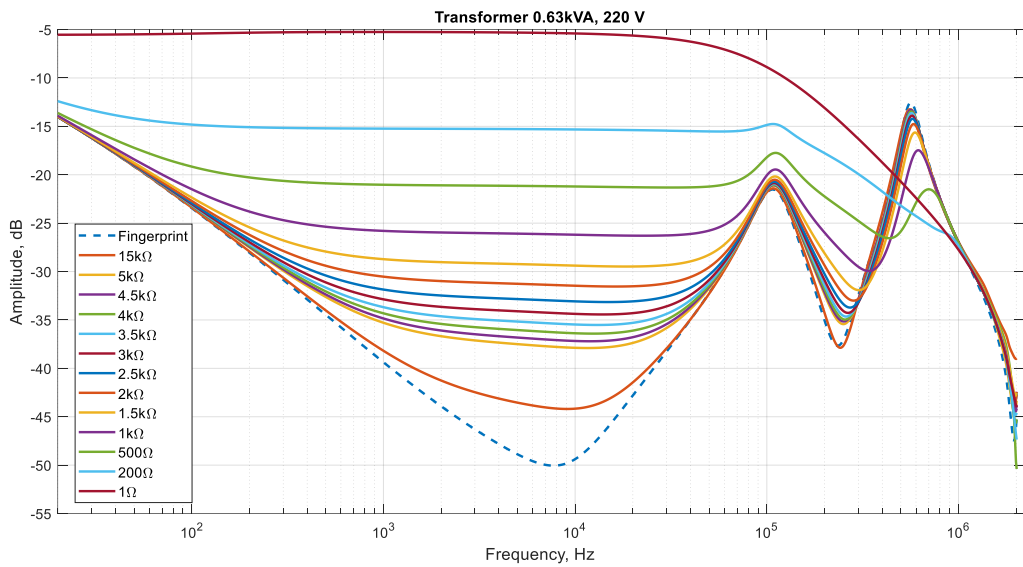


Figure 18A. Transformer 0.63kVA 220 V

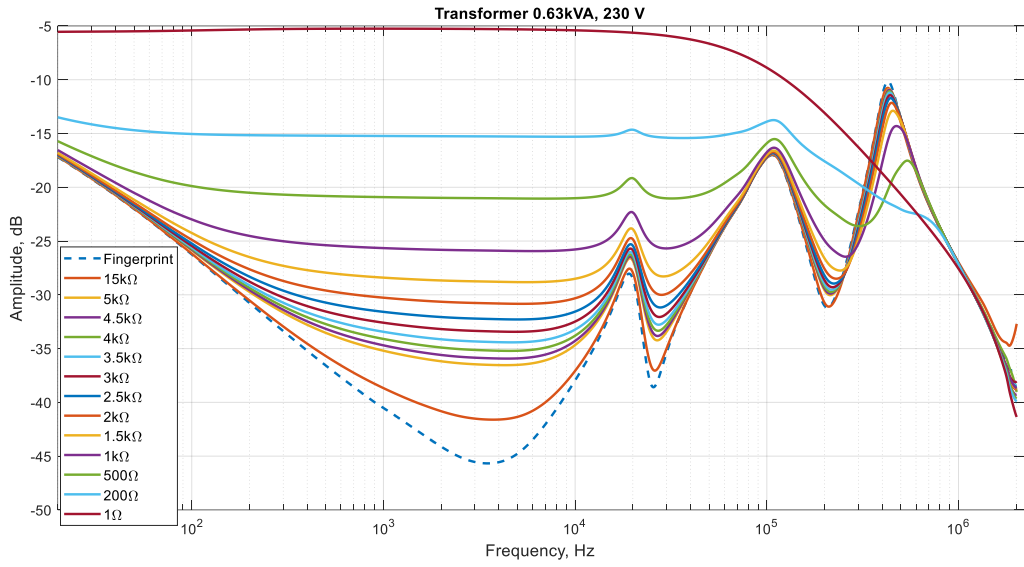


Figure 19A. Transformer 0.63kVA 230 V

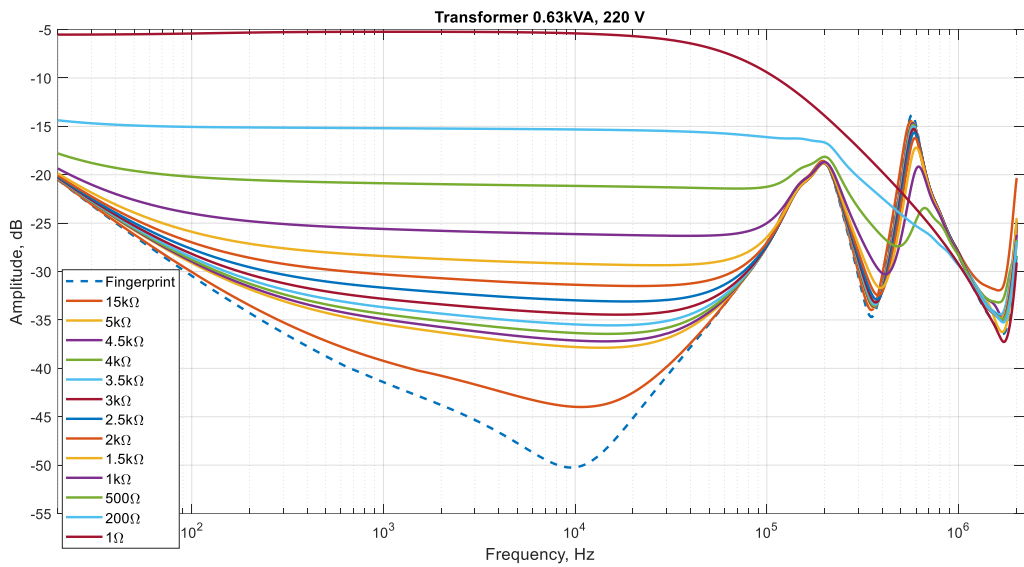


Figure 20A. Transformer 0.63kVA 220 V

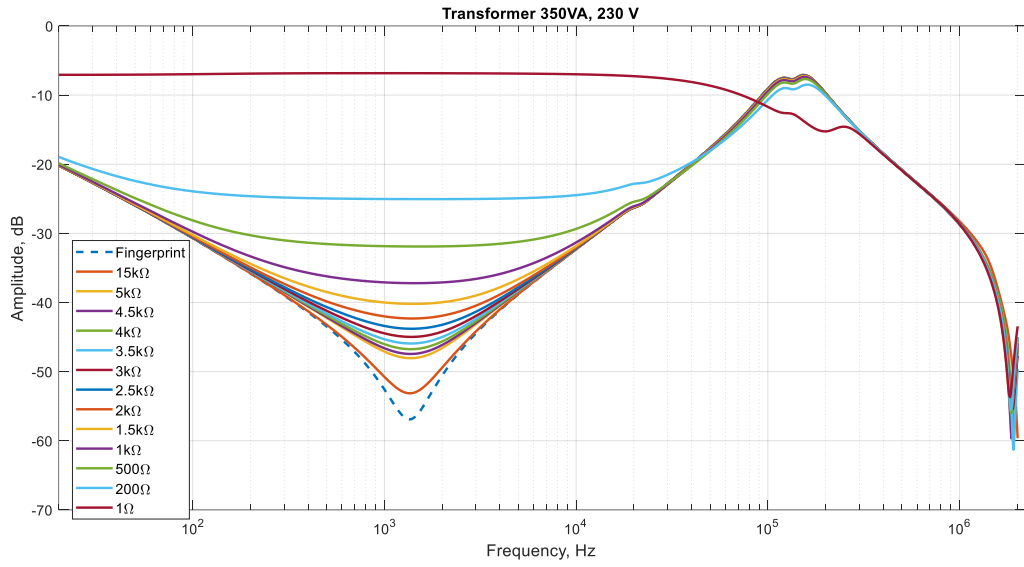


Figure 21A. Transformer 0.35kVA 230 V

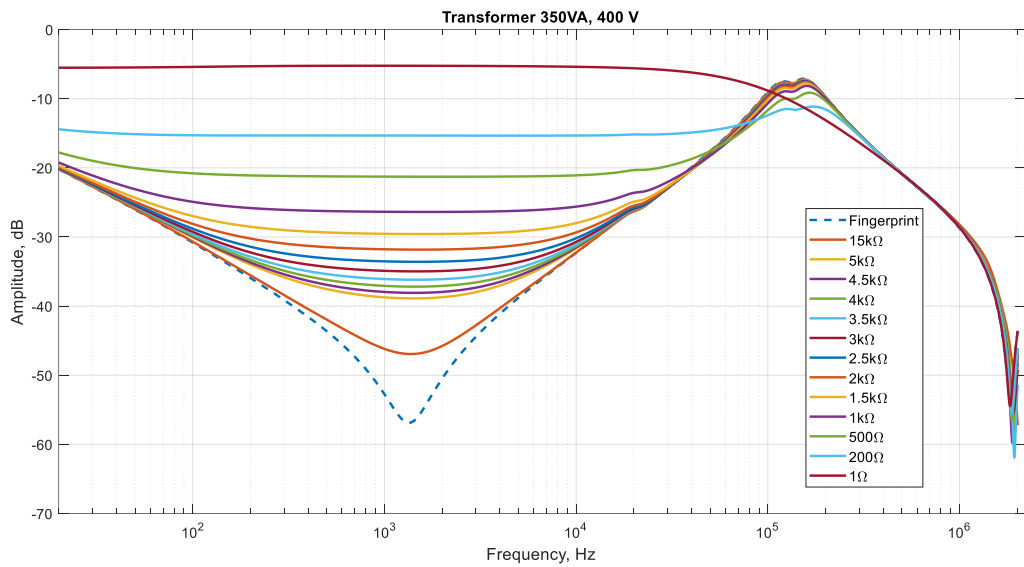


Figure 22A. Transformer 0.35kVA 400 V

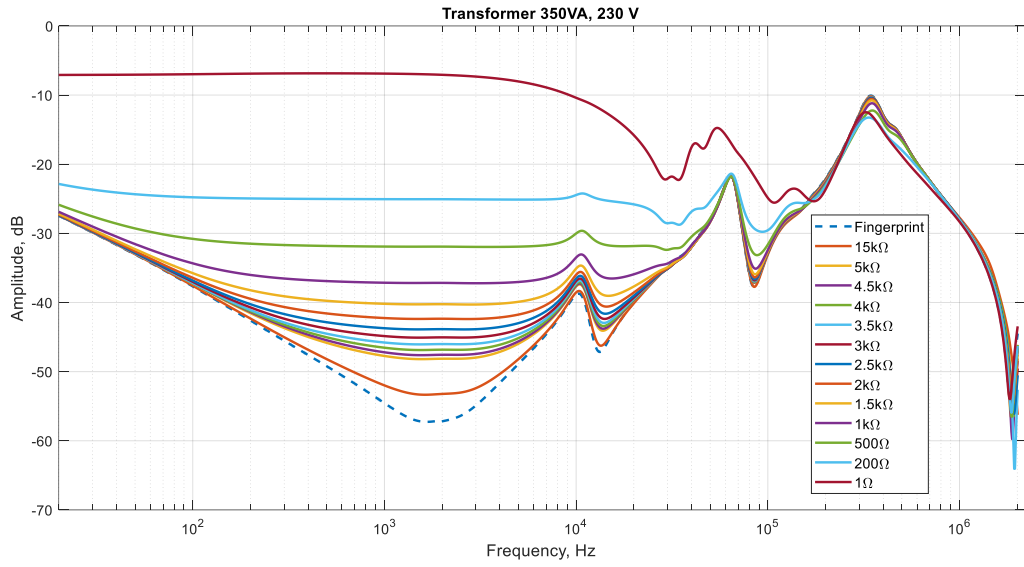


Figure 23A. Transformer 0.35kVA 230 V

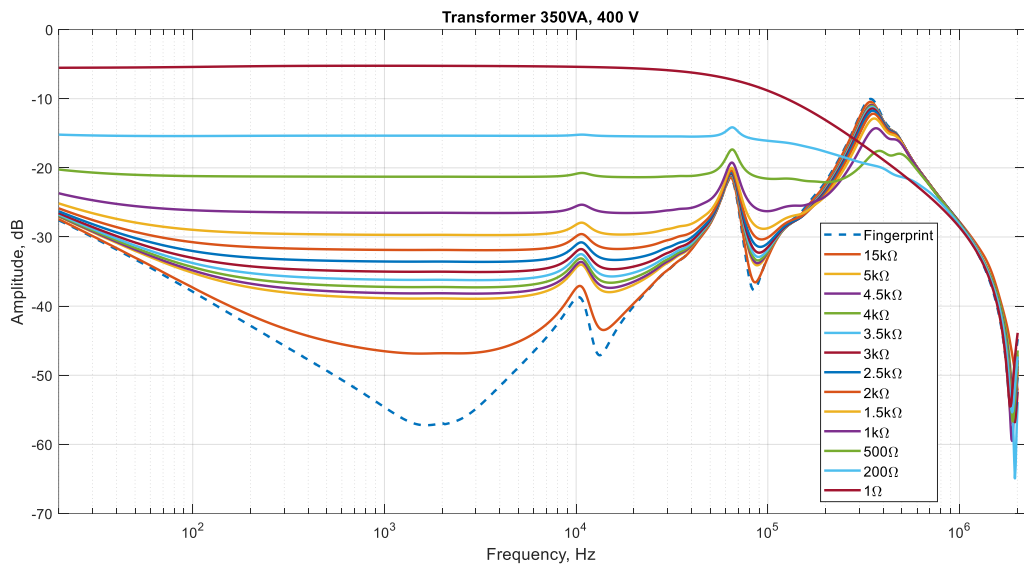


Figure 24A. Transformer 0.35kVA 400 V

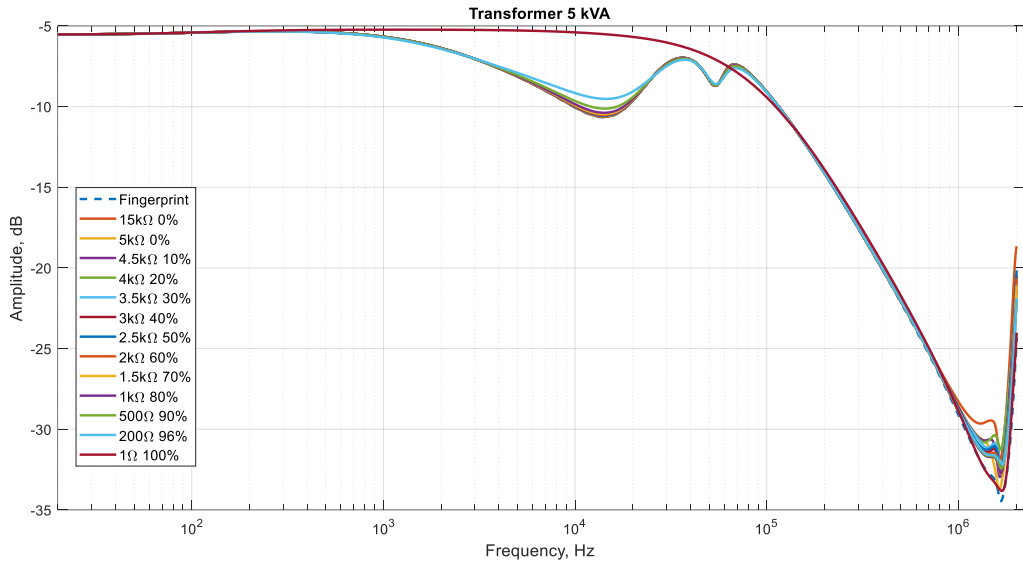


Figure 25A. Transformer 5kVA

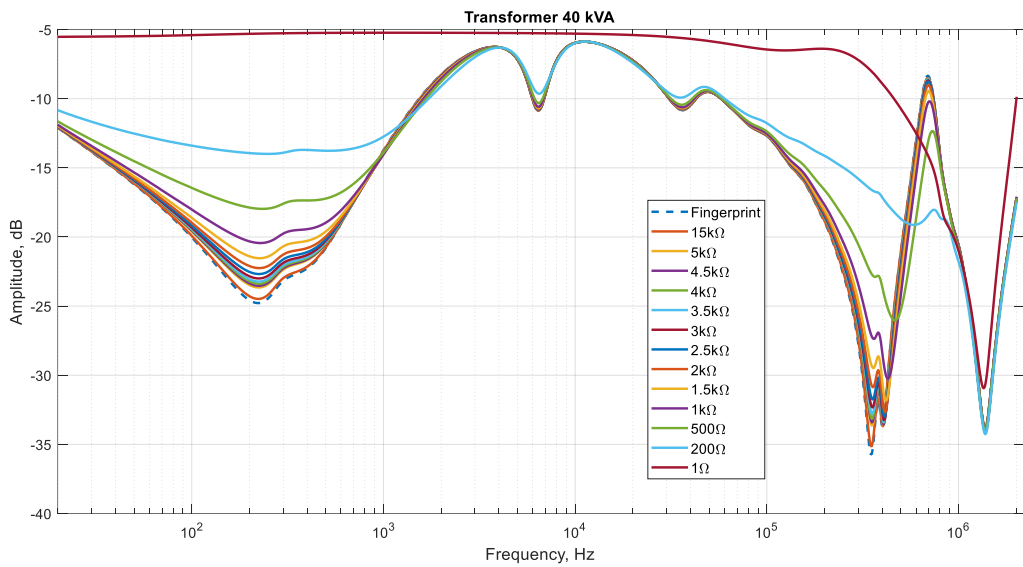


Figure 26A. Transformer 40kVA